Exploring the Potential of Mn/Zno@Mxene Nanocomposite in Biomedical Applications

MS Thesis
by
Hina Murtaza
CIIT/SP24-R06-007/LHR

COMSATS University Islamabad
Pakistan
FALL 2025

Exploring the Potential of Mn/Zno@Mxene in Biomedical Applications

A thesis submitted to

COMSATS University Islamabad

In partial fulfillment

Of the requirements for the degree of

Master of Science
in
Chemistry

By

Hina Murtaza

CIIT/SP24-R06-007/LHR

Department of Chemistry

Faculty of Chemistry

COMSATS University Islamabad

Pakistan

FALL 2025

Exploring the Potential of MnZno@Mxene Nanocomposite in Biomedical Applications

This thesis is submitted to the Department of Chemistry in partial fulfillment of the requirements for the award of the degree of Master of Science in Chemistry

Name	Registration Number
Hina Murtaza	CIIT/SP24-R06-007/LHR

Supervisor Committee

Supervisor

Dr. Sadaf Ul Hassan
Assistant Professor
Department of Chemistry
COMSATS University Islamabad
(CUI)
Lahore Campus

Member

Dr. Zulfiqar Ali
Associate Professor
Department of Chemistry
COMSATS University Islamabad
(CUI)
Lahore Campus

Member

Dr. M. Shahid Nazir
Associate Professor,
Department of Chemistry
COMSATS University Islamabad
(CUI)
Lahore Campus

Certificate of Approval

This thesis titled

Exploring the Potential of MnZno@Mxene Nanocomposite in Biomedical Applications

By

Hina Murtaza
CIIT/SP24-R06-007/LHR

has been approved

for the degree of Master of Science in Chemistry

at COMSATS University Islamabad, Lahore Campus

External Examiner: _____

Dr. Abid Ali
Associate Professor
Department of Chemistry
University of Lahore

Supervisor: _____

Dr. Sadaf Ul Hassan
Assistant Professor
Department of Chemistry
CUI, Lahore Campus

Head of the Department: _____

Dr. M. Shahid Nazir
Associate Professor
Department of Chemistry
CUI, Lahore Campus

Author's Declaration

I Hina Murtaza, CIIT/SP24-R06-007/LHR, hereby declare that I have produced the work presented in this thesis, during the scheduled period of study. I also declare that I have not taken any material from any source except referred to wherever due to that amount of plagiarism is within an acceptable range. If a violation of HEC rules on research has occurred in this thesis, I shall be liable to punishable action under the plagiarism rules of HEC.

Date: _____

Date of Thesis submission

Signature of Student

_____

Hina Murtaza

CIIT/SP24-R06-007/LHR

Certificate

It is certified that Hina Murtaza, CIIT/SP24-R06-007/LHR, has carried out all the work related to this thesis under my supervision at Department of Chemistry, COMSATS University Islamabad, Lahore Campus and the work fulfils the requirement for the award of the degree of MS in Chemistry.

Date: _____

Date of thesis submission

Supervisor:

Sign

Dr. Sadaf Ul Hassan

Assistant Professor

Department of Chemistry

COMSATS University Islamabad

Lahore Campus

Dedication

I offer this thesis as a humble dedication to my parents, whose tireless prayers, love, and devotion have been the pillars of all my success in life. I owe my supervisor, Dr. Sadaf Ul Hassan, deep gratitude for his guidance, encouragement, and support throughout this process, without which this achievement would not have been possible. Lastly, I would like to extend my sincere congratulations to my siblings, whose constant support and prayers kept me going in this venture.

Acknowledgements

All praises to Allah Almighty, the most beneficent and the most merciful whose endless blessings, grace, and mercy have bestowed upon me the guidance, strength, and inspiration needed to complete this dissertation project. I further express my sincerest gratitude to the Holy Prophet Hazrat Muhammad (SAW) whose wisdom and teachings are the sources of light for all mankind.

At this, I want to say that I am very grateful to my beloved Research Supervisor **Dr. Sadaf Ul Hassan,** because of their mentorship, professional advice, timely and positive feedback in all circumstances, and constant support, which has significantly contributed to the completion of this project. This is the personality that has always steered me with professional knowledge and experience. I am proudly and gladly working under this supervisor that is so kind and supportive.

I would like to acknowledge that **Ma'am Muntaha Ijaz** was very supportive and generous to offer the required laboratory facilities to conduct experiments during my research. Her cooperative conduct and help towards my research work and her aids have been very much welcome.

I am deeply grateful to my friend **Saba Iqbal**, all my lab fellows for their company and support throughout my research. Thank you for supporting me and going through it all.

I would like to express my heartfelt thanks to my parents and siblings who have been my support system in every aspect and above all feelings and prayers. As a daughter, I had a hard time in carrying on with this journey, yet you have never failed to support and cheer me as well.

I also owe much of the credit to Chemistry department which supplied me with everything I required to conduct this research.

Hina Murtaza

CIIT/SP24-R06-007/LHR

Abstract

Exploring the Potential of Mn/Zno@Mxene Nanocomposite in Biomedical Applications

By

Hina Murtaza

Mxenes are two-dimensional transition metal composed of carbides and nitrides, which have recently attracted much attention as biomedical application platforms owing to their high electrical conductivity, numerous surface functional groups, and biocompatibility, which is favorable, giving them the best places to design multifunctional nanocomposites. This paper has managed to prepare and characterize a MnZno@Mxene nanocomposite through XRD, FTIR, Raman spectroscopy, UV-Vis spectroscopy, SEM, EDX, elemental mapping, and XPS. The MnZno@Mxene nanocomposite was found to have great antibacterial activity against both Gram-positive and Gram-negative bacterial with the maximum inhibitory zone of 22 mm against Escherichia coli, 18 mm against Staphylococcus aureus, and 19 mm against Pseudomonas aeruginosa, as compared to the standard antibiotics, including gentamicin and ciprofloxacin, and time-kill kinetic analysis revealed successful and sustained bacterial inhibition, especially in E. coli. A wound-healing assessment of a full-thickness excisional wound model in vivo showed that the treated group had a significantly faster healing rat with 95.19% wound closure at 10 days as opposed to 66.76% in the negative control, as well as increased skin regeneration and improved wound morphology. In addition, the nanocomposite also showed significant anti-inflammatory effects in carrageenan induced paw edema model, with paw thickness reducing from 4.39 mm to 6.96 mm after 24 hours, as a result, a change similar to the positive control. The high potential of MnZno@Mxene was further validated by histopathological analysis, which revealed increased re-epithelialization, decreased inflammation, and ordered deposition of collagen in treated tissues, indicating high adaptability and usefulness of MnZno@Mxene as an antimicrobial therapy, wound healing, and inflammation control material.

Table of Contents

Chapter 1 Introduction 1

1.1 Overview of Wound Healing Process 2

1.1.1 Hemostatic Phase 3

1.1.2 Inflammatory Response.....4

1.1.3 Proliferation stage.....5

1.1.4 Tissue Remodeling and Maturation 6

1.2 Clinical Barrier and Challenges in Achieving Effective Wound Repair.....7

1.3 Advancement in wound care through Nanotechnology 7

1.3.1 Therapeutic Uses of Individual Nanoparticles 9

1.3.1.1 Zinc oxide nanoparticles 9

1.3.1.2 Manganese nanoparticles 10

1.3.2 Synergistic Effects in Binary Nanoparticle Systems.....11

1.4 Mechanistic Contributions of Nanomaterials to Wound Recovery: 11

1.4.1 Antimicrobial Activity 12

1.4.2 Controlled and Sustained Drug Release.....13

1.4.3 Modulation of Inflammatory Responses 13

1.4.4 Promotion of Angiogenesis.....14

1.4.5 Challenges and Limitations of Nanoparticle-Based Based Treatments 14

1.5 Introduction to Mxene as a prominent 2D Nanomaterial.....15

1.5.1 Structure Characteristics of Mxene 16

1.5.2 Functional Properties of Mxene 17

1.5.3 Mxenes in Antibacterial and Antimicrobial Applications.....19

1.6 Development of Mxene-Based Nanocomposites 19

1.7 Biomedical Relevance of Mxene composite in Wound Treatment.....20
1.7.1 Mxene -Based Nanoparticles for Drug Delivery.....21
1.7.2 Applications in Tissue Regeneration.....22
1.7.3 Anti-inflammatory Functionalities.....23
1.7.4 Supports of Hemostatic processes.....24
1.8 MnZno@Mxene Nanocomposite in Biomedical Applications.....26
Chapter 2.....28
Literature Review.....28
Chapter 3.....40
Materials and Methods.....41
3.2 Materials Synthesis and Nanocomposite Fabrication.....41
3.2.1 Synthesis of Mxene:.....41
3.2.2 Synthesis of Mn/Zno Nanocomposite.....42
3.2.3 Synthesis of Mn/Zno @Mxene Nanocomposite.....42
3.3 Methodology for Antibacterial potential study:.....43
3.4 Methodology for Wound healing in vivo studies.....44
3.5 Methodology for Anti-Inflammatory Activity:.....44
Chapter 4.....46
Results and Discussion.....46
4.1 FTIR Analysis.....46
4.2 Raman Studies:.....48
4.3 UV-Vis. Studies:.....49
4.4 XRD study:.....50
4.5 SEM/EDX and Elemental Analysis:.....51
4.5 XPS analysis:.....55

4.2 Antibacterial Studies 56

4.8 Time Scale Studies 58

4.9 In vivo wound healing studies 59

4.10 Assessment of the Anti-Inflammatory Response:.....60

4.11 Comparative studies of other reported papers.....61

Chapter 5 Conclusion 65

References.....66

List of Figures

Figure 1: Illustration of the sequential stages involved in wound healing. 2
Figure 2: Wound healing follows a structured progression through four key phases. 6
Figure 3:. Schematic representation of the diverse applications of nanomaterials in wound healing. 8
Figure 4: Mode of Antibacterial Action of Manganese Nanoparticles. 10
Figure 5: Overview of the therapeutic properties and biomedical applications of MnZno nanoparticles. 12
Figure 6: Layered Structure of Mxene nanosheet. 16
Figure 7: Schematics of M2AX, M3AX2, and M4AX3 crystal structures. 17
Figure 8: Illustration of the key physicochemical and biological properties of Mxene nanomaterials. 18
Figure 9: multifaceted biomedical applications of functionalized Mxene nanomaterials... 21
Figure 10: Multifaceted role of Mxenes in promoting wound healing 25
Figure 11: Schematic illustration of the biomedical application of the MnZno@Mxene composite antibacterial activity and enhance wound healing**. 27**
Figure 12: Schematic illustration of the synthesis of Mxene from Ti_3AlC_2 MAX phase via HF etching 41
Figure 13: Schematic representation of the hydrothermal procedure used to prepare MnZno@Mxene nanocomposite. 43
Figure 14: Graphical illustration of the agar well diffusion method for evaluating antibacterial activity. 44
Figure 15: FTIR spectra of Mxene, MnZno, and MnZno@Mxene composite. 47
Figure 16: Raman spectra of MAX phase, Mxene, MnZno, and MnZno@Mxene composite 49
Figure 17: The UV–Visible absorption spectra of Mxene, MnZno, and MnZno@Mxene nanocomposite displays distinct peaks. 50
Figure 18: XRD Analysis of Individual Components and the MnZno@Mxene Nanocomposite. 51
Figure 19: a) SEM image of Max phase, b) EDX spectrum of Max phase c) Elemental mapping of Max phase. 52

Figure 20: a) SEM image of Mxene, b) EDX spectrum of Mxene, c) Elemental mapping of Mxene. 53
Figure 21: a) SEM image of MnZno, b) EDX spectrum of MnZno, c) Elemental mapping of MnZno. 54
Figure 22: a) SEM image of MnZno@Mxene, b) EDX spectrum of MnZno@Mxene, c) Elemental mapping of MnZno@Mxene. 55
Figure 23: XPS full spectra of MnZno@Mxene and High-resolution XPS spectra C1s, O1s, Ti2p. 56
Figure 24: Agar Well Diffusion Results Displaying Antibacterial Activity Again S. aureus, E. coli, and P. aeruginosa. 57
Figure 25: Figure 20 Comparative Analysis of ZOI Induced by MnZno@Mxene Nanocomposite 57
Figure 26: Kinetic Insights into the Antibacterial Mechanism of MnZno@Mxene. 58
Figure 27: Comparative evaluation of wound healing in rats from the MnZno@Mxene treatment group, positive control (medicated gel), and negative control (normal saline) during 10 days**. .....** 62
Figure 28: Evaluation of wound healing progression across treatment, positive control, and negative control cohorts. 60
Figure 29: Paw thickness variation recorded at different time points (0–24 h) after carrageenan-induced inflammation. 61

List of Tables

Table 1: FTIR Absorption Bands and Their Assigned Functional Groups. ...47
Table 2: Overview and comparison of multifunctional materials for antibacterial, wound healing and anti-inflammatory. 63

List of Abbreviations

Abbreviation	Full Form
2D	Two-Dimensional
ATP	Adenosine Triphosphate
BC	Bacterial Cellulose
BET	Brunauer–Emmett–Teller Analysis
CAM	Chorioallantoic Membrane
CeO_2NPs	Cerium Oxide Nanoparticles
COX-2	Cyclooxygenase-2
DNA	Deoxyribonucleic Acid
DFO	Deferoxamine
DLS	Dynamic Light Scattering
ECM	Extracellular Matrix
EDX	Energy-Dispersive X-ray Spectroscopy
FGF	Fibroblast Growth Factor
HIF-1	Hypoxia-Inducible Factor-1
iNOS	Inducible Nitric Oxide Synthase
IL	Interleukin
LCST	Lower Critical Solution Temperature
MDR	Multidrug Resistant
MnZno	Manganese-Doped Zinc Oxide
MRI	Magnetic Resonance Imaging
MRSA	Methicillin-Resistant Staphylococcus aureus

NF-κB	Nuclear Factor Kappa B
NIR	Near-Infrared
NPs	Nanoparticles
PANI	Polyaniline
PDGF	Platelet-Derived Growth Factor
PEGDA	Poly(ethylene glycol) diacrylate
PCL	Polycaprolactone
PVA	Polyvinyl Alcohol
QDs	Quantum Dots
RBC	Red Blood Cells
ROS	Reactive Oxygen Species
SCI	Spinal Cord Injury
SEM	Scanning Electron Microscopy
TEM	Transmission Electron Microscopy
TGF-β	Transforming Growth Factor Beta
TNF-α	Tumor Necrosis Factor Alpha
UV–Vis	Ultraviolet–Visible Spectroscopy
VEGF	Vascular Endothelial Growth Factor
XRD	X-ray Diffraction

Chapter 1
Introduction

Skin is the biggest organ in the human body and plays a variety of functions, including the following. regulating body temperature, enhancing the formation of vitamin D, helping it to be excreted, immune against viral and toxic substances and keeping the body hydrated [1]. Skin, is an active organ that is always renewed. Skin has three major coatings, namely the. epidermis, dermis, and subcutis. The inner one is the subcutis, and the next one is the epidermis. is the outermost. The epidermis is made of keratinocytes, which are segregated. to strata based on the maturity of the cells[2]. The epidermis is deficient in blood supply. its own so it relies on the dermis to transport nutrients and oxygen. The primary role of this layer of fat, the subcutis, is to support the bones and muscles, as well as support the body. warm and fasten the upper layers to the muscle [3]. A chemical protection of the skin is crucial. it is effective in the presence of the immunological and other protective mechanisms of the body; the physical system of protection against the risk of the environment. The complex combination of lipids constituting this barrier consists of ceramides, cholesterol and fatty acids. produces a hydrophobic stratum corneum that prevents the loss of water through too much water loss and blockage. the intrusion of hazardous substances like allergens and infections [4]. Skin pH, which is usually between 4.5 and 5.5, is necessary to maintain the skin's moisture, barrier, etc., microbiological equilibrium. The acid mantle is another slightly acidic layer and it enhances. keeps the skin cells healthy and protects against harmful microorganisms. A change in pH alkaline may be detrimental to the barrier, which will cause the skin to be dry and exposed to the possibility of developing dermatitis. and acne [5]. Damages on the skin would lead to the formation of wounds, regardless of whether they are caused by internal ailments such as underlying illnesses or external forces such as trauma, burns or surgical incisions. These wounds interfere with the continuity of the skin and disrupt its ability to perform critical defensive functions. tasks. By disintegrating the structure of the skin, the underlying tissues are vulnerable to. a complex biological response is induced to repair the environmental hazards. break and reconstruct tissue integrity. The word wound can be interpreted as a wound that is a tissue injury. easy to cure but the health and other nature characteristic of an individual can turn it into a nightmare. complex. This has made

wound healing to attract a lot of care within the biomedical field [6]. Wounds are a very critical health concern in the world as they are experienced by millions of individuals globally. to a great extent influencing their quality of life. As the populations are growing old and illnesses such as. diabetes, wounds are on increase. In highly-developed nations, wounds in themselves are. believed to affect 1-2 percent of the population [7].

1.1Overview of Wound Healing Process

Skin injuries can vary in shape and intensity, yet they all trigger the body's incredible natural healing mechanism. Wound healing is not just one event but a dynamic biological process that occurs through a sequence of linked stages, each essential in restoring tissue integrity. Curiously, this essential process starts right when we are born; the severing of the umbilical cord signifies our initial injury and the first trigger of this survival response [8]. A wound is characterized as an interruption in the skin's protective epithelial layer, frequently penetrating to affect the underlying tissues, consequently altering their typical structure and function. These injuries can occur in various forms, from a precise, intentional incision performed during surgery to more extensive harm resulting from serious trauma or burns. Injuries can also manifest as bruises, hematomas, cuts, or scrapes. Since the skin is crucial for maintaining the body's equilibrium and shield, it is important to restore its integrity promptly to support overall homeostasis.[9]

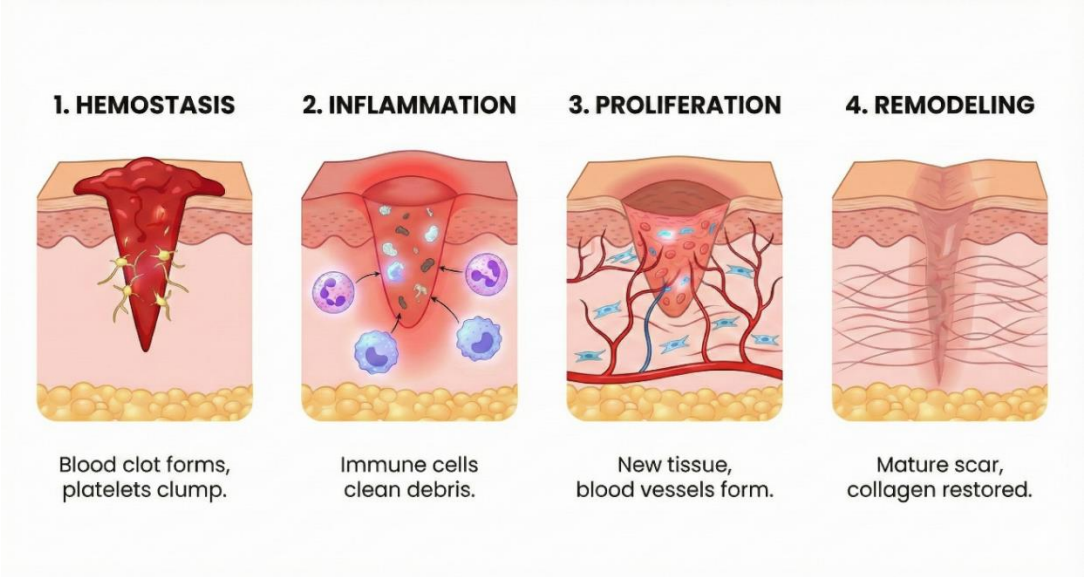

Figure 1: Illustration of the sequential stages involved in wound healing.

Wound healing is a multifaceted process that has four primary phases. The primary aim of these phases is to rejuvenate both the structure and purpose of the skin, enabling it to recover its integrity and protective capabilities. Nonetheless, if this process is interrupted or stalled, persistent wounds may arise. These injuries do not recover within a typical period, resulting in persistent discomfort, restricted movement, and an increased chance of infection.[10]

1.1.1 Hemostatic Phase

Hemostasis is the meticulously regulated process that encompasses blood coagulation, platelet activation, and blood vessel repair. Upon injury, the hemostatic system triggers numerous vascular and extravascular receptors that collaborate with blood elements to cover injured blood vessel and the surrounding area. The coagulation system serves as the primary contributor to this response, whereas platelet activation constitutes the second essential element—assisting in the formation of the hemostatic plug and enhancing coagulation. Ultimately, after stability is reached, circulating inhibitors and proteolytic feedback mechanisms stop both coagulation and platelet function.[11].

Besides being a protective factor in wound healing, hemostasis is also a requirement. The fibrin clot helps in the migration of the fibroblasts and the keratinocytes, acting as a temporary matrix or scaffold. This temporary matrix is the fibrin and fibronectin. Fibronectin is a high fibrin affinity multifunctional adhesion protein that is found in the bloodstream and various tissues. Besides being a chemoattractant to repair cells, it also serves as a collagen fiber deposition template and helps in wound debridement secondary to increased macrophage phagocytic activity and destruction of extracellular matrix (ECM) debris. The consequences of platelet activation are degranulation and the generation of a number of strong cytokines, which are important to initiate tissue regeneration and activate additional immune reactions. Activated platelets also stimulate the new extracellular matrix (ECM) components formation by binding themselves to the revealed collagen fibers within the wound. [12]

Hemostasis is the body’s process for preventing blood loss, carried out through a succession of tightly coordinated physiological and biochemical events that result in the formation of a stable plug to seal the injured vessel. It proceeds through distinct stages: interactions between the vessel wall, adhesive glycoproteins, and platelets; initiation of blood coagulation; and, ultimately, fibrinolysis.[13]

Human platelets typically survive for 5 to 7 days and have a diameter of approximately 2 to 5 μm, while canine platelets generally have a lifespan of around 6 days. The majority of platelet production is driven by thrombopoietin, which is produced by cells in the bone marrow and smooth muscle. Thrombopoietin is cleared from the bloodstream by binding to platelets, establishing a negative feedback system. The ability of platelets to respond to a wide variety of stimuli, despite lacking a nucleus, is largely due to the abundant substances stored within them. Platelets contain preformed materials located within alpha and delta (dense) granules [14].

1.1.2 Inflammatory Response

The regulation of both pro-inflammatory and anti-inflammatory cytokines is essential for successful wound healing. Cytokines such as IL-1β, IL-6, TNF-α, and various chemokines play a crucial role in the initial phases by attracting immune cells that clean the area and improving the action of growth factors. This inflammatory reaction must be managed carefully and promptly to facilitate healing. The shift to advanced phases, in which the initial pro-inflammatory signals encourage angiogenesis and tissue remodeling, is subsequently aided by anti-inflammatory cytokines. [15]

In absence of infection, monocytes at the injured site generate into macrophages that replace the major phagocytic cells in the process of healing. Waste that is ingested by macrophages includes dead neutrophils, bacteria, and fibrin clots. They also produce cytokines and nitric oxide to initiate the healing process. Even though the exact mechanism of action of nitric oxide remains unclear, studies have shown that low concentrations enhance keratinocyte growth and high concentrations enhance differentiation [16]. Due to such an important role, macrophages may be referred to as the "transitional cell between wound inflammation and repair. The wound healing is possible without neutrophils and not without macrophages. Compared to platelets, which release cytokines stored in macrophages continuously produce and secret cytokines which activate cell migration, proliferation and vascular organization. Among the matrix metalloproteinases (MMPs) that are secreted by macrophages and that induce tissue remodeling and debridement, collagenase can be mentioned [17].

Chronic wounds and slow healing are frequently a result of prolonged inflammation. Typically, the stages of wound healing begin with inflammation, which is essential for removing pathogens and damaged cells from the affected tissue. Neutrophils and macrophages are attracted to the injury area through chemotaxis, where they work to fight off bacteria. Once the wound is cleansed, neutrophils undergo programmed cell death, which helps prevent additional tissue damage and reduces the inflammatory response. At the same time, the macrophages that persist release growth factors that stimulate nearby keratinocytes, fibroblasts, and endothelial cells, facilitating subsequent healing stages [18]

In this diseased inflammatory microenvironment, fibroblasts upregulate inflammatory gene expression, while keratinocytes secrete IL-1α and type I interferon, initiating an inflammatory reaction in nearby stromal cells. This, consequently, enhances the movement of immune cells into the damaged area. In conclusion, the prolonged healing of chronic wounds is due to the lack of ECM remodeling resulting from the unregulated immune control of both inflammatory and non-inflammatory cells. [19]

1.1.3 Proliferation stage

Angiogenesis is a complicated activity that results in the development of new blood vessels out of the ones that are already present. It starts with the creation of a hemostatic plug in the first stage of repair, which makes platelets release growth factors like fibroblast growth factor (FGF), platelet growth factor (PDGF), and transforming growth factor (TGF) -B. These growth factors and transcription factors, hypoxia-inducible factor-1 (HIF-1) and vascular endothelial growth factor (VEGF), released under low oxygen concentrations, stimulate the appearance of a number of angiogenic genes and the development of new blood vessels, as well as repair injured blood vessels at the wound site. The tissue surrounding the wound produces a rich system of blood vessels, with many more capillaries than healthy tissue, as the angiogenesis process proceeds.[20] The hallmark of the wound healing process is an angiogenic response which supply nutrients and oxygen to the damaged tissue. This angiogenesis process helps to develop granulation tissue that is required to repair a wound, as well as help in the removal of debris. Many of the soluble factors that have been identified in the various wound models are thought to mediate wound angiogenesis.

During the healing process, angiogenic promoters and inhibitors have been identified, meaning that the net effect of angiogenesis can be variable as the significance of every factor switches between enhancing or inhibiting vessel development [21].

1.1.4 Tissue Remodeling and Maturation

The vascular system forms and undergoes major remodeling once the embryonic heart starts beating and blood circulation begins. This leads to a system of arteries, veins, and capillaries that are distinct in their structure, genetics, and function and are capable of facilitating circulation. Alterations in vessel width, branching patterns, and linkages are all components of this process. Arteriovenous differentiation occurs alongside remodeling, which is vital for embryonic viability.[22] Scar remodeling is widely recognized to take a long time. Failure during the maturation and modeling phase can lead to an overproduction of collagen and the development of hypertrophic scars with significant stiffness, or even the creation of a distinct, hard-to-treat condition known as keloid.

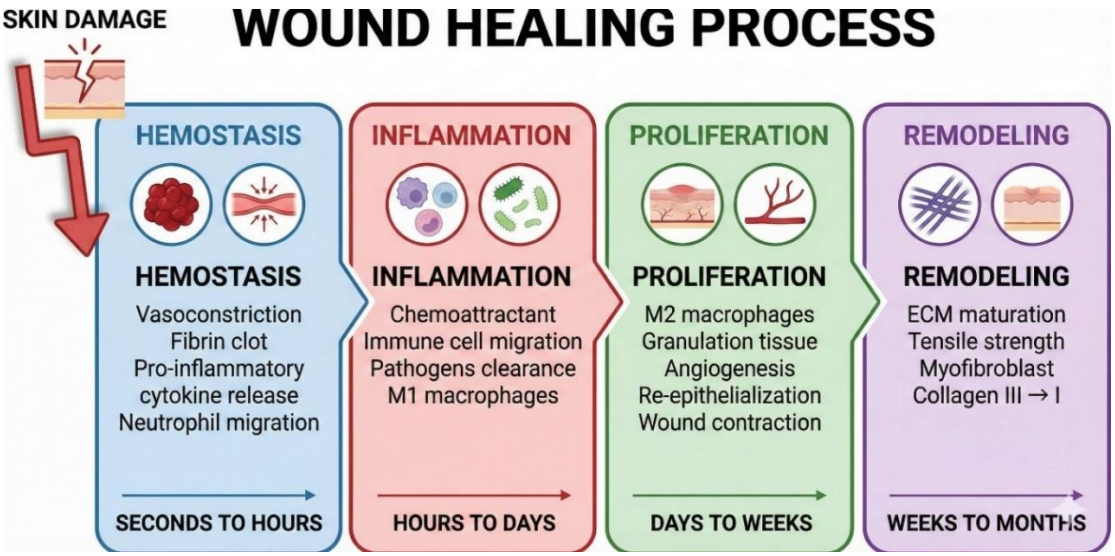

Figure 2: Wound healing follows a structured progression through four key phases.

The connective tissue in keloids resembles the desmoplastic stroma found in certain tumors, particularly pancreatic adenocarcinoma. Fibroblasts derived from keloids bear a close resemblance to cancer-associated fibroblasts from the tumor stroma, not only in the expression of α-SMA but also in the production of transcripts for inflammation-promoting cytokines and/or chemokines [23]. As the wound matures, the extracellular matrix

components experience specific alterations. Physiological outcome of mammalian wound healing shows the development of a scar, which is closely associated with the level of inflammation during the healing process. [24]

1.2 Clinical Barrier and Challenges in Achieving Effective Wound Repair

Chronic wounds present significant clinical challenges due to factors such as high protease action, tenacious infection, excess inflammation, and hypoxia. Challenges also include the conglomeration and complication of chronic or severe wounds, despite the potential of advanced wound dressings and active dressings to enhance healing and counter issues like inflammation, ischemia, scarring, and infection [25]. Furthermore, there is a lack of efficient, evidence-based therapies for specific chronic wounds that yield definitive clinical outcomes. Despite advancements in therapeutic approaches, the clinical assessment and handling of chronic wounds remain difficult, often due to prolonged treatment durations and complex healing processes. Conventional methods like growth factor administration, wound dressings, and skin grafts are not universally applicable, necessitating the development of alternative modalities. While novel technologies like nanotherapeutics, stem cell treatment, and 3D bioprinting goal to improve effectiveness and regeneration [26], and self-healing hydrogels show promise in accelerated closure and tissue regeneration, challenges such as scalability, long-term safety, and inconsistency in clinical outcomes remain. Future directions involve personalized medicine, manufacturing innovation, rigorous clinical trials, and interdisciplinary collaboration [27].

1.3 Advancement in wound care through Nanotechnology

Nanomaterials are revolutionizing wound management due to their unique properties and versatile applications. They offer advanced therapeutic interventions for both acute and chronic wounds. Various types of nanomaterials, including nanoparticles, nanofibers, and nanocomposites, are utilized [28]. Nanomaterials refer to materials whose structural features lie in the nanoscale or less than 100 nanometers that confer them with special physical, chemical, and biological characteristics. Nanomaterials are beneficial to wound healing, due to its special physicochemical properties and size, which is of nanomaterial size. They can be adjusted to permit cellular and molecular interaction by their adjustable surfaces and high surface-to-volume ratio and can be used to provide better wound care. Such materials are useful in

scarring prevention, controlled drug delivery, infection prevention and tissue repair. Nanomaterials such as metallic nanomaterials (silver, gold and zinc oxide), polymeric nanomaterials (hydrogels and nanofibers), lipid-based nanomaterials (liposomes), inorganic nanomaterials (calcium phosphate and silica) have shown promising results in wound healing and tissue functional recovery.

Figure 3:. Schematic representation of the diverse applications of nanomaterials in wound healing.

These materials exhibit strong antimicrobial properties, crucial for preventing infections and biofilm formation, which are significant impediments to healing. Nanomaterials also facilitate controlled drug delivery of growth factors, antimicrobial compounds, and anti-inflammatory agents directly to the wound site, enhancing therapeutic efficacy. Furthermore, they can modulate inflammatory responses, promote cell adhesion and proliferation, stimulate angiogenesis, and enhance extracellular matrix synthesis, thereby fostering tissue regeneration [29]. Nanomaterials integrated into wound dressings can improve mechanical strength, provide a conducive environment for cellular processes, and offer sustained drug release. Despite their promise, challenges related to biocompatibility, potential toxicity, and

extensive production require further research to improve their efficacy and safety for clinical use [30].

1.3.1 Therapeutic Uses of Individual Nanoparticles

Nanoparticles are important for wound healing due to their ability to prevent infection, maintain moisture, promote tissue growth, and reduce inflammation. In particular, are noted for their antibacterial properties and effectiveness in wound healing [31]. Metal nanoparticles integrated into hydrogel scaffolds are also being investigated for their antimicrobial properties and potential to accelerate healing, though further clinical application studies are needed [32]. Biopolymer-based nanoparticles, which come from natural and synthetic materials, offer biodegradability and biocompatibility, demonstrating comparable antibacterial properties and wound healing effectiveness of nanoparticles. [33]. Nanotechnology-based drug delivery systems, including various nano formulations, can overcome limitations of traditional herbal remedies such as poor skin penetration and solubility, thereby enhancing their efficacy in wound healing. Nanomedicine, in general, has advanced wound healing treatments by enabling targeted and personalized therapies that expedite tissue regeneration and recovery [34].

1.3.1.1 Zinc oxide nanoparticles

Zinc oxide nanoparticles (ZnoNPs) show significance in wound healing due to their biocompatibility, low noxiousness, and ability to boost bioactivity. Zinc oxide nanoparticles (ZnoNPs) are very biocompatible and can penetrate the dermis and epidermis layers hence they have become a good agent in wound healing. According to studies done on animal models such as rats, ZnoNPs provide great benefits in improving tissue regeneration by enhancing key tissue regenerative processes such as re-epithelialization, keratinocyte migration, collagen fiber deposition, and the development of granulation tissues. These regenerative properties are closely connected with the action of zinc as a mediator of the activity of matrix metalloproteinases (MMPs) which comprise a family of zinc-dependent enzymes required by the remodeling process of wound healing.[35]

Also, zinc deficient animals have been found to experience a slow rate of healing wounds and this can be improved by zinc supplementation, thus the importance of zinc in efficient

tissue healing. When incorporated in scaffolds, ZnoNPs enhance water uptake, oxygen permeability, porosity, hydrophilicity and biodegradability all of which are critical in creating the most viable environment through which a wound can be healed. Moreover, ZnoNPs also exhibit strong antibacterial effects with Gram-positive and Gram-negative bacteria in the absence of UV radiation, which is why they are applicable in wound infection prevention Their applications in wound healing are supported by their antimicrobial antiviral, antioxidant, anticancer and anti-inflammatory activities. ZnoNPs also work well in conjunction with components that aid in wound healing. Their mechanisms of action include enhancing the generation of reactive oxygen species (ROS) and releasing zinc ions (Zn^{2+}), which can lead to cell death [36]. They can enhance bacterial death and epidermal regeneration, stimulating tissue formation, making them a good platform for the fast healing of infected wounds [37]. Furthermore, ZnoNPs can serve as effective nanocarriers for conventional drugs due to their cost-effectiveness, biodegradability, and biocompatibility [38].

1.3.1.2 Manganese nanoparticles

Manganese-based nanoparticles are a promising area of nanotechnology for various biomedical applications due to their unique properties [39]. These nanoparticles, including manganese oxides (Mn^{2+}, Mn^{3+}, and Mn^{4+}), are being explored for their various morphologies and tunable magnetic properties [40].

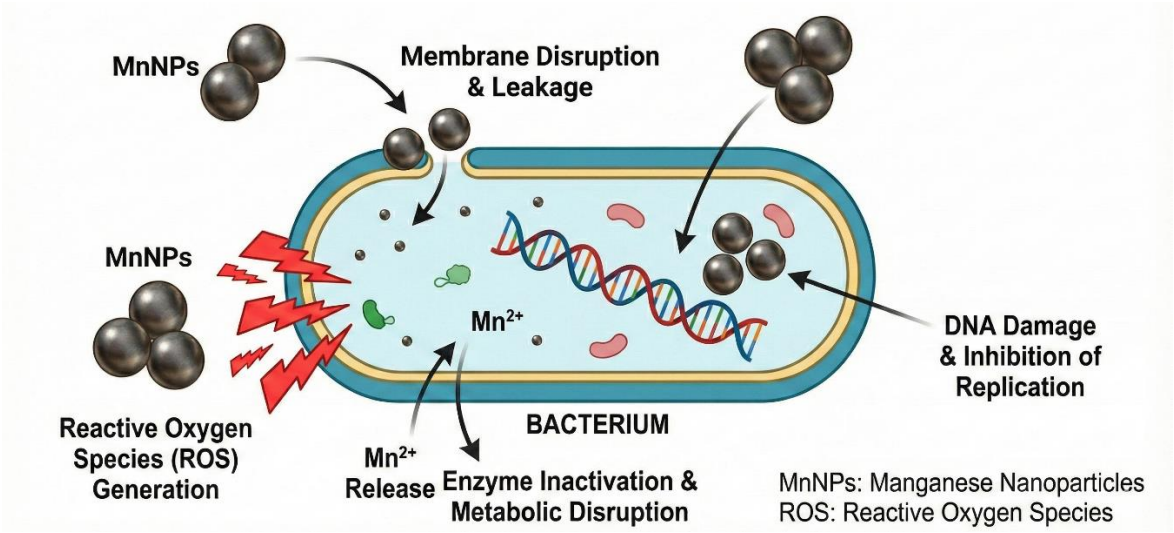

Figure 4: Mode of Antibacterial Action of Manganese Nanoparticles.

Their applications span magnetic resonance imaging (MRI), hyperthermia, and drug delivery. Doping magnetic nanoparticles with manganese can enhance their properties and safety profiles [41]. Specifically, manganese-based nanoplatforms offer multifunctional capabilities, including pH/reducing-responsive MRI, controlled drug delivery, photothermal and chemo dynamic therapy, and immunotherapy [42]. Research is also focused on creating biocompatible magneto-fluorescence nanoparticles for sensing of fluorescent and magnetic hyperthermia [43].

1.3.2 Synergistic Effects in Binary Nanoparticle Systems

MnZno nanocomposites are a hybrid system of nanoparticles whereby Mn ions are embedded in a Zno framework to obtain a hybrid structure with increased physicochemical and biological properties. Zno nanoparticles are suitable in this dual system with good antibacterial properties, UV absorption, and biocompatibility, whereas Mn doping brings other functionalities to this system, including better charge separation, increased ROS modulation, and better antioxidant properties. The reaction between Mn^{2+} and Zno modulates the bandgap, heightens surface defects and enhances the catalytic and biologic responses, leading to better antimicrobial, anti-inflammatory as well as tissue-regenerative outcomes than pure Zno. This bifunctional nanoparticle has enjoyed wide usage in biomedical field-related applications, such as wound healing, biosensing, and anticancer therapies, due to Mn being an efficient redox-active and Zn being a vital ion required in cellular repair. MnZno nanocomposites provide a combination of bioactivity, stability, and multifunctionality and, therefore, are an advanced, promising group of nanomaterials. [44-46]

1.4 Mechanistic Contributions of Nanomaterials to Wound Recovery:

Nanomaterials use their unique characteristics and functionalities to speed up wound healing. They have an influence on the wound-healing process via a number of important processes.

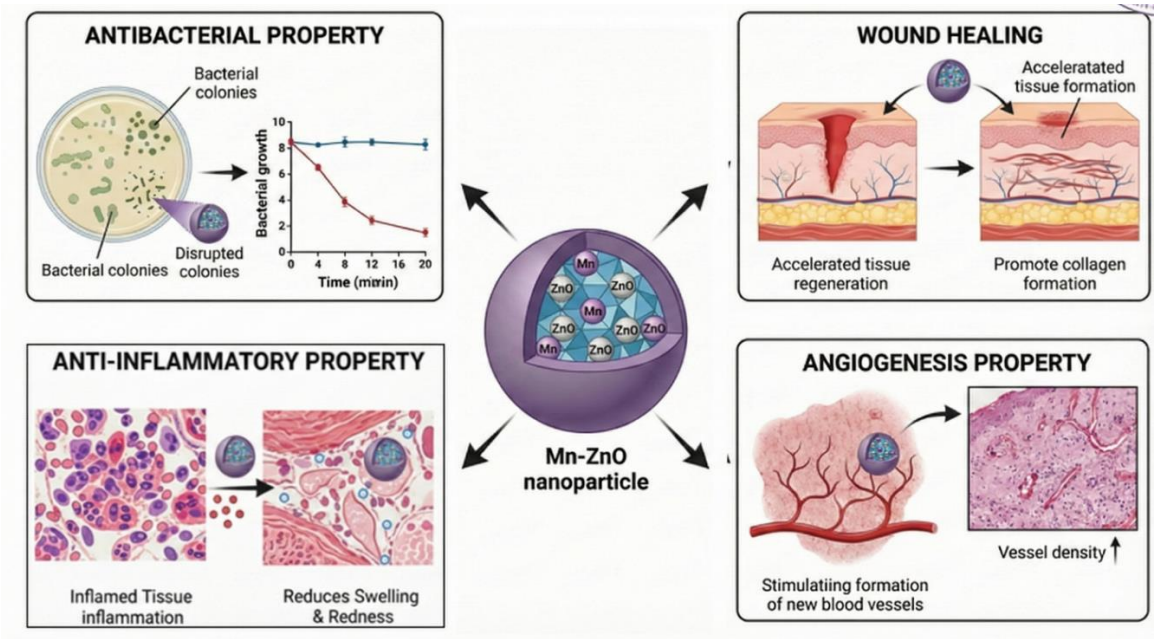

Figure 5: Overview of the therapeutic properties and biomedical applications of MnZno nanoparticles.

1.4.1 Antimicrobial Activity

The antimicrobial efficacy of (Mn) and (Zno), especially in nanoparticle form, has a long-term history (Zno is a proven broad-spectrum antibacterial agent), and Mn in most cases, is a dopant to amplify its effect. The impact of Zno nanoparticles on Gram-positive and negative bacteria can be summarized as the formation of reactive oxygen species, release of Zn^{2+} ions, and direct action on the membrane. Studies also reveal that Mn-doped Zno is capable of further improving this activity by boosting the generation of ROS and increasing ion release to generate more powerful antibacterial effects- namely, Gram-positive bacteria such as S. aureus and B. subtilis. However, Mn doping can also render cytotoxicity to the mammalian cells in such a way that Mn-doped Zno has been found to have improved antimicrobial activities; safety issues are important to consider in the actual practice. [47] Certain reactive oxygen species (ROS) are also generated by nanoparticles, e.g., cerium oxide. additionally inhibit the growth of microbes through oxidative stress. Nanomaterials have the capability to disperse biofilms that are commonly present in chronic diseases is disrupted. bacterial colonies, and decrease resistance. They also moderate the immune responses by a type of interaction with immune cells in the healing process[48].

1.4.2 Controlled and Sustained Drug Release

Nanomaterials provide a viable system of localized and managed drug delivery, directly to wound sites, therapeutic to wound sites, growth factors, and therapeutic agents. effects and reducing the systemic side effects [49]. Bioactive materials can be packed into a carrier like a dendrimer, liposome or polymeric nanoparticles to enable. to be delivered with specific and long-term release [50]. Also, the drugs are concealed against, these carriers preserve drug by means of environmental factors such as light, moisture or enzymes. stability and enhance shelf life. The poorly water-soluble medications are made more soluble by making them. It is possible to enhance their bioavailability and efficacy using nanomaterials. Particle size and surface charge may be varied to offer tailored release profiles that ensure sustained releases. therapeutic action and reduce the frequent dosing. Site-specific drug targeting of nanomaterials allows delivering it to wound settings. ligands (e.g., peptides or antibodies), which enhances efficacy and decreases toxicity.

Also, nanocarriers can be prepared by sequential release or synergistic release methods. can combination therapy, i.e. co-deliver many medications or agents [51]

1.4.3 Modulation of Inflammatory Responses

In various studies, Zinc oxide nanoparticles (Zno NPs) were found to exert anti-inflammatory effects, i.e., preventing the expression of inducible nitric oxide synthase (iNOS), COX-2, and pro-inflammatory cytokines in immune cells and inhibiting activation of signaling pathways, which include the NF-kB and JAK-STAT signaling pathway leading to the accumulation of nitric oxide [52]. With regards to Mn-containing nanomaterials, in a model of the macrophage, in which Zno-MnO_2 nanoparticles were substituted with MnO_2 NPs, the doped nanoparticles induced the production of inflammatory cytokines and ROS formation, but with a lower inflammatory activation (e.g., TNF-α) compared to pure MnO_2 NPs - indicating that Zno doping influences the inflammatory [53].

Some nanoparticles e.g., help keep redox balance in the wound microclimate by means of cerium oxide (CeO_2NPs). alteration of the levels of reactive oxygen species, which are involved in both. triggering and clearing of inflammation [54]. The synthesis of nanomaterials is also susceptible to nanomaterials. interacting with cellular receptors and pathways, and inflammatory mediators. ensuring a checked immune response. Moreover, nanomaterials help

in reducing fibroblast burning, deposition of extracellular matrix, and avoiding overabundance of collagen. accumulation and encouraging suitable tissue repair, so as to avert chronic fibrosis inflammation [55].

1.4.4 Promotion of Angiogenesis

Angiogenesis, which is a very necessary process in the formation of new blood vessels on effective wound. Nanomaterials can be used to fast the healing process. They encourage the migration, vessel formation, and tube formation of the endothelial cells in the wound site, which leads to. the development of the working vasculature. This tissue acceleration is brought about by improved vascularization. restoration and renewal through improvement of the nutrition and oxygen transportation. Nanomaterials are able to bind to surface receptors of cells and stimulate signaling pathways that regulate cell. Differentiation and migration through replication of the natural extracellular matrix (ECM). In particular, multifunctional nanoparticles activate integrin receptors, which enhance cellular Migration, Propagation, and cytoskeletal structure, among other responses. Furthermore, scaffold nanomaterials provide a beneficial three-dimensional framework to guide cell action. and accelerates the mending of wounds [56].

1.4.5 Challenges and Limitations of Nanoparticle-Based Based Treatments

Despite the positive effects shown in nanomaterials in the wound, there has been some negative effect. healing process, their excessive price remains a serious impediment to clinical application. Tactics such as the application of cheaper adjuvants, the development of composite can be employed to cut costs. substance, and the introduction of controlled or sustained drug delivery procedures (e.g., microneedles). Dosages can be reduced, and efficiency increased by being built up in layers (so-called assemblies). Even though a lot of studying is in vitro or on small animals such as mice and rats, they have very different skin. from human skin. Though pigs are a closer fit, they are expensive and complex their utilization. Due to its complexity, it is also difficult to fully understand the healing processes due to the lack of standard models of complex wounds.

Despite the growing use of nano materials in wound management, there is not much information about the molecular processes of its. actions, especially during the later stages of healing, such as the macrophage activity and not to mention other effects. signaling. These

processes are in need of more detailed research in order to improve therapies. Lessen the demerits [57]. It is taken into consideration that there are specific constraints in regard to the conventional. nanomaterials, there is a current trend of searching for new superior nanostructures. multifunctionality. One of them, Mxenes, is a relatively recent family of two-dimensional. The two-dimensional transition metal composed of carbides and nitrides have been very promising as a potential in biological uses.

1.5 Introduction to Mxene as a prominent 2D Nanomaterial

Mxene is a new nanostructure, a 2D that has attracted much attention in the field of biomedical. is used due to its special physicochemical properties. Mxene was first observed in 2011 at Drexel University.

Their overall formula is Mn +1AXn, in which M is an. A is an element (such as molybdenum, titanium, or vanadium) in early transition metals. X is carbon or nitrogen, and n is typically silicon or aluminum, group 13 or 14. They are normally obtained through selective etching of ternary in a layered form. MAX phases are termed as precursors. An element is lost in the etching process, forming multi-layered $Mn+1AX_n$ such that is frequently represented as Mn+1XnTx with surfaces ending in functional groups, e.g. oxygen, hydroxyl, fluorine or chlorine. (-F, -OH and -O). These surface endings confer hydrophilicity and are chemically tunable properties to Mxenes. The reactive property and versatile nature of Mxene are achieved. its surface terminations which have given it a spectacular material framework regarding biomedical and pharmaceutical uses [58]. Mxenes may be in the form of multilayer or. they are sheets that consist of a few layers and are accordion-shaped. They do not resemble other 2D materials. similar to graphene because of a special mixture of abundant surface chemistry, mechanical. ductility, enormous specific surface area, and electrical conductivity. Excellent Mxenes exhibit physicochemical, electrical, and electronic properties, among others. because of their high capacitance [volumetric], optical transparency, and antimicrobial property [59].

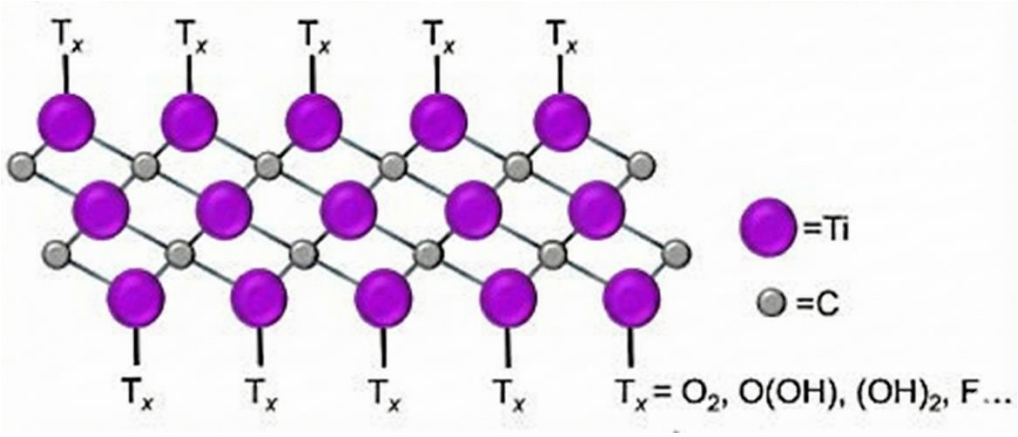

Figure 6: Layered Structure of Mxene nanosheet.

1.5.1 Structure Characteristics of Mxene

The phases are hexagonal layers composed of nearly tightly packed M, which are called the MAX phases separated by layers of A and X atoms, which are also in octahedral position on the inside. the M layers. MAX has strong covalent, ionic and metallic forces that hold M and X atoms together. phases, the M-A bonds are mostly metallic and weaker, so that they allow for selective. A layers are chemically etched to create Mxenes [60]. Mxenes are structurally built out of n+1 layers of transition metal atoms (M) arranged in a hexagonal lattice, between n layers of nitrogen or carbon atoms. Etching of the Mn +1Xn sheets. are accordion-like in appearance. In the case of the A element removal, 2D nanosheets are eliminated. prepared using surfaces that end with functional groups such as -O, -OH, -F or -Cl. These surface terminations are also commonly denoted by the notation $Mn+1X_nT_x$ where T is. to these endings on the surface. The hydrophilicity and chemical reactivity as well as the electrical. These surface groups has a very important role in shaping the features of Mxenes [61].

Mxenes exhibit different stacking sequences depending on n: ABAB stacking is. hexagonal in M_2X (n=1), face-centered cubic (ABC) stacking is more widespread. in M_3X_2 and M_4X_3 (n=2,3). The etched-out A layers separate the M-X layers which are formed. shared-edge octahedral (M_6X) units, which are similar to the rock-salt structure but arranged in 2D sheets. Selective etching produces conductive, strong, and flexible nanosheets by means of. removing M-A metallic ties and preserving M-X bonds, which are stronger [62].

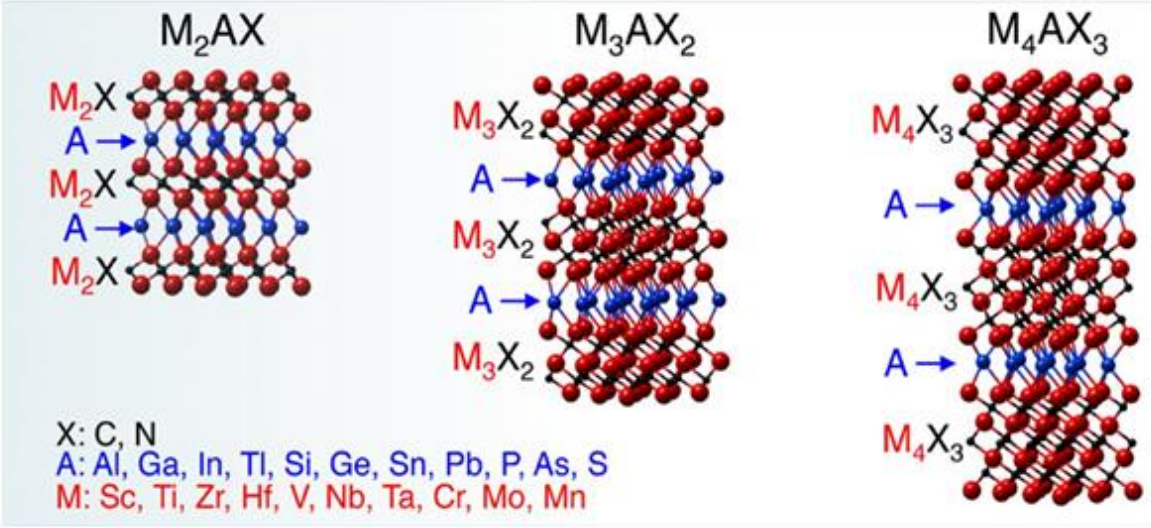

Figure 7: Schematics of M2AX, M3AX2, and M4AX3 crystal structures.

1.5.2 Functional Properties of Mxene

Mxenes have a high surface area, high metallic conductivity, and good mechanical properties, which make them more appropriate to use in optoelectronics, thermoelectric, and biomedical fields. Mxene has shown a good performance biocompatibility and a strong photothermal effect at near-infrared (NIR). That allows it to be broadly used in different biomedical applications including irradiation. biosensing, tumor therapy and tracer imaging. Mxene has anti-inflammatory activity, also shows good antibacterial property and has a great scavenging ability to reactive oxygen species (ROS). It may stimulate cell migration, adhesion and propagation, particularly of fibroblasts and keratinocytes, which are essential in wound. regeneration and wound repair. The anti-inflammatory properties of Mxene are also added. and improved by its good antibacterial property and excellent scavenging ability. oxygen species (ROS).

It has the capability to enhance cellular migration, adhesion and proliferation, particularly that of fibroblasts and keratinocytes, which show a key role in wound healing and tissue. regeneration. The material also encourages angiogenesis in order to accelerate the healing of tissues. and hemostasis. It can easily be chemically modified and its surface functional groups enable its chemical modifications. drug loading, which allows the controlled and stimuli-responsive discharge of therapeutic agents. Moreover, it has been shown that Mxene-based

nanomaterials could be used to regulate. immune reactions and make the wounds damp, which enhances the overall wound healing process. [63, 64].

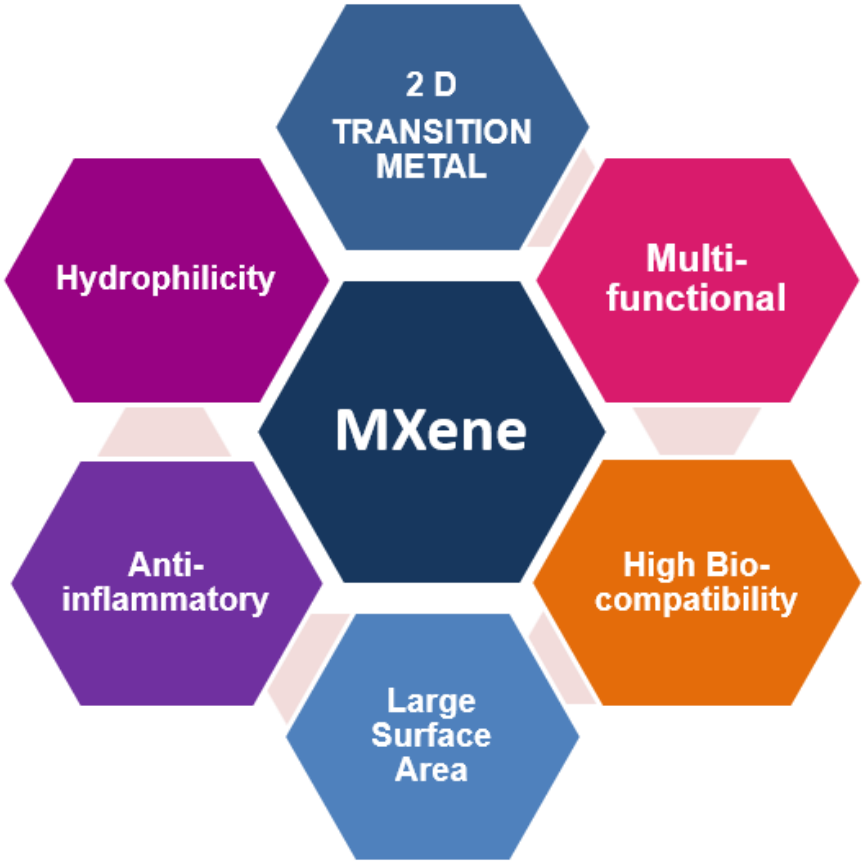

Figure 8:Illustration of the key physicochemical and biological properties of Mxene nanomaterials.

Mxenes with transition metals, e.g., titanium, tantalum, niobium, etc., have shown great physiological stability and biocompatibility in animal. studies without any adverse immunological or pathological effects [65]. They are applicable in producing hydrophilic composites that have high cytocompatibility and tissue adhesion due to their intrinsic hydrophilic and electronegative layer structures, that enable large water dispersibility and homogenous incorporation into aqueous-based. systems. Due to its increased hydrophilicity and processability as compared to other two-dimensional materials. Similar to graphene, Mxene is particularly favorable to be used in biomedical preparations [66]. It has many active sites, which also increases the ability to alter the materials and supply drugs.

The surface functional groups provide a means to bind to therapeutic agents, biological macromolecules and other matrices. Also, the electrical conductivity of Mxene, that may be adjusted between semiconductive and conductive by surface. modification, addresses a vast

collection of biomedical devices [67]. Mxene sharp nanosheets exhibit the mechanistic antibacterial properties that are manifested by their sharp edges. It damages bacterial membranes physically and chemically disrupting microbial cell wall materials by redox reactions. Its NIR absorption is also strong, which is why it can be expanded further. potential of diagnostic imaging and photothermal treatment, making Mxene a. flexible material platform for the next generation biomedical uses[68].

1.5.3 Mxenes in Antibacterial and Antimicrobial Applications

Three mechanisms can be used to explain the antibacterial action of Mxene:

(a) Direct mechanical damage of bacterial membranes by sharp boundaries of nanosheets,

(b) Generation of (ROS) like hydrogen peroxide and hydroxyl. radicals. (c) Photothermal inactivation by the generation of heat using light. Oxidative damage of bacterial proteins, DNA and membranes occurs as a consequence. generation of ROS caused by electrical properties of Mxenes. It's crucial to remember that ROS possess two faces: high levels of ROS may lead to necrosis and apoptosis whereas moderate levels can lead to autophagy. quantities are required to the immunological control and normal cellular activity. To reduce causing harm, regulation of the levels of ROS during the course of therapy is of paramount importance [69]. Other elements parameters that influence the antibacterial properties of Mxenes are the size of the flakes, surface charge, dispersibility, and optical properties. Smaller flakes have a high probability of penetrating bacterial cells. and sharper surface exposed. Whereas the negatively charged Mxenes may require surface. modification, positively charged Mxenes tend to react with the negatively charged bacterial membranes with greater success. Moreover, Mxenes are photothermal that facilitate the production of ROS, lead to protein and DNA damage, and enhance the UV-visible light absorption and conversion to heat on bacterial membranes which is a sign of permeability. [70, 71]

1.6 Development of Mxene-Based Nanocomposites

Layers restacking, which is an issue, may limit Mxenes application in a practical way. poor long-term stability, though of extraordinary qualities, which include oxidation, and good electrical conductivity, large surface area, and changeable surface chemistry. By addition of Mxenes with other materials, such as metal oxides, metal nanoparticles, polymer, etc.

and nanomaterials based on carbon, researchers have given greater focus on the development. To address these challenges and enhance their performance, Mxene-based composites in an attempt to do so functioning. Mxene composite materials have proven to be very promising wound materials. potential in healing due to their high level of biocompatibility, tunable surfaces and multifunctionality. These composites can be developed in order to treat wounds effectively. to possess such desirable properties as large porosity, biodegradability, and strong antibacterial. activity. Mxenes can regulate inflammatory reactions and promote significant healing. when added to wound, processes like cell migration, proliferation and differentiation can take place [72]. Chitosan is a biopolymer that has regenerative and antibacterial properties. was mixed with Mxene nanosheets to offer one of the first studies about Mxene-based. wound dressings. This composite was better biocompatible and more increased. Gram-positive and negative antibacterial activity, and hence, it is an antimicrobial. hopeful therapy in the healing of tissues and prevention of infections. Since then, several Mxene-based composites have been intended to be used as tissue engineering and wound dressing. applications [73]. Smart wound dressing has also been achieved using Mxene composites. that are able to measure such variables as pH, temperature, and humidity besides common indicators. dressings. These allow real-time wound evaluation and specific treatment. smart solutions. In addition, Mxene-based scaffolds have shown promise in. tissue regeneration due to their tremendous mechanical strength and ability to induce. tissue regeneration [74]. All in all, antimicrobial functions can be combined as a result of responsive functions. protection, and structural assistance, Mxene-based composites show much promise. to develop wound care technologies. The aim of the current research is to maximize them. effectiveness and explore their clinical relevance in the future possible therapeutic applications.

1.7 Biomedical Relevance of Mxene composite in Wound Treatment

The nanomaterials of Mxene have been found to possess an immense potential of enhancing natural properties of Mxenes to be used in the biological contexts. Such materials are especially effective in chronic wound treatment due to the ability to increase the wound sterilization, regulate the release of medications, as well as to change cytokine activity at the wound sites. The innovation increases the possibilities of wound management methods that

are available. The next are the applications in terms of which they enhance wound healing.

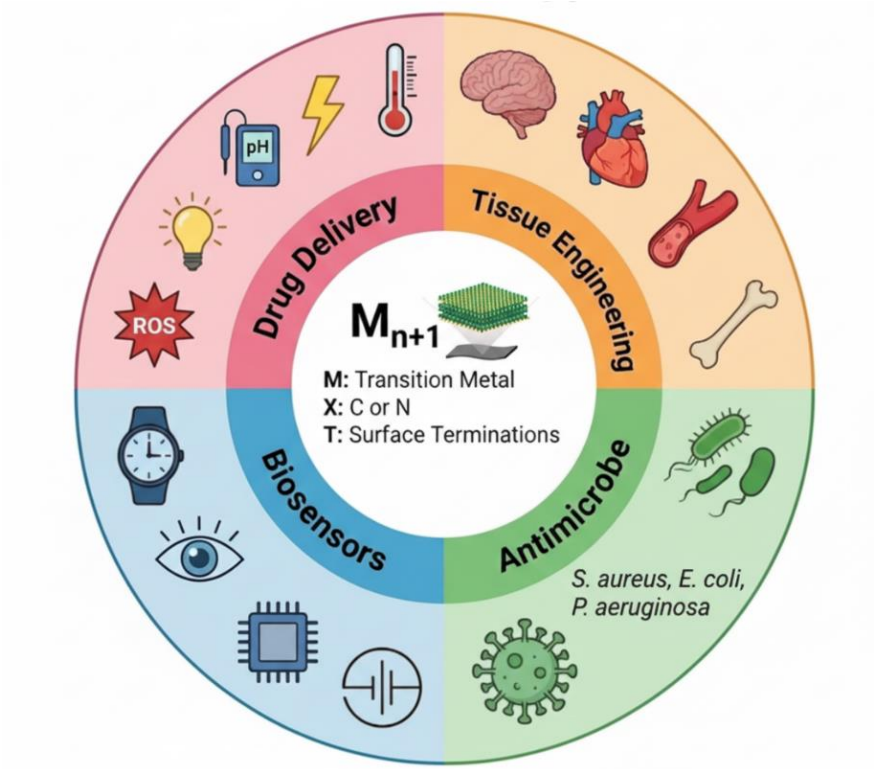

Figure 9: multifaceted biomedical applications of functionalized Mxene nanomaterials.

1.7.1 Mxene -Based Nanoparticles for Drug Delivery

Mxenes are the best to deliver a drug to a specific target and at a specific rate due to their unique properties. physicochemical characteristics. Via chemical bonding or physical adsorption, they may be loaded with medicinal substances such as medicines, proteins and nucleic acids. 20 large specific surface area. Besides enabling a more focused release of a longer period of time, the loaded chemicals on the target site and with such structural capacity, stability is assured throughout the process. storage [75]. Changing the surface functional groups, changing the spacing between layers or It is possible to fine tune the release behavior of by adding stimuli-responsive components. medications from Mxenes. As an example, pH responsive Mxenes are engineered to liberate. their cargo under acid conditions, typical of tumors and inflamed tissues, thus improving site-targeted therapeutic effect and reducing systemic side effects [76]

. Mxenes are also incorporated into an array of further to enhance their performance. delivery

systems, such as hydrogel, microneedles, and composite. Because Mxene-based hydrogels offer an ideal alternative with regard to their biocompatibility and high absorption. wound healing atmosphere. These hydrogels decide angiogenesis which is essential in. cell regeneration, promote cell growth, and permit progressive and controlled. medication release. In addition, Mxenes enhance mechanical properties of. hydrogels, including elasticity and rigidity that play an important role in wound covering, etc. protection [77, 78]. PDGF (platelet-derived growth factor) had better tissue regeneration and faster. wound healing. Equally, when loaded with magnetic Mxene colloids when wrapped. in the case of Ag nanoparticles, a two-network hydrogel was formed consisting of poly(N-isopropyl. acryl amide) and alginate exhibited a temperature-dependent release upon exposure to NIR light. The contraction of the hydrogel occurs when it is heated above the lower critical solution. The controlled release of silver nanoparticles (Ag NPs) by means of temperature (LCST) predetermines that. aids in wound healing [79, 80]. Mxene has electrical conductivity which adds to the angiogenesis also in promotion. Ti_3C_2Tx (Mxene) and polyaniline (PANI) can be used as an example. implanted in a hydrogel of polyvinyl alcohol (PVA) provided conductivity and structural strength. Mxene stimulated the growth of blood vessels, deposition of collagen, and antibacterial action besides photothermal action of the hydrogel which increased. temperature and also aided in the release of drugs, under near-infrared exposure [81].

1.7.2 Applications in Tissue Regeneration

The use of Mxene-composites has attracted significant interest in tissue regeneration. because of its remarkable amalgamation of the mechanical strength, superb electrical conduction, ultrathin arrangement, and surface adjustability. Mxene-based composites have attracted much attention to the issue of tissue regeneration. They are ideal candidates because of their characteristics that can be used in scaffolds in the development of tissues. technology and hi-tech dressings. Besides support physical cell, Mxenes, when incorporated in hydrogels or porous scaffold mechanisms, generate. a bioactive environment which supports essential regeneration mechanisms like cell adhesion, migration, proliferation, and differentiation. By modifying cellular reactions and promoting. angiogenesis or the formation of new blood vessels, electrical stimulation of the wound site. has been shown to accelerate tissue regeneration in a dramatic way. This is one of the main benefits of Mxenes [82]. For example,

Ti_3C_2Tx (Mxene) and bacterial cellulose (rBC) were applied by Mao et al. to form a composite hydrogel which demonstrated an outstanding level of flexibility, conductivity, and biodegradability. The healing of was enhanced by this rBC/Mxene hydrogel. On rats when used in full-thickness skin lesions is more effective than when using traditional Tegaderm films. applied together with external electrical stimulation [83].

In another example, Scaffolds of HPEM were produced by researchers via the combination of Mxene nanosheets polluted with polydopamine. polyglycerol-ethylene amine and treated them with oxidized hyaluronic acid. In addition to the encouragement of tissue adhesion and proliferation of cells, these scaffolds also enhanced gene expression. associated with collagen III, muscle actin, and vascular endothelial growth factor (VEGF), which enhanced tissue regeneration and angiogenesis [84]. Moreover, the HPEM scaffolds significantly improved patient recovery and reduced infection in an MRSA model. infected wounds. It has been shown that Mxene composites and photothermal, as well. The two approaches are complementary to one another. In the presence of the near-infrared (NIR) light, they can. generate localized heat which stimulates collagen synthesis, fibroblast proliferation, and tissue. remodeling. These examples demonstrate the multiple applications of the Mxene-based materials. regeneration of support tissues [85].

1.7.3 Anti-inflammatory Functionalities

Mxenes have great anti-inflammatory capabilities and can therefore be used effectively. promoting tissue regeneration and wound healing. Inflammation is a natural occurrence, although it is not at its best response to injury; overreacting or taking long to respond to injury may slow recovery. By inhibiting the secretion of pro-inflammatory cytokines and chemokines, Mxenes such as Ti_3C_2Tx and TiN modulate this response and offer a more balanced immunological situation that promotes healing. The ability to influence macrophage polarization (cell change). the conversion of the pro-inflammatory M1 to the tissue-repairing M2 is a crucial process [86, 87]. As an example, Li et al. designed a hydrogel injectable constructed of. polydopamine-coated Ti_3C_2Tx Mxene and dopamine grafted hyaluronic acid which had high potency as an anti-inflammatory agent through reactive oxygen and nitrogen species scavenging and stimulating M2 macrophage polarization.

This formula is used in diabetic wound models. enhanced cell migration and re-

epithelialization and at the same time reduced oxidative stress [88]. Similarly, Nb2C Mxene hydrogel exhibited efficient ROS. cell injury reduction, less tissue injury, and faster healing through increased angiogenesis and collagen deposition [89]. Also, a hydrogel made of poly(acrylamide) includes. Mxene was found to have a 96% ROS scavenging rate which was attributed to the Mxene. electron transferring properties and antioxidant polymer chains. Using a gelatin-based another study showed antibacterial and anti-inflammatory properties when it came to the Mxene@TiO2 hydrogel implanted. This was caused by the photothermal stimulation and ROS reduction. the wound shifts to a proliferative stage, as opposed to an inflammatory one [90]. These examples demonstrate that Mxene materials have great potential to treat chronic and infectious diseases. wounds because they not only alleviate harmful inflammation, but also stimulate the. biological processes involved in effective tissue regeneration.

1.7.4 Supports of Hemostatic processes

Mxenes have great potential in improving wound treatment and bleeding management. due to their outstanding hemostatic quality. Their individual physical and chemical. The porous design and immense specific surface area of the properties permit it. to achieve rapid absorption and entrapment of blood constituents such as fibrinogen, platelets, etc. and red blood cells. Besides helping to concentrate the components of blood quickly. their aggregation is also accelerated by this connected porosity structure at the place of damage. The Mxenes, that is, substantially charged on the surface, which promotes platelet activation and enhances a large contributing donor to their hemostatic activity, is cell adhesion. This activates the coagulation cascade successfully and produces a rapid hemostasis through the formation of a stable clot[91, 92]. Moreover, the surface chemistry of Mxenes can also be adjusted to be better. their action of interacting with the blood components. To enhance platelet adherence and stimulate. activation of clotting factors, such as functional groups as carboxyl and amine, may be added. For example, Mxene@polydopamine (PDA)-decorated chitosan nanofiber dressing displays improved platelet and blood cell adhesion in vitro and in vivo. This impact was ascribed with the hydroxyl groups of PDA, which were numerous and permitted a powerful affinity towards blood. components as well as, on contact with the plasma fibrin, was successful in causing of the. development of a clot [93].

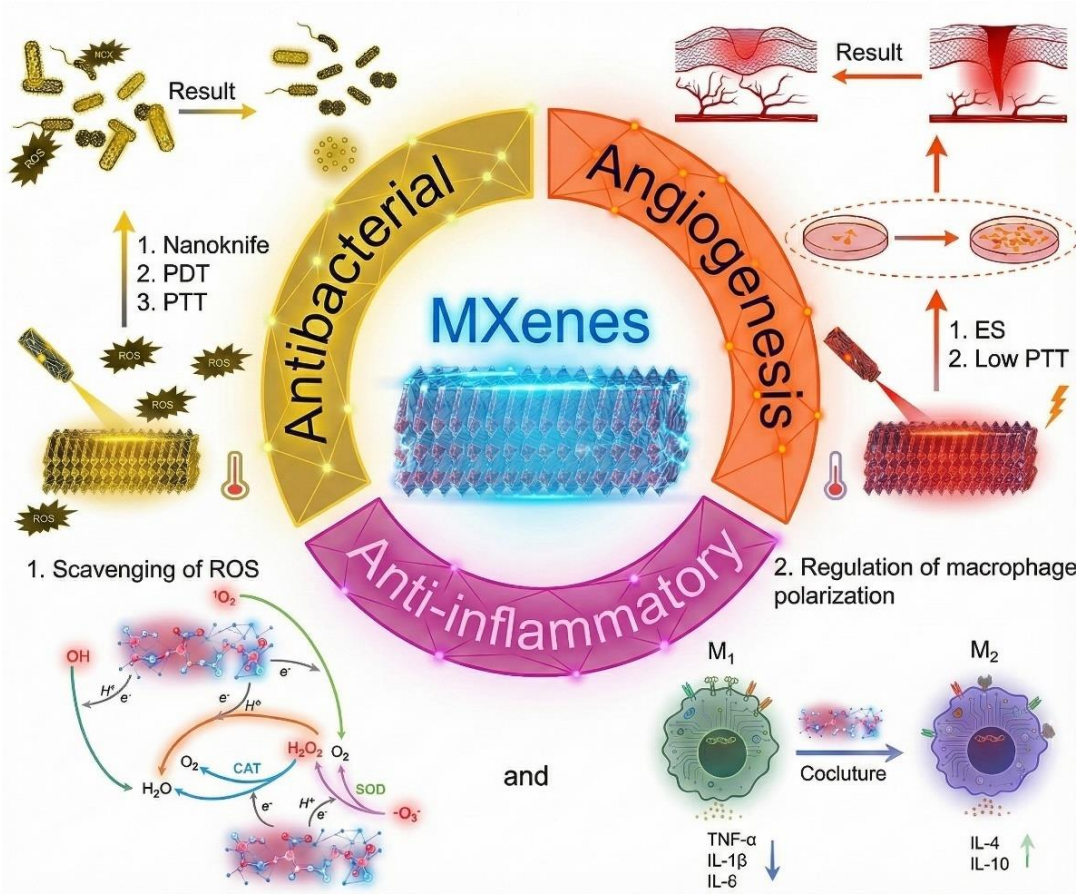

Figure 10: Multifaceted role of Mxenes in promoting wound healing

More so, Mxene-based composite scaffolds have. has exhibited multifunctionality with the ability to regenerate, be hemostatic and antimicrobial. qualities. A polydopamine polycaprolactone (PCL) electrospun scaffold. such as coated Mxene/Ag_3PO_4 bio heterojunctions (MX@AgP bio-HJs) is one notable example. This scaffold generated Ag^+ ions when responding to near-infrared (NIR) light, which had a. strong antibacterial effect and also promoted the healing of tissue and blood coagulation. The polydopamine layer is a nanofibrous membrane that is photothermally controlled. effectively reduced bleeding, lowered the chance of infection, and favored the deposition. of collagen and epithelial tissue, the result of which was a favorable environment in wound healing, as is found in vivo [94]. Overall, Mxenes promote activation of platelets, aggregation of blood cells, and stable clotting due to their high potential. it has a surface charge, a high surface area, and a chemically modifiable surface. This allows for quick hemostasis. Their multitasking nature, together with other characteristics such as antibacterial activity. and tissue adhesion, enables

Mxenes to be a versatile platform in controlling bleeding. and supplementing wound healing and wound regeneration.

1.8 MnZno@Mxene Nanocomposite in Biomedical Applications

The present research is aimed at the creation of an innovative bioactive MnZno@Mxene nanostructure to meet the increasing need of the multifunctional therapeutic agents that can overcome the complicated issues of wound healing. The manganese- and zinc-doped zinc oxide (MnZno) nanoparticles were chosen purposefully with a 2D Mxene platform of complementary biological functions of each. Zn^{2+} ions stimulate angiogenesis, increase cell proliferation, and help to become antibacterial, Mn^{2+} ions have potent antioxidant activity, regulate inflammation, and aid tissue regeneration. The Zno matrix provides high antimicrobial activity and can stabilize the balance of ROS, which is necessary to ensure good healing.

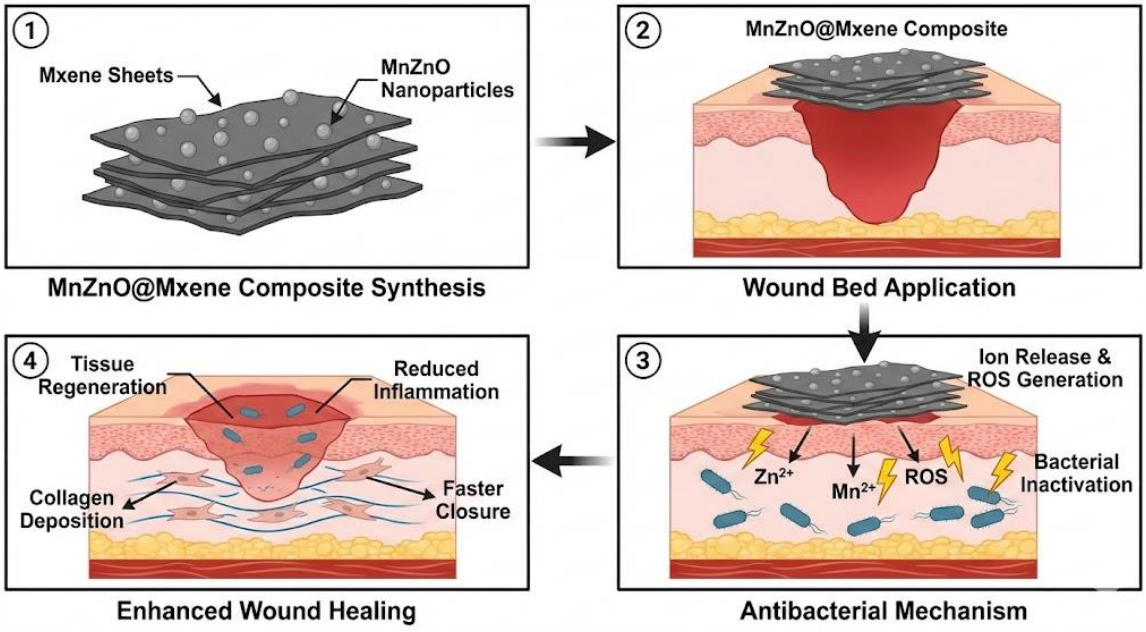

Figure 11: Schematic illustration of the biomedical application of the MnZno@Mxene composite antibacterial activity and enhance wound healing.

Mxene is a stable, biomedical, and highly conductive carrier with a large surface area and hydrophilic surface that enhances the dispersion of nanoparticles, their interaction with the body, and controlled ion release. The MnZno, collectively in the form of MnZno@Mxene, is designed together to exhibit combined antibacterial, antioxidant, anti-inflammatory, and pro-angiogenic properties-essential mechanisms in wound repair which are fast and

complete. Even though there are applications of individual nanomaterials within wound healing, no studies have been performed to combine MnZno and Mxene, and combining these materials is a promising approach to developing advanced nanomedicine. The proposed work will address the shortcomings of traditional therapies, such as drug resistance and insufficient healing conditions, and synthesize and characterize a multifunctional hybrid material and assess its antibacterial, antioxidant, and tissue-regenerative activity to achieve better wound healing.

Chapter 2
Literature Review

The modern biomedical research has been working on the production of materials that will benefit. in both the natural curing of wounds and in dealing with clinical outcomes. with bacterial infections and chronic inflammation. Researchers have been in recent years; they have been investigating a great variety of nanomaterials to enhance wound healing. their interaction at the cellular level with biological systems and adjustable makes them. physicochemical characteristics. It is best to start with a baseline of understanding of skin architecture. and wound healing processes, in this literature review, the researcher tries to explore significant. discoveries in the area. It subsequently describes the deficiencies of the existing. therapies. It then evaluates the role of nanotechnology in terms of metal and metal oxide. Nanoparticles, which is also known as nanoparticles, is being utilized more and more to facilitate therapeutic outcomes. Additionally, new types of materials, such as Mxenes, are studied concerning their characteristics, structural. attributes, and possible uses in medicine. Old single, dual, and hybrid. Particular attention is paid to nanocomposite systems that have the ability to cure wounds. Besides stating research needs nowadays, this critical analysis of the body of research also points out the existing gaps in the body of research. The experimental approach to this will be based on literature that will provide the background information. work.

The article by Khan et al. (2017) examines the manganese-doped zinc oxide nanoparticles and indicates that the incorporation of Mn alters the structural and optical characteristics of Zno and increases antimicrobial activity. Their study is consistent with previous research showing that Zno nanoparticles has its mechanism of action through ROS generation, Zn^{2+} release, and damage of membrane and that transition-metal doping can enhance these effects by modifying defect structures and band-gap behavior. They verified the successful Mn substitution using XRD, SEM/TEM, EDX and UV-Vis and attributed these alterations to enhanced biological performance.The necessity of conducting more mechanistic research and thorough cytotoxicity analyses to guarantee safe biomedical use of doped Zno nanoparticles is also mentioned in the literature [45].

Davidson et al. (2023) designed chitosan nanovesicles containing bioactive Mn (Chi-Mn)

that combines the positive wound-healing properties of chitosan and the multi-functional properties of manganese ions. Their paper demonstrates evidence of proof-of-concept that Chi-Mn has sustained antioxidant activity, a broad-spectrum antimicrobial effect (against E. coli and P. aeruginosa), compatibility with traditional antibiotics, and compatibility with key skin cells, including fibroblasts and macrophages. This study is an excellent prospective in creating a multi-functional wound-healing formula, which tackles infection, oxidative stress, and tissue regeneration in one system. Their results are consistent with previous literature that indicates the increasing interest in metal-ion-loaded nanomaterials as wound repair agents, and they show that the surface integration of the biological benefits of chitosan with the bioactivity of manganese presents a viable platform of future wound-healing preparations [95]. Wu et al. (2021) invented manganese-doped calcium silicate (MCS) nanowires composite hydrogels that could be used to treat melanoma and ensure wound healing. The inclusion of Mn gave it superb photothermal qualities where tumor destruction in the case of near-infrared radiation was made possible. The therapeutic Si and Mn ions also leached out of the hydrogels which promoted angiogenesis, improved cell migration, and tissue regeneration. The hydrogel matrix was based on alginate, which enhanced biocompatibility and provided the ability to regulate ion delivery. In animal models, the material had a high tumor-killing effect as well as wound healing. In general, the paper provides a theragnostic biomaterial with multiple functions that can be used to combine cancer therapy and skin repair [96].

The paper by Popescu et al. (2020) examined surfactant-modified manganese-doped zinc oxide (Mn-Zno) nanoparticles and their impacts on ROS generation and DNA, on the murine fibroblast cells. They demonstrated that the type of surfactant and Mn doping affected the morphology, size, surface area and Mn incorporation of the particles, which affected the cellular responses. Smaller and highly surface-area particles generated a larger amount of ROS and viably destroyed more DNA whereas higher levels of Mn doping diminished the oxidative stress and genotoxicity implying a protective effect of Mn. XRD was used to determine the crystal structure of the nanoparticles, morphology and elemental composition of the nanoparticles were determined by TEM/SEM and EDX respectively, and surface area was determined by BET. Their results also emphasize that the optimal functionality of nanoparticles can be achieved by controlling the synthesis of Mn-Zno nanoparticles at the expense of biocompatibility offering a future of safer biomedical

applications [97]. Yin et al. (2024) examined the impact of adding iron (Fe), cobalt (Co), and manganese (Mn) to zinc oxide (Zno) nanoparticles on their antimicrobial properties and cytotoxicity. They prepared nanoparticles with different types of dopants, concentrations as well as calcifications and characterized them through methods like XRD, SEM/TEM and surface area analysis. Mn- and Co-doped Zno had greater antibacterial capabilities against E. coli although Mn-doped particles were more cytotoxic to mammalian cells. The research has shown that the production of ROS and the release of Zn^{2+} ion are the most important factors leading to antimicrobial effects and toxicity. Altogether, Co-doped Zno at the optimal doping concentration provided a good compromise between potent antibacterial properties and less toxicity to cells, which could be used in biomedical applications [47].

Gnanasekar et al. prepared manganese-doped zinc oxide (Mn-Zno) nanoparticles and used them as bioactive nano coatings on titanium scaffolds to enhance the antimicrobial and regenerative properties. They verified the successful incorporation of Mn into the Zno lattice and even deposition of the metal on the Ti surface using TEM, SEM, RBS and EDX analyses. Mn-Zno/Ti biomaterials had high antibacterial efficacy with more than 80 percent inhibition against Staphylococcus aureus and significant decrease of Pseudomonas aeruginosa. At the same time, the coated scaffolds demonstrated excellent cytocompatibility with the human fetal osteoblast cells and a pronounced stimulation of the osteogenic markers of ALP, IBSP, and SPARC. Their results, in general, prove that Mn-doped Zno coatings are effective combinations of antimicrobial protection and osteogenic stimulation, and therefore, can be considered viable applications in bone-related regenerative medicine [98]. Alam et al. (2022) prepared manganese-doped zinc (Mn-Zn) nanoparticles with the help of the Carica papaya leaf extract, which is an economical and environmentally responsible green synthesis pathway. The XRD, SEM, EDX and DLS characterization demonstrated a nanosheet-like morphology, a crystallite size of approximately 19 nm, the successful incorporation of Mn and Zn and good colloidal stability with a negative surface charge. The nanoparticles were found to have a good antioxidant capacity in various tests, which shows that they have the potential to scavenge free radicals. They were also found to be very efficient in the pathogenicide effect on Salmonella typhi, E. coli, S. aureus and Klebsiella pneumoniae with the maximum effect being on S. typhi.

Also, the Mn-Zn nanoparticles exhibited good catalytic activity, had the ability to degrade dyes including Eriochrome black T, methyl red and methyl orange and also reduce p-nitrophenol to p-aminophenol. In general, it is important to note that the research identifies the multifunctional character of phyto-synthesized Mn-Zn nanoparticles that may find application in the spheres of catalysis, wastewater treatment, and biomedicine [99].

Haque et al. (2021) have also conducted a review of manganese-based advanced nanoparticles and highlighted their increasing role in biomedical applications in terms of Mn redox activity, nanozyme-like enzyme-mimicking behavior, and responsiveness to diseased microenvironments. They explain, how the Mn nanoparticles can control the reactive oxygen species, release Mn^{2+} in acidic or glutathione rich conditions to achieve better T1 MRI imaging, and regulate drug delivery making it useful in cancer treatment, in antimicrobial therapy, and in regenerative medicine. Other issues that are brought out in the review are the possibility of Mn-related toxicity, the uncertainty of long-term biodistribution, and the necessity of standardized synthesis and safety testing. On the whole, the authors make manganese-based nanomaterials one of the most promising that still needs to be optimized prior to clinical translation [39].

Jiang et al. (2024) came up with hybrid manganese dioxide-gold (MnO2-Au) nanoflowers impregnated into a hydrogel dressing to manage diabetic wounds by excessive reactive oxygen species (ROS). The MnO2 component is a nanozyme, catalystically disproving H 2 O 2 and ROS scavenging, whereas the gold increases stability and bio-compatibility to nanoparticles. The hydrogel promoted in vitro migration and collagen expression of fibroblasts and in vivo, the hydrogel had a significant effect on promoting wound healing and tissue regeneration in a diabetic rodent model. Detailed characterization was used to verify the structure of nanoparticles, elemental composition and the ability to release Mn^{2+} in a sustained manner. As the research shows, MnO2-Au nanoflower hydrogels provide a versatile platform, ROS-scavenging and pro-regenerative, to diabetic wound healing, although the authors state that additional long-term safety, biodistribution, and comparative studies are necessary before the implementation of the system [100]

Jiang et al. (2024) prepared a nanocomposite of Mxene and M2 macrophage. derived exosomes (FM-Exo) to assist diabetic wounds to heal. The immune high glucose suppression leads to hard to heal wounds and it augments them. the danger of being

infected, underdevelopment of blood vessels, and inflammation. The FM Exo nanocomposite was effective in antibacterial effect and generated exosomes. consistently for a week. FM-Exo induced macrophages to move in high-glucose environments. conversion into M2 state that promotes healing by activating an important cellular process. repair signaling pathway. This enhanced the growth of blood vessels and fibroblasts. FM-Exo improved collagen organization, reduced inflammation, elevated VEGF levels to a minimum. stimulates development of blood vessels, faster healing and reduced scarring in diabetic. mice [101].

Gao et al. (2025) made a tissue-adhesive hydrogel that was made of Mxene and deferoxamine. Multidrug-resistant diabetic wound microspheres loaded with (DFO) to heal wounds. (MDR) bacteria. The hydrogel showed excellent mechanical strength, powerful. Good biocompatibility, biodegradability and tissue adhesion after it has been made out of a strong crosslinking methodology. Mxene when subjected to near-infrared (NIR) light. produced heat that was effective in killing bacteria such as P. aeruginosa and MRSA and helped. in the quick degradation of bacterial biofilms. In the meantime, DFO was slowly set at liberty. and stimulates the formation of new blood vessels in the hydrogel and assists in angiogenesis. As the hydrogel created removed hazardous reactive oxygen species (ROS), it also helped in the reduction of inflammation. n laboratory studies, it induced tube. cell migration and formation; in animal models, it increased wound healing more. more effectively than possibly commercial dressings. The antibacterial and strength of this hydrogel make it combined. resistant to oxidation, and promotion of angiogenesis is an efficient but simple one. efficient way of treating infected diabetic lesions [102].

Hu et al. (2024) interacted sodium alginate, agar, Mxene (Ti_3C_2Tx), and zinc ions to form. a new hydrogel dressing (MSG-Zn^{2+}) to treat infected wounds. Because of the synergies between the antibacterial properties of zinc and photothermal heating properties of Mxene, the hydrogel was shown to be strong in antibacterial activity. When subjected to near-infrared. The Mxene is then rapidly heated by (NIR) light, and the heat, when added to the zinc ions, reacts to form zinc oxide. it releases, and is able to kill E. coli and S. aureus effectively. Moreover, Zn^{2+} is used to support the hydrogel. good bacterial adherence enhancing sterilizing. Other than having antibacterial effects, the hydrogel proved to be highly biocompatible to cell experiments and promoted. cell migration, that assisted in wound healing. It is suitable to clinical use. it exhibits a high swelling capacity, is

hydrophilic and can be readily and cheaply manufactured. The hydrogel structure allows easy use, as well as fit well on the surfaces of. wounds. Considering everything mentioned, MSG-Zn^{2+} hydrogel is a cheap and versatile one. wound healing and prevention of bacterial infection method [103].

Sang et al. (2024) developed a near-infrared (NIR) sensitive NIR-sensitive hydrogel composed of Zno quantum. dots (QDs) were used to coat Mxene (Zno-Ti3C2@H) and aid the recovery of spinal cord injury (SCI). The hydrogel reduces the harmful reactive oxygen species (ROS) in the mitochondria. allows free zinc ions to be released at the level of injury. With up to 80% effectiveness, the Zno-TiC2 nanozyme removes ROS, which induces neuron and blood vessels healing, lowering the death of nerve cells, and repairing mitochondrial activity. The hydrogel heats the damaged location up to 42.9degC with exposure to NIR, enhancing the blood circulation and bringing Zn^{2+} to the desired location. Treated animal models were also found to have increased motor activity. recommend functional recovery. Also, the substance enhanced protein expression. part in the formation of nerves and vessels. This multipurpose and biocompatible. platform offers a promising, low-toxicity method of successful SCI therapy [104].

Li et al. (2023) researched the regenerative properties of Mxene nanosheets in skeletal. muscle restoration had been studied and emphasized their bioactivity of tissue regulation. oxidative stress, regeneration and inflammation. Ti3C2Tx Mxene that possesses unique. Antioxidative and anti-inflammatory and photoelectromagnetic properties, was evaluated in terms of antioxidative, anti-inflammatory, and myogenic actions in vitro and in vivo. Mxene is successful in the scavenging of reactive oxygen. species (ROS), reducing oxidative injury in macrophages and promoting a shift. between pro-inflammatory M1 and anti-inflammatory M2 macrophages. According to in vitro Mxene suppressed inflammatory markers such as TNF-a and IL-1b and reduced them. increasing the expression of myogenic genes such as MyoD, MyoG and MHC to favor myoblast. development. Besides, Mxene stimulated angiogenesis by activating the migration, Proliferation, and differentiation of vascular tubes of endothelial cells, and by increasing. the busheling of the angiogenic markers ANG and VEGF. All of these factors worked jointly to stimulate the vascular net development and production of myotubes. When Mxene was used in vivo on defects in tibialis anterior muscle rat, it enhanced muscle fibers. vascularization and production, its ability to regenerate is proven [105].

Wu et al. (2024) developed a photo responsive hydrogel system that is smart to promote osteo. vascularization and overcome the issue of big bone defects fixation. Ti_3C_2Tx Mxene nanosheets that are grafted with polydopamine (MP) and acidic fibroblast growth factor. The implantation of (aFGF) in a hydroxypropyl chitosan/gelatin (HG) matrix is done to create the. hydrogel (HG/MPa). This designed system enables by responding to near-infrared (NIR) light. in the on-demand synthesis of aFGF and mild heat stimulation, both of which are functional in conjunction in favor of angiogenesis and bone tissue regeneration. The NIR-triggered release elevates aFGF action in the wound location, and this initiates the rapid production of blood. vessels.At the intermittent exposure to NIR, HG/MPa facilitates angiogenesis and osteogenic. differentiation in vitro and cell adhesion, cell proliferation and migration. It competently recruits endogenous stem cells and enhances the expression of markers associated to angiogenesis and osteogenesis. The hydrogel was confirmed in animal models. stimulates the formation of new bone, promotes formation of solid vascular. networks, and promotes the repair of bone defects of critical sizes [106].

Cheng et al. (2023) designed the TTZM hydrogel, which is a hydrogel wound dressing based on. modified oxidized bacterial cellulose (TBC) with Mxene and tannic acid coated metal. organic frameworks (TA@ZIF-8). This is especially true in the near-infrared (808 nm). this compound dressing, which was composed of light, was found to be highly antibacterial. Effective bacterial $Zn^{2+,}$ together with Mxene produced eradication, which inhibited. metabolism of bacteria and ruptured walls. The hydrogel increases wound healing by atherosclerosis and vascular maturation. It supported in vitro killing of S. aureus and E. coli and healthy cell growth. Studies conducted in vivo confirmed that infected wounds recover and regenerate faster. In addition to being The hydrogel was easy since it was biocompatible and possessed heat-reactive antibacterial characteristics. to make [107].

A freeze-drying method of in situ synthesis was used by Zhang et al. (2025). To form Mxene nanosheets that are silver nanoparticles (AgNPs) and bacterial cellulose (BC). a multi-purpose wound treatment sponge. Large porosity, fluid uptake, and better. The final BCP-MAg composite has photothermal and antibacterial properties. sponge. It kills bacteria such as S. aureus and E. coli and prevents bleeding to a great extent in 36 seconds. It decreases the levels of toxic proteins and thus lowers inflammation in the process. stimulates the formation of skin layers, collagen and new tissue and helps in the healing

process. On the seventh day, the sponge had covered 83.7 percent of the wounds on the rat models. Also, it was shown to be compatible with organs, blood, and cells. Because it has these properties, it can be a potentially useful all-in-one wound care substance. can be applied to control bleeding, infection and aid in tissue restoration [108].

Ou et al. (2025) developed a multifunctional nanocomposite hydrogel (KC@PF@TA). order to manage chronic diabetic wounds. This hydrogel is made with the use of paeoniflorin (PF). tissue regeneration, Mxene (Ti_3C_2Tx), and silver have strong antibacterial and photothermal properties. To enhance mechanical power, the conversion of heat below. The material was optimized in terms of near-infrared light and safe cell interaction. In the laboratory it accelerates wound healing and was tested on experiments with diabetic animal models who had wounds, reduced inflammation, lysed bacteria and stimulated tissue regeneration. These PF facilitated effects and stimulated cell migration and proliferation. Besides, the safety and biodegradability of the hydrogel were determined. Despite having proven itself safe in preclinical trials, further research is needed to determine its safety over the long term. greater performance of animals, and response to environmental factors such as pH and temperature. It is all said and done that the hydrogel possesses tremendous potential in terms of future therapy of. hard-to-treat diabetic wounds [109].

Li et al. (2024) discussed whether Mxenes can be used as the future of tissue materials. wound healing and engineering. Mxenes possess anti-bacterial, anti-inflammatory, and antioxidant properties due to their 2-dimensional structure and outstanding. physicochemical characteristics. They are very suitable in biomedical applications. due to these attributes especially in skin restoration. The incorporation of Mxenes This is underlined in terms of into wound dressings and their implication on the enhancement in healing outcomes. study. Mxenes assist in reducing the microbial infections, inflammation control and encouraging tissue repair. Their controlled release and drug loading are achievable. large surface area and surface functions. It has been found that they are compatible according to the latest research. contain skin cells and enhance cell adhesion and cell growth. The multifunctionality of The authors highlight Mxenes as a major advantage in comparison with conventional materials [110].

Cheng et al. (2023) designed three 2D-2D composite membranes made of Mxene: GO@Mxene, O-g-C3N4@Mxene and BiOCl@Mxene on a polyethersulfone (PES).

substrate. These have been developed to enhance the antibacterial and the separating properties of water purification. qualities. Better antibacterial activity was exhibited in S. aureus and E. coli. by all modified membranes. The best bacteriostatic rate was exhibited by the M4 BiOCl@Mxene membrane 50 per cent E. coli and 82.4 per cent S. aureus. SEM imaging revealed reduced membranes on comparison with pure Mxene that had been modified. density of microorganisms. The membranes showed a separation efficiency of dyes with a value of less than. There is 67% on top of their antibacterial properties. Also, the composite membranes. performed better than unmodified Mxene in their resistance to biofouling. The additional improvements were eventually brought about by 2D materials, which had synergies. This work proposes another way of reducing biological contamination in membrane technology [111].

The paper by Liu et al. (2022) developed a versatile and adaptable hydrogel of polyvinyl alcohol. To enhance skin wound healing, (PVA), Mxene (Ti3C2Tx), and polyaniline (PANI) were incorporated. The Mxene increased the strength of the hydrogel when it was stimulated by near-infrared (NIR) light. and provided antibacterial properties. The polyaniline improved the structure of the hydrogel and was used as an electrical material. The mixture resulted in a strong hydrogel. antibacterial quality, high strength in terms of mechanics and excellent conductivity. According to studies have been carried out on lab and animal models, the hydrogel can kill. helpful bacteria, facilitate the proliferation and migration of the skin cells, and increase the speed. wound healing through the induction of collagen and blood vessels. All things in view, this hydrogel has high potential to be used as a long-term and. efficient wound dressing [81].

Li et al. (2022) used Mxene-based nanomaterials in accordion-shaped, intercalated. single-layer nanoparticles, and nanoparticles loaded with gold nanoparticle (AuNP) to form a continuum. multifunctional chitin/Mxene composite sponges. These composites were meant to do the following. increase the capacity of chitin sponges to enhance the healing of wounds. The addition of Mxene improved mechanical properties, hemostatic activity, and blood and water absorption. They were able to prevent excessive loss of blood and accelerate blood clotting. Because of the joint effect of the action of bacteria capture and photothermal, the sponges are also. exhibited great antibacterial effects on S. aureus and E. coli. The hemostatic The ability was also improved and normal skin cell migration was promoted by the. addition of AuNPs. On day nine, CH/Au@sMX sponges were found to

have an 84 percent wound closure rate. These sponges aided the healing of the skin, had anti-infection qualities and quickly stopped bleeding. They are versatile hence can be utilized in the treatment of infected. injuries at any phase of healing. It is all said and done, this piece of work expands the biomedical. applications of nanomaterials in wound care using Mxene [112].

Zhou et al. (2021) designed multifunctional and biodegradable scaffolds (HPEM) to treat. staphylococcus aureus (MRSA) infected wounds treated with Ti_3C_2Tx. Mxene@PDA nanosheets. These scaffolds were obtained through the reaction of Mxene@PDA, oxidized hyaluronic acid, and poly(glycerol-ethylenimine), which led to a conductive. and self-healing hydrogel. High conductivity to electricity, and strong tissue adhesion and HPEM demonstrated quick hemostatic action in all of them. With ~90% effectiveness against MRSA, it exhibited a high level of antibacterial effect and promoted growth of healthy ones. skin cells and doing minimal harm. Collagen deposition, via elevated angiogenesis. markers such as granulation tissue development, and overexpression of such in vivo data are indicated. faster wound closure (~91%). The multipurpose structure of the scaffold fosters rapid skin. regeneration and anti-inflammatory responses. The paper focuses on application of 2D—Mxene@PDA in the production of high-tech wound care products. For the treatment of bacterial infections that are both drug-resistant and improve the outcome of wound healing, HPEM is a promising antibiotic-free therapy [84].

Sun et al. (2021) developed a novel microneedle patch with adenosine and Mxene in it. promote wound healing. Adenosine is dynamically covalently bound to the patch. PEGDA hydrogel procedure with 3-(acrylamido)phenylboronic acid (PBA). When Mxene has photothermal properties, enabling it to be exposed to the near-infrared (NIR) radiation. controlled drug discharge. Such a drug release assists in preserving therapeutic signaling at. the wound site. The ability of the patch to induce angiogenesis has been established. vitro research. The patch stimulated the blood vessel growth in animals considerably. This angiogenesis accelerated and enhanced wound healing. Drug The microneedle shape makes distribution painless and effective. Its versatility combines photothermal reaction with controlled drug delivery. All facts put in, the Mxene patch as a microneedle patch has a strong potential in the field of wound care and in other aspects. biomedical uses [113].

Ye et al. (2024) have indicated that Mxenes have potential applications in the field of biomedicine due to. their exceptional properties, which are large surface area, rigorous

electrical properties, and functional diversity. Some studies show that they are generally lowly toxic. and good biocompatibility in normal cells, and toxicity increased in cancer cells. because of oxidative stress mechanisms. Tissue integration is good in animal in vivo studies. and minimal side effects. Moreover, Mxenes are biodegradable through pH-sensitive. and enzymatic processes, reducing long-term cumulative risk. To completely prove so as to maximize their medicinal potential and ensure their safety, further research in higher animals is necessary. necessary [114].

Maleki et al. (2024) provided a comprehensive introduction of Mxenes, which is a form of two-dimensional. transitional metals-based nitride-, carbonitride-, and carbides-based materials, highlighting. its growing significance in biological use. They become appealing targets to drug. delivery, regenerative medicine, biosensing and infection or cancer treatment due to. their different physicochemical and biological properties. The study focused in specific on the way Mxene-based hydrogels may enhance the mechanical and electrical. properties of nonconductive scaffolds, especially of electroactive tissue engineering. applications: heart and nerve tissues. Several in vivo, despite their promise, were not revealed. areas are yet to be addressed, such as long-term stability and biosafety [115].

Blinov et al. (2023) improved and created a sol-gel method to produce zinc oxide. zinc acetate with nanoparticles (Zno NPs). In the absence of temperature, pH 8, and zinc. Gels were made the most stable with concentrations between 0.05 and 0.2 M. Gel polysaccharides had a great influence on characteristics, and the most suitable stabilizer was identified. to be hydroxyethyl cellulose. The size of the particles in Zno NP gels was 150-1400 nm. and they exhibited evident hysteresis in terms of their rheological behavior. When an equilibrium with the gel was achieved. Zno NPs were in contact with polysaccharides via the charged hydroxyl groups. When Zno NP gels with fewer than microparticles per have better comparison with control treatments compared to microparticle based and control treatments. Hydroxyethyl cellulose significantly enhanced the healing process in vivo research on burn wounds. The healing rate of the nanoparticle treated group was found to be 24.33% faster than the control group. and 16.23% quicker than that of the microparticle group [116].

Dutta et al. (2021) demonstrated that zinc oxide nanoparticles (Zno NPs) possess a broad spectrum of. biological applications due to their small size (nanoscale) and high surface

area, biocompatibility, and favorable physicochemical characteristics. These are nanoparticles that are commonly sized. between 1 and 100 nm, are deemed harmless, and their toxicity is minimal, which explains the reasons. the perfect candidates that can be used in nanomedicine. The research identifies the advantages and disadvantages of both synthesis strategies especially in relation to scalability, cost and environmental effect, and categorizes various synthesis processes into three: Zno NPs conjugation and surface modification, chemical, green, and biological. become special, and may significantly enhance their therapeutic potency and lower their toxicity. attention. How these nanoparticles interact with have also been critically analyzed. biodistribution, surface chemistry and toxicity of biological systems. Antimicrobial, anticancer, anti-inflammatory, antidiabetic, wound-healing, bioimaging, and the delivery of drugs is not their only numerous biological applications [117].

The research conducted by Hassan et al. (2021) explored the angiogenic and wound-healing qualities of zinc. Zno nanorods were produced in a green (environmentally friendly) way using eggshells. albumin as a bio template. Zno nanorods have been known to be biocompatible. ability to generate reactive oxygen species (ROS) that can activate pro-angiogenic. receptors such as VEGF and therefore induce angiogenesis. Conversely, excess $Zn^{2+\cdot}$ release may lead to a negative outcome on angiogenic outcomes. The experiment proved that Zno. The ideal concentrations of nanorods enhanced the development of blood vessels, epithelialization, and. wound repair on an excision wound model in the chorioallantois membrane (CAM) assay. The results proved that Zno nanorods possess a high potential as a potential regenerative substance of promoting vascularization and skin regeneration and that they cause angiogenesis in dose-dependent manner [118]. Batool et al. (2021) employed a green and biogenic procedure to produce zinc oxide nanoparticles (Zno). NPs) on the basis of Aloe barbadense leaf extract. Good antimicrobial effect was demonstrated by these Zno-NPs with bacteria and fungi strains. The wound healing of mice was significantly. faster when Zno-NPs were introduced into a dressing made of silica gel (Zno-NP/SG). Zno-NP/SG-30 ppm showed 95% wound contraction without using any additional substance within 11 days. inflicting irritation or inflammation. It decreased edema and enhanced the coagulation of the blood, platelet activity and skin elasticity. As per the research, Zno-NPs are effective wound. anti-bacterial and healing agents. Zno-NP/SG dressings were found to be controlled. degradation, repairing

characters, and non- irritating characters. Improved skin healing and wound shrinking were confirmed as having been subject to macroscopic inspections. Nevertheless, more Regarding other types of wounds, histological examination and mechanistic studies are necessary [119]. Sukri et al. (2019) examined a green process of producing zinc oxide nanoparticles. (Zno-NPs) that use the extract of the peel of the pomegranate fruit, Punica granatum, as. a natural stabilizing reducing agent. Zno-NPs at varying temperatures of annealing. were produced, which produced particles of shape spherical and hexagonal. With particle sizes between 32.98 nm and 81.84 nm, XRD analysis confirmed the growth of the particles strongly. crystalline Zno-NPs, especially at high temperatures (600-700 deg C). Zno-specific UV-Vis and FTIR spectroscopy were used to validate the bands, and various nanostructures were studied. shown by TEM. The E. coli and E. faecalis were both inhibited. biosynthesized Zno-NPs, of which the smaller nanoparticles are the most antibacterial. activity. The cytotoxicity of normal and colon cancerous human cell lines was investigated. discovered dose-dependent toxicity, the larger particles the higher the cytotoxicity. As the results of the study show, Zno-NPs were developed based on environmental friendliness. processes can be used extensively in biomedical applications, including antibacterial. and anticancer treatments. It is recommended to make further modifications that would enhance their selectivity. toxicity in cancer cells [120].

Mihai et al. (2019) examined the recent advances in the use of nanomaterials, namely metal-based nanoparticles, to enhance wound healing and infection. The traditional wound care is based on topical medications that facilitate healing. and avoid infection. However, it has been rocked by the emergence of drug-resistant diseases. to the necessity of more remedies. Nanotechnology has innovative practices to offer. and especially when metal nanoparticles have good antibacterial and wound-healing. They use properties, including silver, gold, zinc, among others. Other advantages of these nanoparticles involve maintenance of a wet wound setting, reduction in the incidence of. dress changes, and improving patient compliance. Agents that may be used are nanoparticles. modern wound care due to their large surface-area-volume ratio and biocompatibility. Silver, zinc, and gold nanoparticles in particular are antibacterial. low toxicity properties. Moreover, to cure chronic wounds and infections. associated with biofilms, sophisticated formulations with nanoparticles of growth factors, The investigation of genes, or stem cells, is underway [121].

Chapter 3
Materials and Methods

3.1 Chemicals and reagents:

Titanium aluminum carbide (Ti_3AlC_2), hydrofluoric acid (HF), zinc nitrate hexahydrate, manganese chloride tetrahydrate, sodium hydroxide (NaOH), deionized water, dimethyl sulfoxide (DMSO), and ethanol were purchased from Sigma-Aldrich, Germany.

3.2Materials Synthesis and Nanocomposite Fabrication

3.2.1 Synthesis of Mxene:

1 g of Ti3AlC2 powder was then added to 10 mL of 40 percent hydrofluoric acid (HF) and stirred. This was done at room temperature over a period of 24 h to selectively etch away the layers of aluminum to form a layered Mxene structure. After removing the suspension was centrifuged at 7000 rpm to take off the solid product, which was washed several times with fresh distilled water. The washing method continued with a cycle of about 5 min and proceeded until the condition of the supernatant was nearly neutral with a pH of 6, indicating that all traces of the acid were eliminated. The obtained wet solid was dried at 60 ° C overnight to produce multilayered Ti_3C_2Tx Mxene. In the case of delamination, the multilayered Mxene, 0.6 g of the material was dispersed with 6 mL of dimethyl sulfoxide (DMSO) and continuously stirred over a period of 24 h to facilitate intercalation. The centrifugation was then done at 5000 rpm and lasted 30 min to isolate the few-layered product. The sample was dried at 60 ° C by vacuum-filtering the sediment to remove all the excess DMSO. The process resulted in a few-layer Ti_3C_2Tx Mxene that was better at exfoliation and dispersibility and could be further used [122, 123].

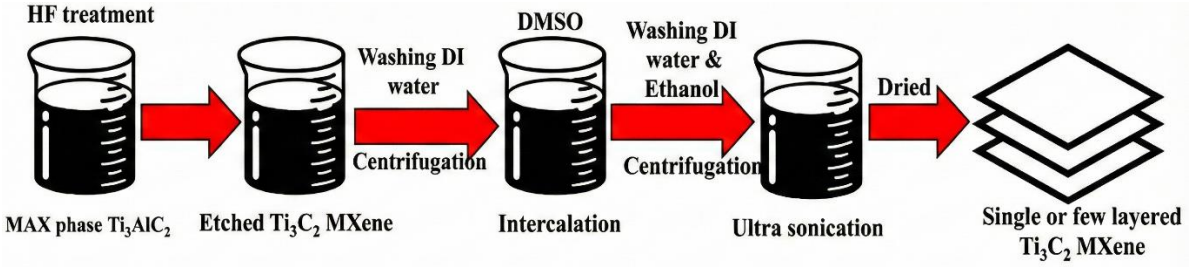

Figure 12:Schematic illustration of the synthesis of Mxene from Ti_3AlC_2 MAX phase via HF etching.

3.2.2 Synthesis of Mn/Zno Nanocomposite

A precursor solution was first prepared by dissolving 2.08 g of zinc nitrate hexahydrate $Zn(NO_3)_2.6H_2O$, and 0.197 g of manganese chloride tetrahydrate ($MnCl_2 \cdot 4H_2O$) in 40 mL of deionized (DI) To achieve a complete dissolution and homogeneity of the metal precursors, the solution was constantly stirred on hotplate. Afterward, 0.2M solution of sodium hydroxide (NaOH) was introduced gradually and in 15 min, the pH was adjusted to 10 of reaction mixture. The mixture was stirred further at 80 ^{o}C after adjusting its pH in order to ensure that precursor species were uniformly nucleated and grew. This was then suspended in a Teflon autoclave, capped and hydrothermal treatment in 180 C was applied to the suspension in 12 h. When the hydrothermal reaction was complete, the autoclave was left to cool at RT. To remove the remaining ions and unreacted species, the solid product was obtained by filtration and several times washed with DI water and ethanol correspondingly. The precipitate obtained was dried in an oven at 80 ^{o}C, and then dried. Lastly, the dry powder was heated at 400 ^{o}C and 2 h to enhance the crystallinity and purity of the phases to give the final product [124].

3.2.3 Synthesis of Mn/Zno @Mxene Nanocomposite

Ti_3C_2Tx Mxene was added to the 0.340 g of ethanol and ultrasonicated in it to create a homogeneous suspension 20 min. Then $Zn(NO_3)_2.6H_2O$ and ($MnCl_2 \cdot 4H_2O$) (2.08 g and 0.197 g, respectively) were added and stirred. The pH was subsequently adjusted by adding 2 M NaOH in 15-minute increments. Mixing was done at 80 °C for 2 h to ascertain homogeneous nucleation and growth. The suspension thus obtained was put in a 100 mL Teflon-lined autoclave and heated at 180 °C for 12 h. When the mixture was allowed to cool naturally to room temperature, the precipitate was then filtered. To ensure that no impurities were left, the product was completely washed using deionized water and ethanol. The dried solid was dried at 80 ^{o}C with a duration of 3 h. Lastly, the sample was dried and calcined at 400 °C for 2 h to get the final composite material [124].

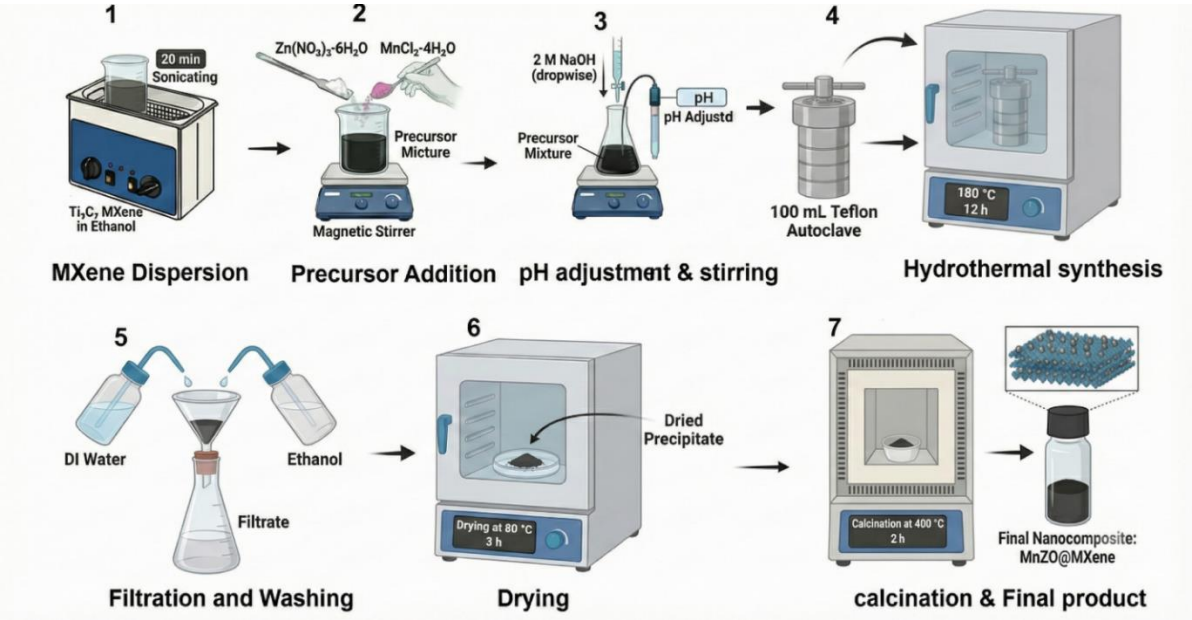

Figure 13: Schematic representation of the hydrothermal procedure used to prepare MnZno@Mxene nanocomposite.

3.3 Methodology for Antibacterial Potential Study:

The antibacterial activity of the synthesized nanocomposite based on the agar well diffusion method (with minor alterations) [139] was done on three bacterial species: Staphylococcus aureus, Pseudomonas aeruginosa and Escherichia coli. The M-H agar plates were prepared by placing 3.8 g of M-H medium in distilled water which was then sterilized by autoclaving but poured into sterile Petri dishes to solidify. After the solidification, the standardized bacterial cultures were spread uniformly on every plate surface. To standardize the bacterial inoculums, they were matched with the 0.5 McFarland standard in terms of turbidity so that all samples had equal cell density. The calibrated inoculum was placed randomly on the agar surfaces. Stock nanocomposites of 5 mg/mL, 2.5mg/mL and 1.25mg/mL stock solutions were made. A sterile borer was used to make four wells on each plate with 40 µL of each concentration, respectively and the fourth well was used as a negative control with DMSO. As a positive control with all strains, gentamicin discs were employed. Each plate was incubated at 37 ^{o} C and 24 hours. The antibacterial effect was then identified by measuring the diameter of the zones of inhibition (in millimeters) around each well after incubation. Experiments were conducted in three replicates to achieve the reproducibility and accuracy of the results.[125]

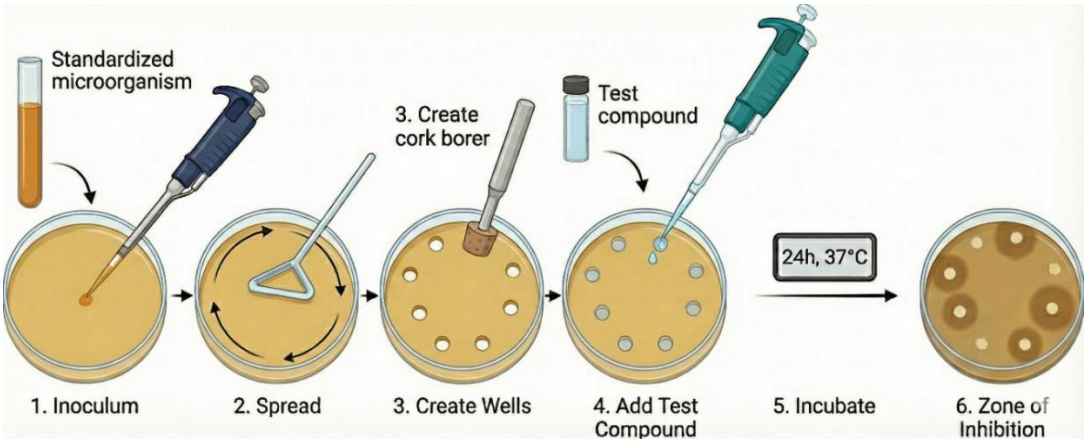

Figure 14: Graphical illustration of the agar well diffusion method for evaluating antibacterial activity.

3.4 Methodology for Wound healing in vivo studies:

The study involved a total of nine mice to be split into three groups of three mice each. Group I was used as the positive control and was to be treated with medicated gel, Group II treated with Mn/Zno@Mxene and Group III was used as the negative control. The dorsal area of all mice was shaved, followed by full-thickness excision wounds in 6 mm diameter under chloroform anesthesia with a sterile surgical blade. The medicated gel was applied to the positive control group, whereas 1 mL of synthetic Mn/Zno@Mxene (2 mM) confined in niosomes was given to the treatment group. The negative control sample was applied with standard saline (1 mL).These equations were included in a 2 × 2 cm 2 dressing and the dressing directly covered the wound bed after each 10-day. The wound contraction was observed at day 0, 2, 4, 6 and 8 to determine the healing trend. Each of these days, digital images of the wounds were taken on the control and treated groups and subsequently, the photos were analyzed in order to determine the healing process. [126]

3.5 Methodology for Anti-Inflammatory Activity:

To determine the anti-inflammatory activity against acute soreness, the animals were randomly separated into three groups. Group A was used as control of carrageenan and it was not treated orally. The positive control Group B was used as treated with diclofenac sodium, and Group C was used as treated with 500 0MnZno@Mxene. The model employed to

investigate the anti-inflammatory effect was the carrageenan-induced rat paw edema model. The 100 μL of a freshly made 1% solution of carrageenan in distilled water was injected in the right hind paw of the rat to induce edema. Animals under Groups B and C received a pre-treatment of a single oral dosage of diclofenac sodium or MnZno@Mxene formulation, respectively, 30 min before carrageenan injection. The paw thickness was recorded at 0 h (just prior to administration of carrageenan) and then at 1, 2, 3, 4 and 24 h after administration. The extent of edema was established by finding the change in the paw thickness of each time point compared to the baseline paw thickness at 0 h.[127]

Chapter 4
Results and Discussion

An inclusive set of analytical techniques was employed to confirm the successful synthesis of the MnZno@Mxene nanocomposite. X-ray diffraction (XRD) was used to determine the phase composition and crystallinity of the material, while Fourier-transform infrared spectroscopy (FT-IR) was performed to identify characteristic functional groups. Ultraviolet-visible (UV-Vis) spectroscopy was utilized to investigate the optical properties of the nanocomposite. The surface morphology and microstructural features were examined in detail using scanning electron microscopy (SEM), and elemental composition was analyzed through energy-dispersive X-ray spectroscopy (EDX) attached to the SEM. Furthermore, Raman spectroscopy was employed to probe the structural characteristics and confirm the presence of Mxene layers and metal oxide interactions. X-ray photoelectron spectroscopy (XPS) provided detailed information on the elemental states and chemical bonding within the nanocomposite. Collectively, these techniques offered a thorough characterization, confirming the successful formation and structural integrity of the MnZno@Mxene nanocomposite.

4.1 FTIR Analysis

The formation and the interfacial interaction of the nanocomposite material are indicated by the FTIR spectra of Mxene, MnZno and MnZno with Mxene nanocomposite. The spectrum of the Mxene shows a weak band of C–H stretching at about 2932 cm^{-1} and the maximum at 1048 cm^{-1} which show the C -F and/or C -O stretching of the termination groups including O, OH, and F that are formed during the exfoliation process; the peak absorbed at 534 cm^{-1} are considered to be Ti -O and Ti -O -Ti bonds. [128, 129] The MnZno spectrum presents a typical band at around 845cm^{-1} and a peak at 607cm^{-1}, 468cm^{-1} that can be assigned to the metal -oxygen stretching vibrations of (Mn, Zn) -O, and thus the presence of mixed metal oxide nanoparticles [130] [131]. In the MnZno@Mxene nanocomposite show CH stretching at 2912 cm^{-1} is observed, and the peak at 1065 cm^{-1} can be attributed to C- F stretching of Mxene surface groups, and the peak at 865 cm^{-1} is attributed to (Mn, Zn)- O vibrations; a strong absorption at 577 cm-1 can be attributed to overlapping TiO and (Mn,Zn)O stretching bands. These characteristic peaks as in the composite are slight shifts, show strong interfacial

interactions, and effective anchoring of MnZno nanoparticles on the Mxene surface.

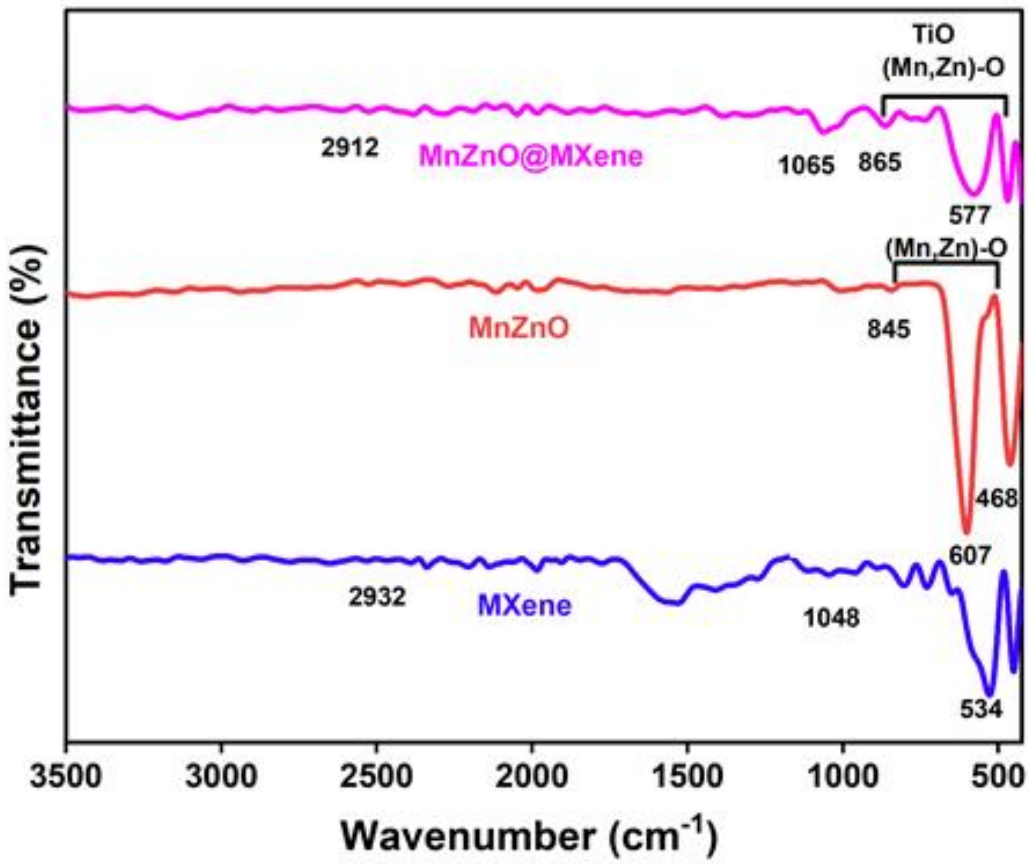

Figure 15: FTIR spectra of Mxene, MnZno, and MnZno@Mxene composite.

Table 1: FTIR Absorption Bands and Their Assigned Functional Groups.

Bands (cm^{-1})	**Mxene**	**MnZno**	**MnZno@ Mxene**	**Vibration Modes**
2932–2912	2932	–	2912	C–H stretching
1065–1048	1048	–	1065	C–F stretching
607 – 845	–	607, 845	865	(MnZn)–O and lattice vibrations

534–577	534	–	577	Ti–O, Ti–O–Ti Vibrations

4.2 Raman Studies:

The Raman spectrum of Mxene (Ti_3C_2Tx), MnZno nanoparticles and the MnZno@Mxene composite show some vibrational properties that are indicative of their structural and interfacial properties. Upon Al etching, Mxene (Ti_3C_2Tx), spectrum is characterized by typical Ti -O, Ti -C -O and Ti -C vibrational modes at about 133, 214, 382 and 626 -1, and broadened D and G bands at about 1379 and 1595 cm -1, which are ascribed to disordered and graphitic carbon due to functionalization of the surface and also partial oxidation [132]. The MnZno nanoparticles exhibit bright E 2(high) and A 1(LO) modes at approximately 333 and 527 cm^{-1} respectively, which belong to the wurtzite crystal structure and are the evidence of the Mn doping-induced lattice deformation and appearance of lattice oxygen vacancies [130, 133]. The Raman spectrum of the MnZno@Mxene composite still has the main vibrational characteristics of both MnZno and Mxene, which points to the effective combination of the two substances. The composite shows vibrational modes at about 131, 319, 384, 628, 1403, and 1620 cm^{-1} with low frequency modes being due to the interaction of MnZno vibrations with TiO and TiC O vibrations of Mxene. Also, the minor blue shift of TiO vibration (~628 cm^{-1}) and the shifts in D and G band (1403 and 1620 cm^{-1}) suggest a strong interfacial bonding and electronic interaction between MnZno and Mxene. In general, the presence of Zno, TiC, TiO, and C vibrations in the coexistence and systematic changes prove that a highly coupled MnZno/Mxene heterostructure was formed.

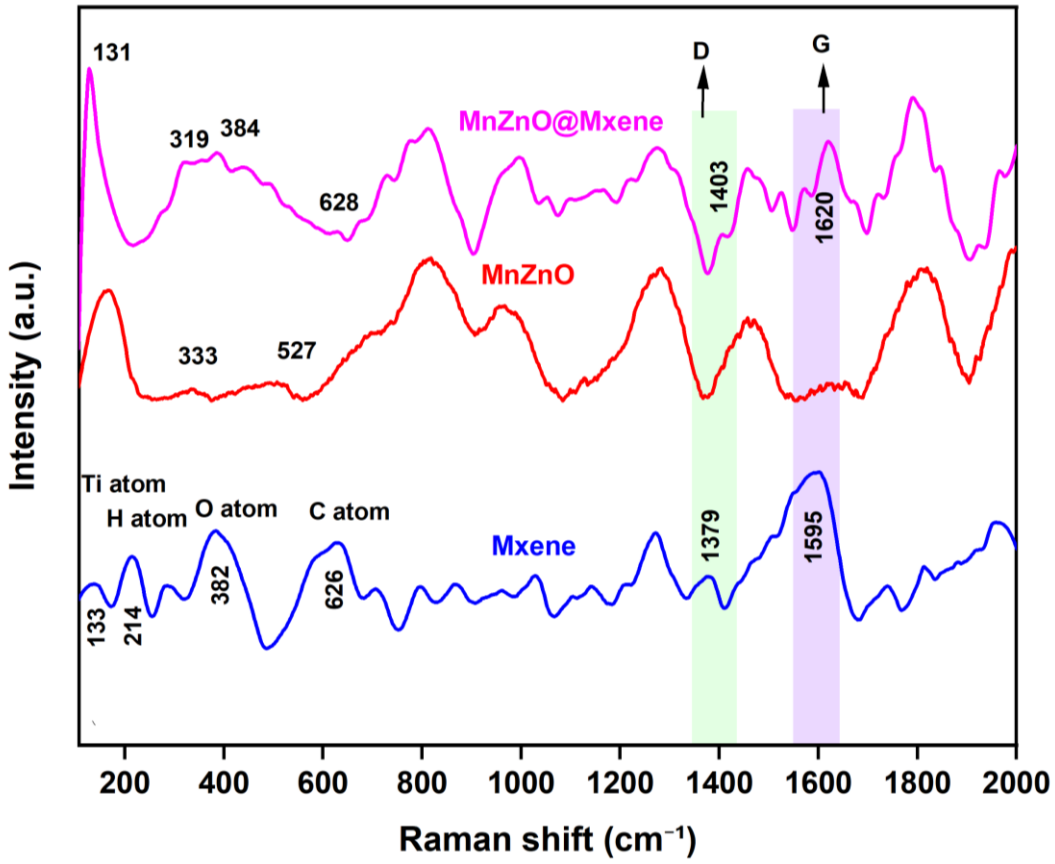

Figure 16: Raman spectra of MAX phase, Mxene, MnZno, and MnZno@Mxene composite.

4.3 UV-Vis. Studies:

The UV Vis absorption spectrums of Mxene, MnZno, and the MnZno@Mxene nanocomposite show unique optical properties that relate to each separately and at their interface. Pristine Mxene exhibits a high absorption peak at about 270 nm which is ascribed to electronic transition of surface termination groups that include -OH, -O and -F groups that occur during etching and delamination reactions [134]. The appearance of the MnZno nanoparticles is represented with a broad absorption band at around 310nm, which corresponds to the fundamental bandgap transition of Mn-doped Zno. [135]. The presence of Mxene and MnZno phases can be reflected by both absorption features at 270 nm and 310 nm, and this is also apparent as a red shift as compared to Mxene in the MnZno@Mxene composite. In addition, the little differences in the peak position and their intensities in relation to the pristine materials indicate that there was high interfacial coupling and charge transfer between MnZno and Mxene, thus proving

the successful implementation of the MnZno@Mxene hybrid nanostructure.

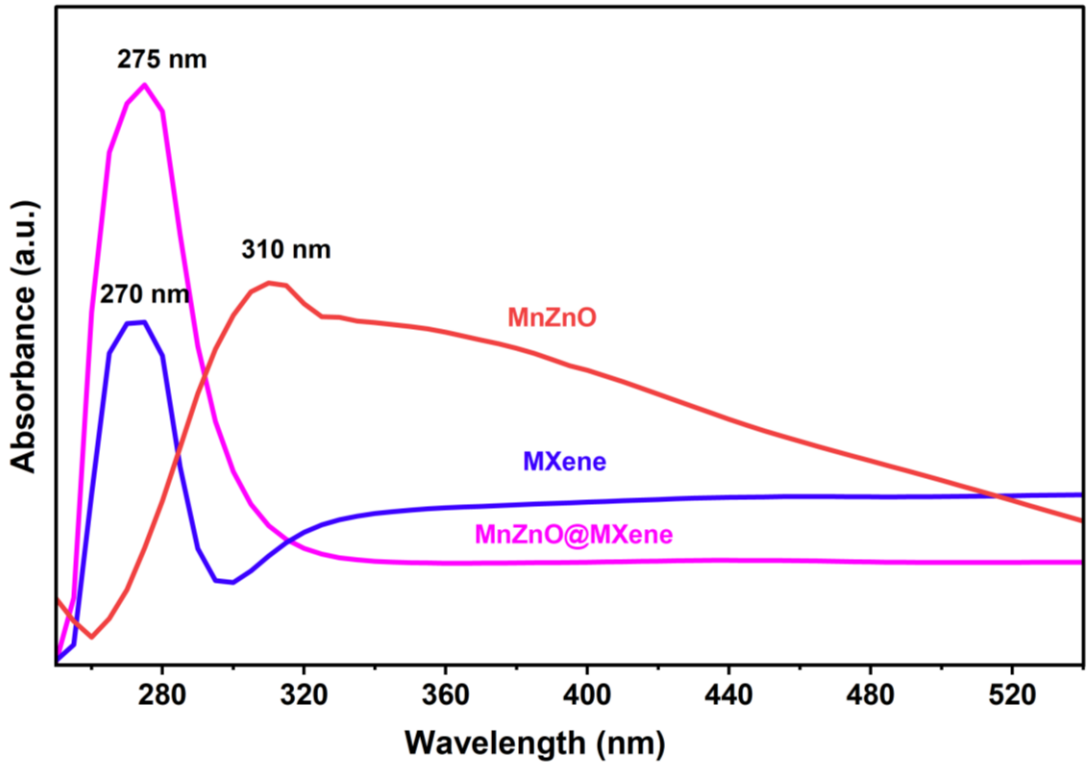

Figure 17: The UV–Visible absorption spectra of Mxene, MnZno, and MnZno@Mxene nanocomposite displays distinct peaks.

4.4 XRD study:

The X-ray diffraction (XRD) pattern of Mxene shows clear reflections with a 2θ value of 9.6, 19.1, and 39 relates to the (002), (004), and (104) planes, which confirms the successful etching of the MAX phase and the creation of the layered (Ti_3C_2Tx) structure [136] Other diffraction peaks that are found at 34.04, 38.64, 41.6, 45, 56.38, 60.1, 65.47 and 73.9 degrees, which are attributed to the (101), (104), (105), (106), (108), (109), (110) and (116) planes, respectively (JCPDS 52-0857), also confirm the highly crystallized [137]. The XRD of Mn-doped Zno nanoparticles reveals characteristic peaks at 29.41 ° C, 32.79 ° C, 36.45 ° C, 44.73 ° C, 51.16 ° C, 58.9 ° C, 60.21 ° C and 64.89 ° C that are attributed to the (100), (002), (101), (102), (110), (200), (112) and (201). The fact that the additional reflections are slight and the secondary impurity phases are absent altogether, speaks in favor of the fact that the incorporation of Mn^{2+}

ions into the Zno lattice was successful. The diffraction intensity of the Mn/Zno nanoparticles slightly decreases and this effect can be explained by the distortion of the lattice caused by the increase in ionic radius of the Mn^{2+} ion [138]. The typical Mn/Zno diffraction peaks of 44.73 (102) and 60.21 (112) in the Mn/Zno@Mxene composite have been found to experience a significant loss in intensity, thereby indicating successful intercalation and even distribution of Mn/Zno nanoparticles in the Mxene layers, and as such, the successful incorporation of the composite structure.

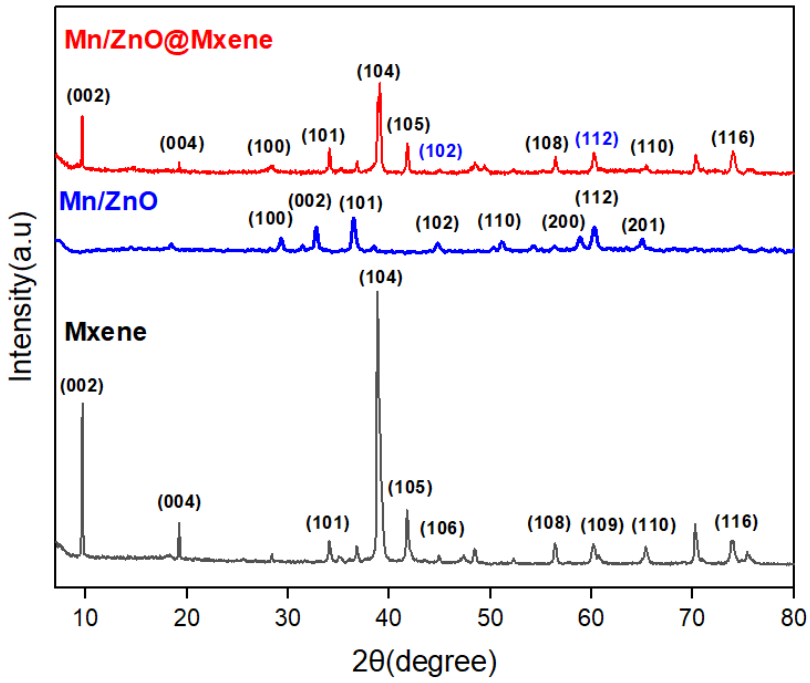

Figure 18: XRD Analysis of Individual Components and the MnZno@Mxene Nanocomposite

4.5 SEM/EDX and Elemental Analysis:

The productive synthesis and compositional development of the MAX phase, Mxene, MnZno nanoparticle, and the MnZno@Mxene nanocomposite is evidenced by SEM and EDX analyses. The morphology in the MAX phase is thick and compact in layered structures typical of Ti_3AlC_2 and the EDX spectrum depicts that the weight percentages of Ti, C, and Al are 62.30, 21.97, and 15.73, respectively, and the uniform distribution of elemental content, which is evidence that the structure is of the MAX phase shown in the figure 19 [139]. The Mxene has a topography after selective etching that has a rough

and partially exfoliated appearance. There is an important element of Al and the presence of Ti (69.46 wt%), O (23.60 wt%), C (6.37 wt%) with small signals of F and Cl, and the uniform distribution of elemental content in elemental mapping which is the indication of successful elimination of Al and the appearance of surface-terminated Mxene sheets shown in the figure 20 [140].

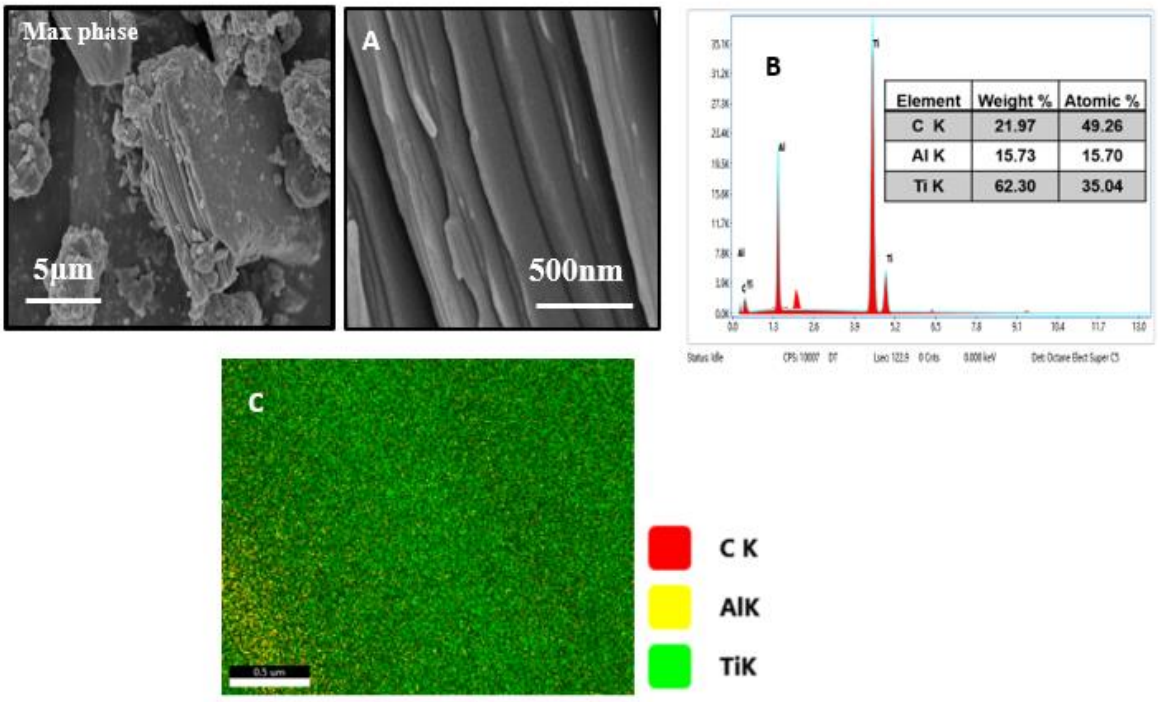

Figure 19: a) SEM image of Max phase, b) EDX spectrum of Max phase c) Elemental mapping of Max phase.

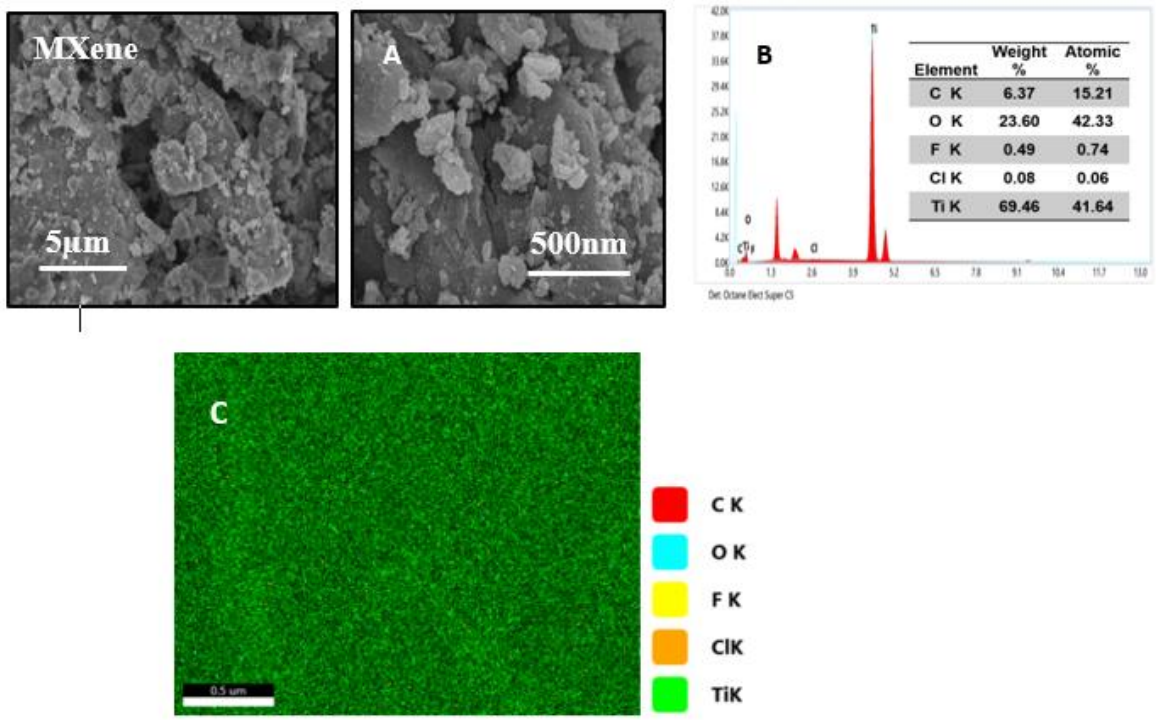

Figure 20: a) SEM image of Mxene, b) EDX spectrum of Mxene, c) Elemental mapping of Mxene.

The MnZno nanoparticles have a clear cubic morphology and EDX spectrum analysis reveals that all elements of nanoparticles are present. EDX table shows that Mn (79.83 wt%), O (19.90 wt%) and Zn (0.27 wt%) are present, and elemental mapping shows the equal distribution of elements, confirming the formation of Mn-doped Zno nanostructures shown in the figure 21 [141]. SEM images of MnZno@Mxene nanocomposite demonstrate the presence of a nanoflake like structure in which MnZno nanoparticles are evenly attached to the Mxene face. The EDX spectrum of the composite shows that it contains Ti, C, O, Mn, and Zn with the weight percentage of 15.90, 11.53, 62.96, 8.83, and 0.50, respectively, and traces of F and Cl, which confirms the successful integration of MnZno nanoparticle into the Mxene matrix. The uniform distribution of elemental content and the hierarchical structure of nanoflakes give it a high surface area and sharp sites, which can be attributed to the improved antibacterial, wound-healing and anti-inflammatory properties of the MnZno@Mxene nanocomposite shown in figure 22.

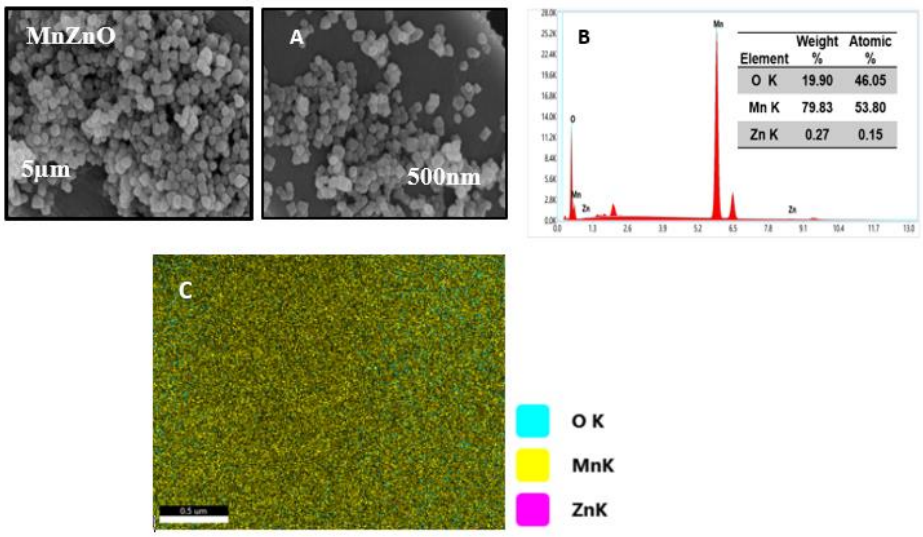

Figure 21: a) SEM image of MnZno, b) EDX spectrum of MnZno, c) Elemental mapping of MnZno.

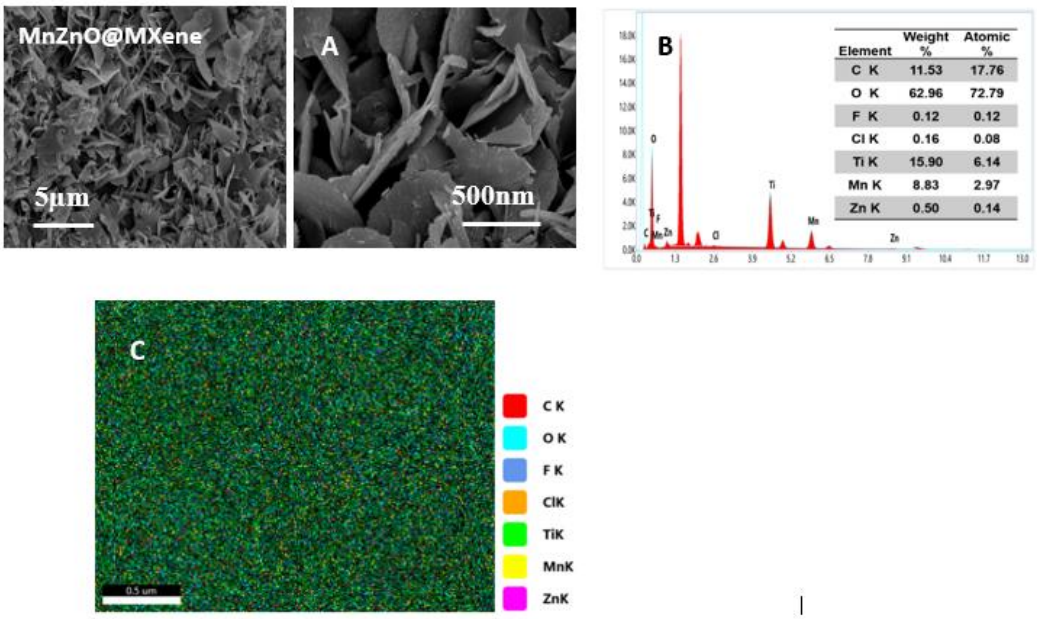

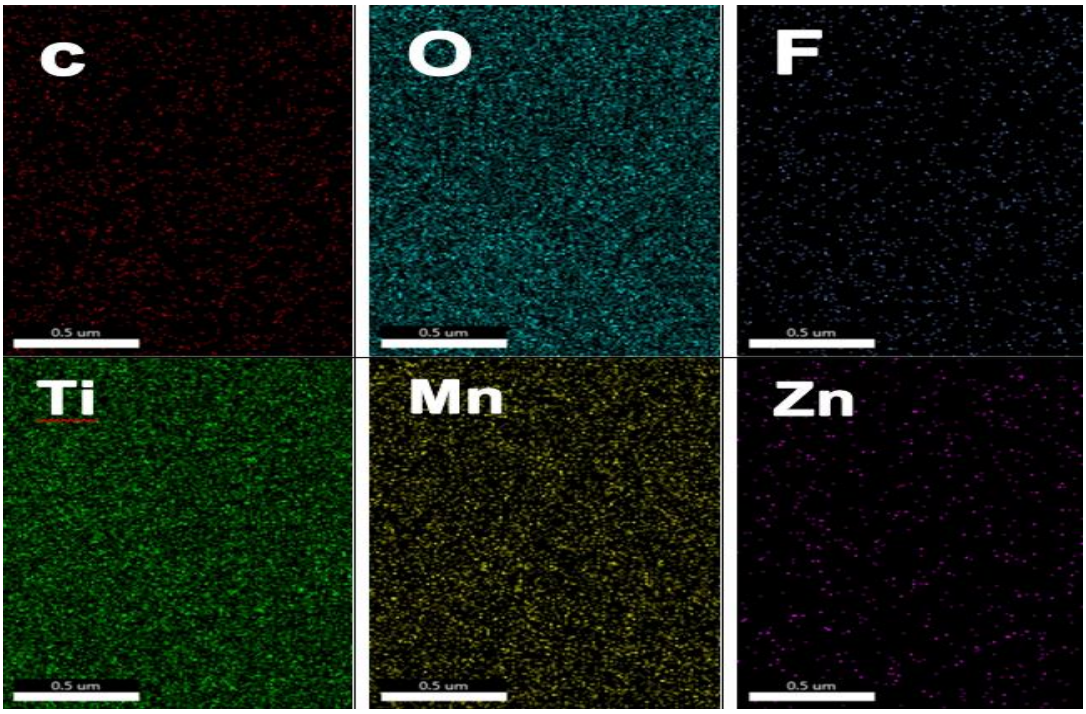

Figure 22: a) SEM image of MnZno@Mxene, b) EDX spectrum of MnZno@Mxene, c) Elemental mapping of MnZno@Mxene.

4.5 XPS analysis:

X-ray photoelectron spectroscopy of the MnZno Mn-doped Zno on the Mxene backbone and the existence of major elemental and chemical oxidation states are confirmed by the X-ray photoelectron spectroscopy (XPS) of the MnZno Mn-doped Zno on the Mxene backbone. The spectrum of the survey gives the elemental composition of the composite with Mn, Zn, Ti, O, and C as the peaks. The O 1s spectra at high-resolution have various components, which are associated with the various oxygen environments.

Peaks with correlation to Ti,Mn,Zn-O, Zno, and MnZn O bonds at heights of about 529.7 eV, 530.6 eV and 531.5eV respectively, and a peak at about 532.5 eV, which is attributed to the surface hydroxyl (OH) group, confirm the existence of oxygen in both metal-oxide and surface-bound hydroxyl forms. The Ti 2p high-resolution spectrum shows the existence of Ti 2p 3/2 and Ti 2p 1/2 peptides with deconvolution showing that TiO 2 (~458.5 eV), Zn -O -Ti (~457.5 eV), Ti -C or surface -OH (~455.5 eV) and F -Ti -C (~464 eV) were involved. This assures of the retention of Ti-based Mxene framework in the course of establishing connections with Zno and Mn species. The C 1s spectrum contains the peaks that are related to the C-C (~284.6 eV), C-O (~286 eV), C-Ti-O (~285

eV), and C-F (~288 eV) bonds which prove the existence of Mxene carbon, surface oxidation, and functional groups. On the whole, the obtained XPS outcomes confirm the effective production of the MnZno@Mxene composite, and well-integrated Mn-doped Zno nanoparticles and surface functionalities which can potentially improve its antibacterial and wound-healing ability. [139, 142, 143]

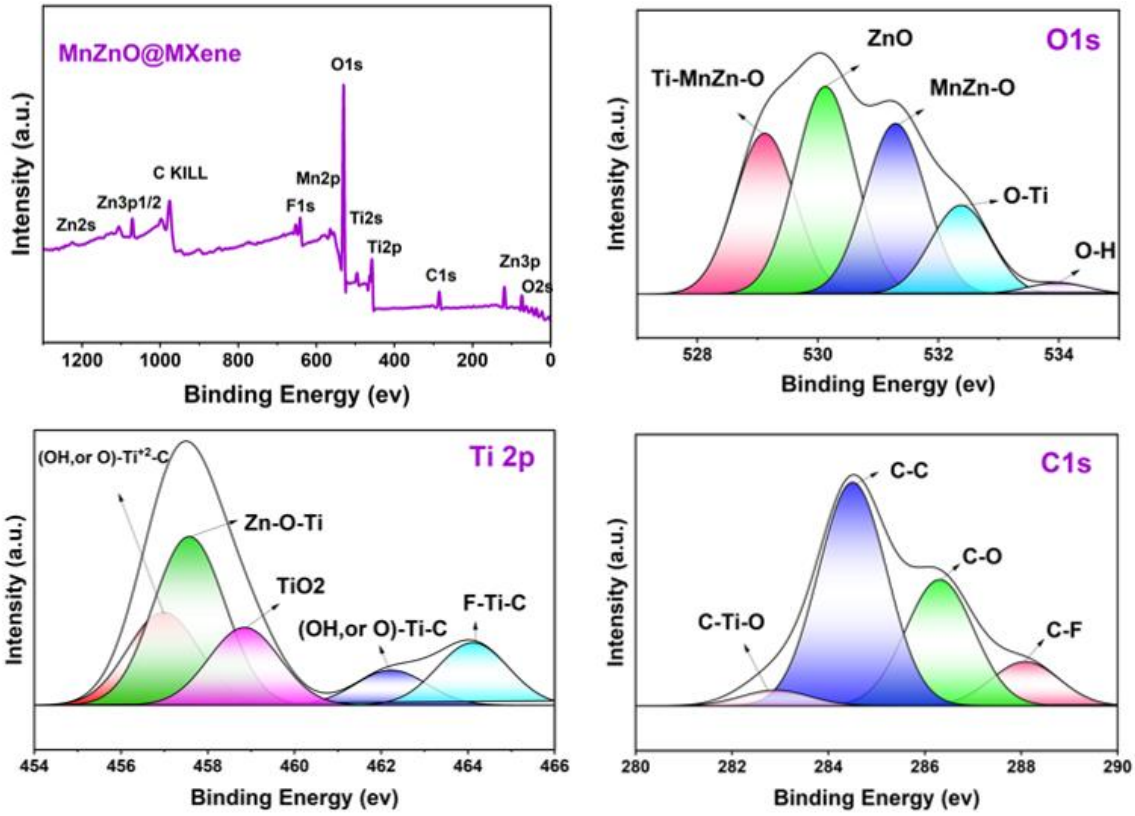

Figure 23: XPS full spectra of MnZno@Mxene and High-resolution XPS spectra C1s, O1s, Ti2p.

4.6 Antibacterial Studies

The method of agar well diffusion assay was used to determine the antibacterial action of MnZno@Mxene nanocomposite against Staphylococcus aureus, Escherichia coli and Pseudomonas aeruginosa. Out of the tested concentrations, the nanocomposite with a concentration of 5 mg/mL presented the best antibacterial activity with the maximum zones of inhibition (ZOI) being recorded against all bacteria. In particular, it was found that the maximum values of ZOI against S. aureus, E. coli and P. aeruginosa were 17 mm, 22 mm and 18 mm, respectively.

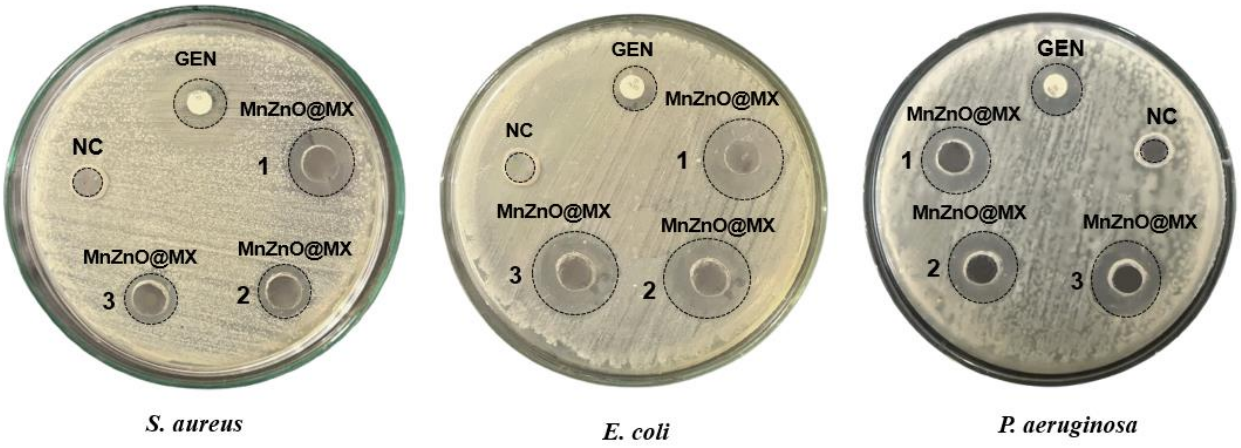

Figure 24: Agar Well Diffusion Results Displaying Antibacterial Activity Again S. aureus, E. coli, and P. aeruginosa.

As would be expected, the negative control not show any zone of inhibition, whereas the positive control showed the best antimicrobial effect, especially on E. coli. The findings are in line with the already published findings that bacterial growth inactivation increases as the concentration of nanoparticles used in the well increases [144]. The differences between the antibacterial reactions of the tested microorganisms may be explained by the differences in the size of nanoparticles, concentration, and the structural peculiarities of bacterial cell walls. The relative antimicrobial activity of MnZno Mxene against bacteria is indicated in the following figure 25.

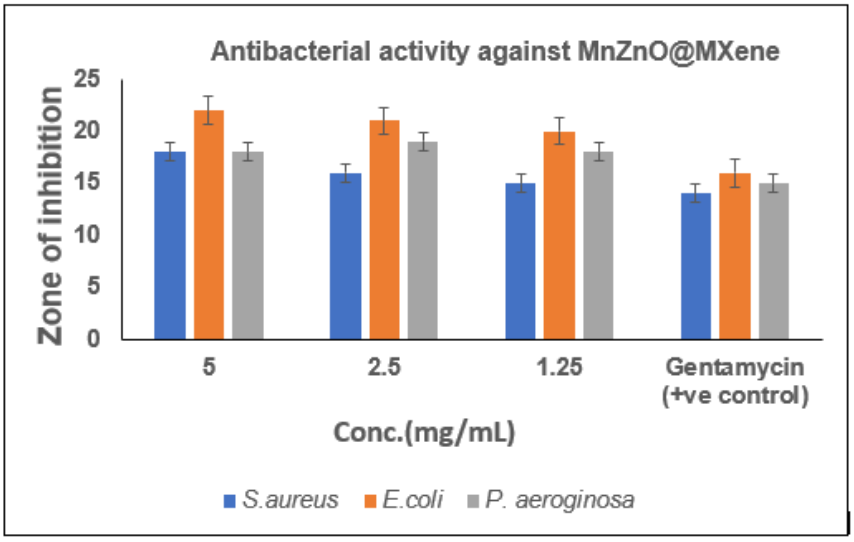

Figure 25: Figure 20 Comparative Analysis of ZOI Induced by MnZno@Mxene Nanocomposite.

4.8 Time Scale Studies

The growth-kinetic behaviors of Staphylococcus aureus, Escherichia coli, and Pseudomonas aeruginosa under the presence of MxeneMnZno behave in a time-dependent manner with rising optical density, which is a characteristic of standard bacterial growth behavior. [145] The strain with the lowest growth rate was S. aureus, where the OD value at the start of the experiment was about 0.15 and grew to about 0.40 after 40 h of growth, which is associated with a long lag phase and sluggish entry into the exponential stage. The growth tendency of E. coli was moderate, and the values of OD increased approximately between 0.30 and almost 0.80 during the same time, which indicates an intermediate susceptibility to the nanocomposite. Conversely, P. aeruginosa showed the quickest growth with the values of the OD rising, starting at about 0.35 to nearly 1.20 after 40 h, indicating a relatively lesser sensitivity and early penetration of the exponential growth phase.

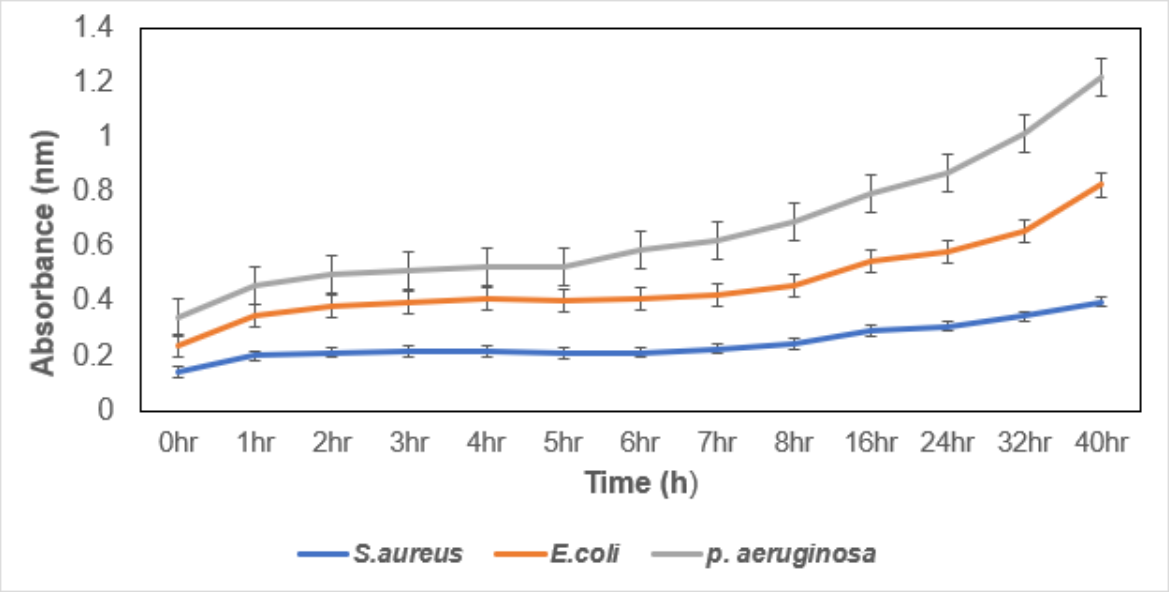

Figure 26: Kinetic Insights into the Antibacterial Mechanism of MnZno@Mxene.

All in all, the growth curves that are gradually increasing with time (1-40 h) and species-specifically are in harmony with the known characteristics of bacterial growth kinetics, and indicate that the growth curves obtained can be confidently considered to be idealized forms of microbial behavior.

4.8 In vivo wound healing studies

The efficacy of the synthesized nanocomposite on wound healing was estimated on an excision wound model within 10 days, with the assistance of three experimental groups, the treatment group, the positive and the negative control.

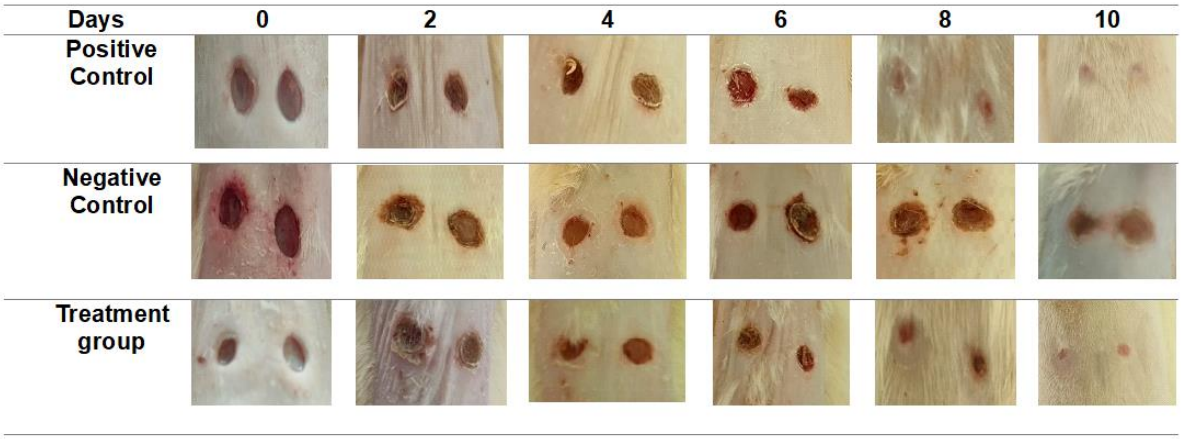

Figure 27: Comparative evaluation of wound healing in rats from the MnZno@Mxene treatment group, positive control (medicated gel), and negative control (normal saline) during 10 days.

Through the research, no wounds in the treated market showed any trace of infection, exudate or active bleeding and slight inflammation was reported in the negative control market and slowed tissue regeneration. The rate of wound contraction was measured on day 2, 4, 6, 8 and 10, and the amount of wound contraction was significantly higher in the group treated with nanocomposites with visible progress showing starting on day 6, versus the negative control. On day 10, the positive control recorded the highest healing efficiency of 95.19% wound closure as compared to the negative control with 66.76% wound closure, whereas the treated group recorded 95.19% wound closure. These findings demonstrate clearly that the nanocomposite is better in terms of the wound healing performance compared to the untreated group. The visual observation also proved increased healing on the treated wounds that is evident in the form of a smooth skin texture and a faster decrease in the wound diameter than the negative control, which supports the therapeutic effect of the nanocomposite in wound management applications.

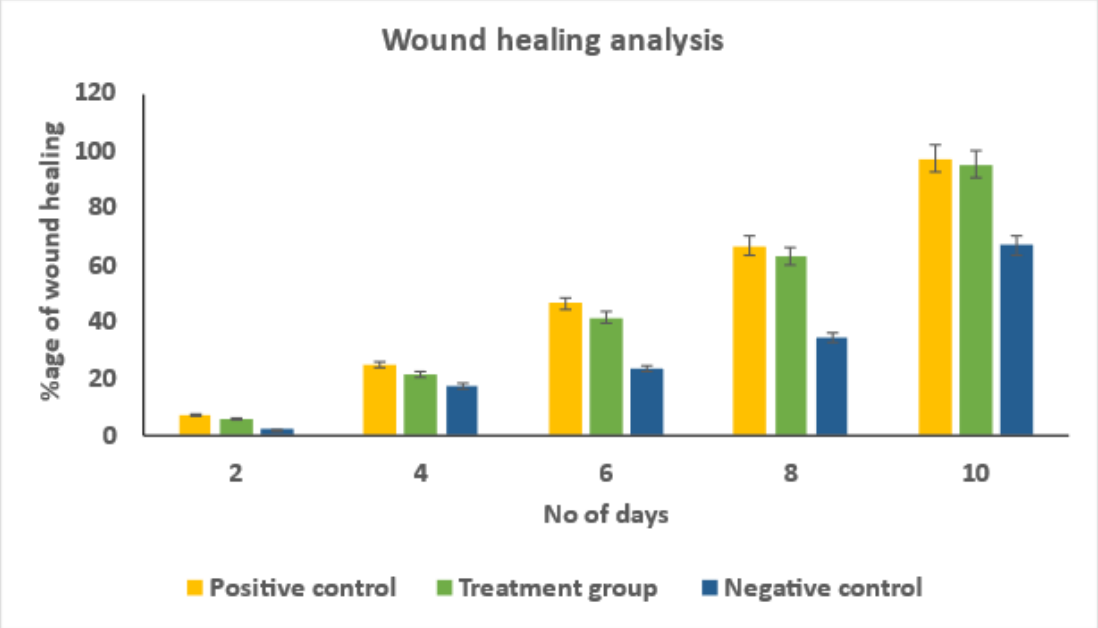

Figure 28: Evaluation of wound healing progression across treatment, positive control, and negative control cohorts.

4.9 Assessment of the Anti-Inflammatory Response:

The anti-inflammatory efficacy of the MnZno@Mxene nanocomposite was evaluated by the carrageenan-induced paw edema in rats which is a proven method of investigating acute inflammation. [146]. This model enables quantitative tracking of the development and resolution of edema with time. The animals were categorized into three groups; a negative control group (no anti-inflammatory treatment), a positive control group (anti-inflammatory drug of standard use), and a treatment group, which was administered with MnZno@Mxene nanocomposite. The carrageenan paw thickness was recorded when the injection was done at baseline (0 h) and at intervals of 1, 2, 3, 4, 5, and 24h. At 0 h, all groups did not differ on paw thickness (4.08 mm in treatment group, 4.06 mm in positive control and 4.07 mm in negative control), and this was the case of homogenous baseline conditions. The paw edema rose to the peak at the 3 rd hour in all three groups with values of 6.96 mm in the treatment group, 6.35 mm in the positive control, and 7.23 mm in the negative control representing intense inflammation. Subsequently, the gradual decrease in paw thickness could be observed in both the treated and the positive control group but slower and a smaller amount significant in the negative control group. At the 5th hour, the thickness of paws was reduced

to 6.01 mm in the MnZno@Mxene-treated group and 5.66 mm in the positive control, whereas it was still higher in the negative control (6.54 mm). This was further decreased at the 6th hour, and the values of the paw thickness dropped to 4.39 mm and 4.12 mm (treatment and positive control, respectively) in comparison to 5.21 mm in the negative control. The faster edema removal in MnZno@Mxene-treated group compared to the untreated one shows a significant anti-inflammatory effect, which is almost similar to that of the standard drug. In general, the results suggest that MnZno@Mxene can be successfully used to prevent carrageenan-induced inflammation and has a great potential to be utilized as a biocompatible anti-inflammatory agent.

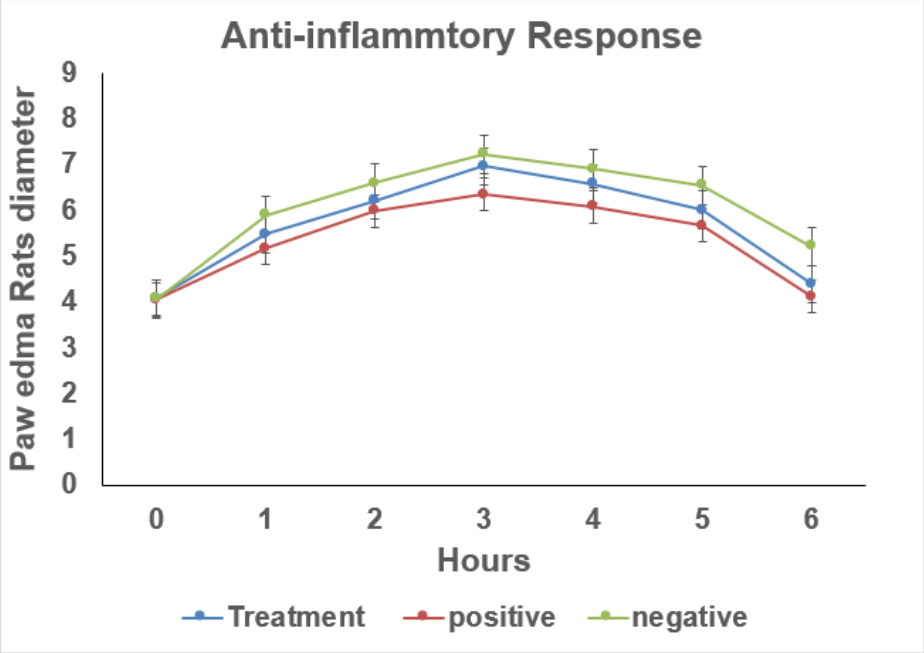

Figure 29: Paw thickness variation recorded at different time points (0–24 h) after carrageenan-induced inflammation.

4.10 Comparative studies of other reported papers

The table summarizes the major research works on the investigation of antibacterial and wound-healing characteristics of Mxene-based and metal-oxide nanocomposites. The CIP Ti_3C_2Tx@ alginate entrapped in a biocompatible sodium alginate framework. The system has good antibacterial activity; its inhibition zone (against Staphylococcus aureus) and inhibition zone (against Escherichia coli) are 18-20 mm and 16-18 mm, respectively, which implies that the system can suppress both Gram-positive and Gram-negative bacteria. In vivo studies through a mouse full-thickness skin wound model show that the wound-healing

process achieves a closing percentage of approximately 61 per cent. at day 7 and 90 per cent. at day 14, indicating faster healing than the untreated wounds. The controlled release of drugs through the alginate network is seen to be the main cause of the anti-inflammatory effect that allows the reduction of infection-related inflammation with minimum local toxicity. The design is multifunctional, which is why the material is especially appropriate in the case of infected wound dressings[147]. The photothermal effect of Zno@Mxene is aimed at achieving rapid antibacterial, particularly against drug-resistant bacteria. It contains over 90% of methicillin-resistant Staphylococcus aureus (MRSA) killing in 5 minutes, which should be mainly attributed to photothermal heating and the formation of reactive oxygen species (ROS). Though no antibacterial data against E. coli and Pseudomonas aeruginosa is carried out in the study, the wound-healing outcome is very encouraging, with almost 100 percent wound closure in a span of some 12 days. This anti-inflammatory effect is attributed to the controlled levels of ROS and local heating, which destroy bacteria and preserve the amount of oxidative damage to the adjacent tissues. This system has high potential of treating antibiotic-resistant wound infection [148] .

Mn-doped Zno nanoparticles synthesized by microwave also focus on the synthesis of materials that are environmentally friendly and antibacterial. The measured zones of inhibition of 15 mm against E. coli and 18 mm against S. aureus of these nanoparticles support the moderate to strong antibacterial activity. No in vivo wound-healing or anti-inflammatory result is reported in this study, however. Consequently, although the material has potential as an antibacterial agent, its applicability to clinics in wound repair has not been sufficiently proven because there is no biological support other than bacteria inhibition.[149]. MnZno@Mxene nanocomposite. It has great and wide-spectrum antibacterial activity and has inhibition zones of 22 mm against E. coli, 18 mm against S. aureus, or 19 mm against P. aeruginosa, which are said to be more powerful than those of the conventional antibiotics. This nanocomposite is applied in wound-healing research where 95.19% of the wounds are healed by day 10, in comparison to the negative control group, which heals 66.76% of the wounds. Also, the material shows significant anti-inflammatory effect, which diminishes paw edema at 6.96 mm to 4.39 mm in 24 hours, which is similar to the effect of a conventional anti-inflammatory medication. The synergistic interaction of Mxene and Mn-doped Zno homogenate achieves antibacterial

activity, skin regeneration, and good anti-inflammatory results. Overall, as the table demonstrates, Mxene-based nanocomposites, especially those containing Zno on their basis or using Mn-doped Zno, can serve as a versatile wound management method due to their combination of high antibacterial properties, wound healing, and wound inflammation control. The most balanced and biologically tested material, which was reviewed is MnZno, and Mxene emerges as the most promising system, and Zno, based on the reviewed materials, has the greatest potential to combat antibiotic-resistant infections. On the whole, these articles have repeatedly shown that Mxenes-hybrids and doped metal-oxide nanostructures do not only show powerful antibacterial properties, but, assessed in vivo, can enhance wound healing and stimulate tissue revival, partially by means of anti-inflammatory actions.

Table 2: Overview and comparison of multifunctional materials for antibacterial, wound healing and anti-inflammatory.

NO.	Material	Bacteria tested (reported ZOImm) *S.aureus, E.coli, P.aeruginosa*	Wound-healing	Anti-inflammatory	Reference
1.	**CIP–$Ti_3C_2T_x$ @ sodium-alginate**	*S. aureus*: 18–20 mm; *E. coli*: 16–18 mm	Mouse full-thickness skin wounds: ~61.0% closure (day 7) and ~90.1% closure (day 14)	Reduced infection-related inflammation via controlled drug delivery	[147]

2.	**Zno@Mxene** (photothermal platform)	>90% kill of MRSA within 5 min, *(E. Coli, P. aeruginosa not reported in this paper.)*	≈100% wound closure by ~12 days	Reduced inflammation caused by ROS damage	[148]
3.	**Microwave green-synthesized Mn-doped Zno NPs**	**Quantified ZOI** Inhibition zones: *E. coli*: 15 mm; *S. aureus*: 18 mm. (*P. aeruginosa* not reported in this paper.)	Not Reported	Not Reported	[149]
4.	**MnZno@Mxene Nanocomposite**	**Inhibition zones:** *E.coli* (22 mm), *S.aureus* (18 mm), *P. aeruginosa* (19 mm); stronger than standard antibiotics	95.19% closure by day 10 vs 66.76% (negative control); Enhanced skin regeneration	Paw edema reduced from 6.96 mm to 4.39 mm at 24 h; Comparable to the positive control	

Chapter 5
Conclusion

In this research, MnZno@Mxene nanocomposite was effectively prepared and showed great promise in biomedical applications, such as antibacterial, wound-healing, and anti-inflammatory. The nanocomposite had good antimicrobial properties as it had a maximum inhibitory zone of 22 mm against E. coli, 18 mm against S. aureus, and 19 mm against P. aeruginosa, which was better than that of the conventional antibiotics like gentamicin and ciprofloxacin, indicating its high antimicrobial activity. The time-kill analyses also showed successful bacterial suppression, especially with E. coli. The positive outcome was observed in the wound-healing studies, with the treated group demonstrating a faster recovery rate as demonstrated by the 95.19 percent wound closure after the first 10 days as opposed to the 66.76 percent wound closure in the negative group; the skin regeneration rate and the morphology of the wound. Anti-inflammatory activity which was assessed by the carrageenan-induced paw edema model showed that the swelling reduced significantly with a paw thickness range of 6.96 mm reducing to a range of 4.39 mm at 24 hours which is similar to that of the positive control and significantly lower than that of the negative control. These findings were supported by histological analysis, which showed an improvement in the epidermal structure, decreased inflammation, and aligned collagen in treated tissues. In general, MnZno@Mxene nanocomposite has a good chance of therapeutic application and therefore can be used in infection treatment, wound healing, and inflammation control.

References

1. Borena, B.M., et al., *Regenerative skin wound healing in mammals: state-of-the-art on growth factor and stem cell based treatments.* Cellular Physiology and Biochemistry, 2015. **36**(1): p. 1-23.
2. Matsui, T. and M. Amagai, *Dissecting the formation, structure and barrier function of the stratum corneum.* International immunology, 2015. **27**(6): p. 269-280.
3. Lai-Cheong, J.E. and J.A. McGrath, *Structure and function of skin, hair and nails.* Medicine, 2013. **41**(6): p. 317-320.
4. Baker, P., et al., *Skin barrier function: the interplay of physical, chemical, and immunologic properties.* Cells, 2023. **12**(23): p. 2745.
5. Proksch, E., *pH in nature, humans and skin.* The Journal of dermatology, 2018. **45**(9): p. 1044-1052.
6. Monika, P., et al., *Challenges in healing wound: role of complementary and alternative medicine.* Frontiers in Nutrition, 2022. **8**: p. 791899.
7. Pino, P., et al., *Antimicrobial nano-zinc oxide biocomposites for wound healing applications: a review.* Pharmaceutics, 2023. **15**(3): p. 970.
8. Strodtbeck, F., *Physiology of wound healing.* Newborn and infant nursing reviews, 2001. **1**(1): p. 43-52.
9. Enoch, S. and D.J. Leaper, *Basic science of wound healing.* Surgery (oxford), 2008. **26**(2): p. 31-37.
10. Fu, W., et al., *Opportunities and challenges of nanomaterials in wound healing: Advances, mechanisms, and perspectives.* Chemical Engineering Journal, 2024. **495**: p. 153640.
11. Versteeg, H.H., et al., *New fundamentals in hemostasis.* Physiological reviews, 2013. **93**(1): p. 327-358.
12. RAF, C., *Wound repair. Overview and general considerations.* The molecular and cellular biology of wound repair, 1994.
13. Dodds, W.J., *Hemostasis*, in *Clinical biochemistry of domestic animals*. 1997, Elsevier. p. 241-283.
14. McMichael, M., *Primary hemostasis.* Journal of veterinary emergency and critical care, 2005. **15**(1): p. 1-8.

15. Mahmoud, N.N., et al., *Investigating inflammatory markers in wound healing: understanding implications and identifying artifacts.* ACS Pharmacology & Translational Science, 2024. **7**(1): p. 18-27.
16. Stallmeyer, B., et al., *The function of nitric oxide in wound repair: inhibition of inducible nitric oxide-synthase severely impairs wound reepithelialization.* Journal of Investigative Dermatology, 1999. **113**(6): p. 1090-1098.
17. Simpson, D.M. and R. Ross, *The neutrophilic leukocyte in wound repair: a study with antineutrophil serum.* The Journal of clinical investigation, 1972. **51**(8): p. 2009-2023.
18. Holzer-Geissler, J.C., et al., *The impact of prolonged inflammation on wound healing.* Biomedicines, 2022. **10**(4): p. 856.
19. Wang, Z., et al., *Inflammatory microenvironment of skin wounds.* Frontiers in immunology, 2022. **13**: p. 789274.
20. Soliman, A.M., et al., *Role of microRNA in proliferation phase of wound healing.* Frontiers in genetics, 2018. **9**: p. 38.
21. Nissen, N.N., et al., *Vascular endothelial growth factor mediates angiogenic activity during the proliferative phase of wound healing.* The American journal of pathology, 1998. **152**(6): p. 1445.
22. Furtado, J. and A. Eichmann, *Vascular development, remodeling and maturation.* Current Topics in Developmental Biology, 2024. **159**: p. 344-370.
23. Čoma, M., et al., *Molecular changes underlying hypertrophic scarring following burns involve specific deregulations at all wound healing stages (inflammation, proliferation and maturation).* International Journal of Molecular Sciences, 2021. **22**(2): p. 897.
24. Reinke, J. and H. Sorg, *Wound repair and regeneration.* European surgical research, 2012. **49**(1): p. 35-43.
25. Das, S. and A.B. Baker, *Biomaterials and nanotherapeutics for enhancing skin wound healing.* Frontiers in bioengineering and biotechnology, 2016. **4**: p. 82.
26. Mamun, A.A., et al., *Recent advances in molecular mechanisms of skin wound healing and its treatments.* Frontiers in immunology, 2024. **15**: p. 1395479.
27. Omidian, H., R.L. Wilson, and E.J. Gill, *Advancements and challenges in self-healing hydrogels for wound care.* Gels, 2024. **10**(4): p. 241.

28. Chakrabarti, S., et al., *Aspects of nanomaterials in wound healing.* Current drug delivery, 2019. **16**(1): p. 26-41.
29. Sri Venkatesh, U., et al., *Nano Materials for Wound Healing.* Journal of Neonatal Surgery, 2025.
30. Goyal, K., S. Ahalwat, and V. Jogpal, *Transforming Wound Management: Advancement in Nanomaterials-based Therapeutics.* Recent Advances in Inflammation & Allergy Drug Discovery, 2024.
31. Selvaraj, X. and C. Guamán, *The Role of Nanoparticles in Wound Healing: Synthesis, Characterization, and Mechanisms of Action.* Health Leadership and Quality of Life, 2025. **4**: p. 774-774.
32. Sheikh-Oleslami, S., et al., *A review of metal nanoparticles embedded in hydrogel scaffolds for wound healing in vivo.* Gels, 2023. **9**(7): p. 591.
33. Darghiasi, S.F., F. Rajabi, and A. Farazin, *Maximizing the therapeutic benefits of biopolymer-derived nanoparticles in wound healing.* Iranian Journal of Basic Medical Sciences, 2025. **28**(7): p. 835.
34. Srikrishna, T. and N. Harikrishnan, *Recent advancement in Nano-drug delivery for Topical Wound Healing.* Research Journal of Pharmacy and Technology, 2022. **15**(5): p. 2320-2326.
35. Khalid, A., et al., *Bacterial cellulose-zinc oxide nanocomposites as a novel dressing system for burn wounds.* Carbohydrate polymers, 2017. **164**: p. 214-221.
36. Asif, N., M. Amir, and T. Fatma, *Recent advances in the synthesis, characterization and biomedical applications of zinc oxide nanoparticles.* Bioprocess and Biosystems Engineering, 2023. **46**(10): p. 1377-1398.
37. Saddik, M.S., et al., *Tailoring of novel azithromycin-loaded zinc oxide nanoparticles for wound healing.* Pharmaceutics, 2022. **14**(1): p. 111.
38. Mandal, A.K., et al., *Current research on zinc oxide nanoparticles: synthesis, characterization, and biomedical applications.* Nanomaterials, 2022. **12**(17): p. 3066.
39. Haque, S., S. Tripathy, and C.R. Patra, *Manganese-based advanced nanoparticles for biomedical applications: future opportunity and challenges.* Nanoscale, 2021. **13**(39): p. 16405-16426.
40. Manavalan, R.K., et al., *Review on medical applications of manganese oxide (Mn^{2+},*

Mn^{3+}, and Mn^{4+}) magnetic nanoparticles. Journal of Nanomaterials, 2024. **2024**(1): p. 1073915.

41. Farinha, P., et al., *A comprehensive updated review on magnetic nanoparticles in diagnostics.* Nanomaterials, 2021. **11**(12): p. 3432.
42. Qian, X., et al., *Manganese-based functional nanoplatforms: Nanosynthetic construction, physiochemical property, and theranostic applicability.* Advanced Functional Materials, 2020. **30**(3): p. 1907066.
43. Sichamnan, A., et al., *Fabrication of biocompatible magneto-fluorescence nanoparticles as a platform for fluorescent sensor and magnetic hyperthermia applications.* RSC advances, 2021. **11**(56): p. 35258-35267.
44. Hasan, M., et al., *A comparative study on green synthesis and characterization of Mn doped Zno nanocomposite for antibacterial and photocatalytic applications.* Scientific Reports, 2024. **14**(1): p. 7528.
45. Khan, S.A., et al., *Synthesis, characterization and evaluation of biological activities of manganese-doped zinc oxide nanoparticles.* Tropical Journal of Pharmaceutical Research, 2017. **16**(10): p. 2331-2339.
46. Thakur, D., et al., *Manganese-doped zinc oxide nanostructures as potential scaffold for photocatalytic and fluorescence sensing applications.* Chemosensors, 2020. **8**(4): p. 120.
47. Yin, H., et al., *Cytotoxicity and Antimicrobial Efficacy of Fe-, Co-, and Mn-Doped Zno Nanoparticles.* Molecules, 2024. **29**(24): p. 5966.
48. Khan, M.M., et al., *Antibacterial activities of zinc oxide and Mn-doped zinc oxide synthesized using Melastoma malabathricum (L.) leaf extract.* Bioprocess and Biosystems Engineering, 2020. **43**(8): p. 1499-1508.
49. Mallick, S., et al., *Engineered nanotechnology: an effective therapeutic platform for the chronic cutaneous wound.* Nanomaterials, 2022. **12**(5): p. 778.
50. Lokare, P., et al., *Applications of plant-based nanomedicines for wound healing–An emerging paradigm for effective therapy.* Materials Today: Proceedings, 2023. **73**: p. 494-501.
51. Ko, N.R., et al., *Reductively-sheddable cationic nanocarriers for dual chemotherapy and gene therapy with enhanced release.* Colloids and Surfaces B: Biointerfaces, 2015. **126**: p. 178-187.

52. Xie, J., et al., *Recent advances in Zno nanomaterial-mediated biological applications and action mechanisms.* Nanomaterials, 2023. **13**(9): p. 1500.
53. Alsaleh, N.B., et al., *Synthesis, characterization, and toxicity assessment of zinc oxide-doped manganese oxide nanoparticles in a macrophage model.* Pharmaceuticals, 2024. **17**(2): p. 168.
54. Rather, H.A., et al., *Antioxidative study of Cerium Oxide nanoparticle functionalised PCL-Gelatin electrospun fibers for wound healing application.* Bioactive materials, 2018. **3**(2): p. 201-211.
55. Wierzbicki, M., et al., *Graphene oxide in a composite with silver nanoparticles reduces the fibroblast and endothelial cell cytotoxicity of an antibacterial nanoplatform.* Nanoscale research letters, 2019. **14**(1): p. 320.
56. Cui, L., et al., *Nanomaterials for angiogenesis in skin tissue engineering.* Tissue Engineering Part B: Reviews, 2020. **26**(3): p. 203-216.
57. Wang, M., et al., *Nanomaterials applied in wound healing: Mechanisms, limitations and perspectives.* Journal of Controlled Release, 2021. **337**: p. 236-247.
58. Solangi, N.H., et al., *Recent trends in Mxene-based material for biomedical applications.* Environmental Research, 2023. **222**: p. 115337.
59. Anasori, B., M.R. Lukatskaya, and Y. Gogotsi, *2D metal carbides and nitrides (Mxenes) for energy storage*, in *Mxenes*. 2023, Jenny Stanford Publishing. p. 677-722.
60. Zhou, J., et al., *Atomic scale design of Mxenes and their parent materials─ from theoretical and experimental perspectives.* Chemical reviews, 2023. **123**(23): p. 13291-13322.
61. Pogorielov, M., et al., *Mxenes—a new class of two-dimensional materials: structure, properties and potential applications.* Nanomaterials, 2021. **11**(12): p. 3412.
62. Akhter, R. and S.S. Maktedar, *Mxenes: A comprehensive review of synthesis, properties, and progress in supercapacitor applications.* Journal of Materiomics, 2023. **9**(6): p. 1196-1241.
63. Zhang, Z., et al., *Applications of Mxene and its modified materials in skin wound repair.* Frontiers in Bioengineering and Biotechnology, 2023. **11**: p. 1154301.
64. Naguib, M., et al., *25th anniversary article: Mxenes: a new family of two-dimensional materials.* Advanced materials, 2014. **26**(7): p. 992-1005.

65. Sundaram, A., et al., *Engineering of 2D transition metal carbides and nitrides Mxenes for cancer therapeutics and diagnostics.* Journal of Materials Chemistry B, 2020. **8**(23): p. 4990-5013.
66. Lin, X., et al., *Fascinating Mxene nanomaterials: emerging opportunities in the biomedical field.* Biomaterials science, 2021. **9**(16): p. 5437-5471.
67. Huang, H., et al., *Recent development and prospects of surface modification and biomedical applications of Mxenes.* Nanoscale, 2020. **12**(3): p. 1325-1338.
68. Begum, S., et al., *2D and heterostructure nanomaterial based strategies for combating drug-resistant bacteria.* ACS omega, 2020. **5**(7): p. 3116-3130.
69. Dunnill, C., et al., *Reactive oxygen species (ROS) and wound healing: the functional role of ROS and emerging ROS-modulating technologies for augmentation of the healing process.* International wound journal, 2017. **14**(1): p. 89-96.
70. Xu, X., et al., *A multimodal antimicrobial platform based on Mxene for treatment of wound infection.* Colloids and Surfaces B: Biointerfaces, 2021. **207**: p. 111979.
71. Rizi, K.S., *Mxene nanosheets as a novel nanomaterial with antimicrobial applications: a literature review.* Journal of Molecular Structure, 2022. **1262**.
72. Zhu, H., et al., *Electroactive oxidized alginate/gelatin/Mxene (Ti3C2Tx) composite hydrogel with improved biocompatibility and self-healing property.* Polymers, 2022. **14**(18): p. 3908.
73. Zarepour, A., et al., *Mxene-based composites in smart wound healing and dressings.* Nanoscale Advances, 2024. **6**(14): p. 3513-3532.
74. Chen, L., et al., *Superhydrophobic functionalized Ti3C2T X Mxene-based skin-attachable and wearable electrochemical pH sensor for real-time sweat detection.* Analytical Chemistry, 2022. **94**(20): p. 7319-7328.
75. Persson, P.O. and J. Rosen, *Current state of the art on tailoring the Mxene composition, structure, and surface chemistry.* Current Opinion in Solid State and Materials Science, 2019. **23**(6): p. 100774.
76. Zhang, W.-J., et al., *ROS-and pH-responsive polydopamine functionalized Ti3C2Tx Mxene-based nanoparticles as drug delivery nanocarriers with high antibacterial activity.* Nanomaterials, 2022. **12**(24): p. 4392.
77. Li, T., Y. Wang, and B. Lei, *Photothermal-antibacterial bioactive noncrystalline nanosystem promotes infected wound tissue regeneration through thermo-ions*

activation. Chemical Engineering Journal, 2024. **491**: p. 151799.

78. Wang, P., et al., *Mxenes-integrated microneedle combined with asiaticoside to penetrate the cuticle for treatment of diabetic foot ulcer.* Journal of nanobiotechnology, 2022. **20**(1): p. 259.
79. Luo, X., et al., *Tissue-nanoengineered hyperbranched polymer based multifunctional hydrogels as flexible "wounped treatment-health monitoring" bioelectronic implant.* Applied Materials Today, 2022. **29**: p. 101576.
80. Yang, X., et al., *Multiple stimuli-responsive Mxene-based hydrogel as intelligent drug delivery carriers for deep chronic wound healing.* Small, 2022. **18**(5): p. 2104368.
81. Liu, S., et al., *Flexible, high-strength and multifunctional polyvinyl alcohol/Mxene/polyaniline hydrogel enhancing skin wound healing.* Biomaterials Science, 2022. **10**(13): p. 3585-3596.
82. Yu, S., et al., *Application of nanomaterials in diagnosis and treatment of glioblastoma.* Frontiers in Chemistry, 2022. **10**: p. 1063152.
83. Wang, L., et al., *Multifunctional hydrogel as wound dressing for intelligent wound monitoring.* Chemical Engineering Journal, 2022. **433**: p. 134625.
84. Zhou, L., et al., *Conductive antibacterial hemostatic multifunctional scaffolds based on Ti3C2T x Mxene nanosheets for promoting multidrug-resistant bacteria-infected wound healing.* ACS nano, 2021. **15**(2): p. 2468-2480.
85. Mao, M., et al., *Mxene-based wearable self-powered and photothermal triboelectric nanogenerator patches for wound healing acceleration and tactile sensing.* Chemical Engineering Journal, 2024. **482**: p. 148949.
86. Ozulumba, T., et al., *Moderating cellular inflammation using 2-dimensional titanium carbide Mxene and graphene variants.* Biomaterials science, 2021. **9**(5): p. 1805-1815.
87. Chin, S.M., et al., *Functional graphene for peritumoral brain microenvironment modulation therapy in glioblastoma.* Small, 2023. **19**(18): p. 2208227.
88. Li, Y., et al., *Artificial nonenzymatic antioxidant Mxene nanosheet-anchored injectable hydrogel as a mild photothermal-controlled oxygen release platform for diabetic wound healing.* ACS nano, 2022. **16**(5): p. 7486-7502.
89. Chen, J., et al., *Tailored hydrogel delivering niobium carbide boosts ros-scavenging*

and antimicrobial activities for diabetic wound healing. Small, 2022. **18**(27): p. 2201300.

90. Qiu, X., et al., *From hemostasis to proliferation: Accelerating the infected wound healing through a comprehensive repair strategy based on GA/OKGM hydrogel loaded with Mxene@ TiO2 nanosheets.* Biomaterials, 2024. **308**: p. 122548.
91. Tang, M., et al., *Surface terminations of Mxene: synthesis, characterization, and properties.* Symmetry, 2022. **14**(11): p. 2232.
92. Liu, C., et al., *Mussel-inspired degradable antibacterial polydopamine/silica nanoparticle for rapid hemostasis.* Biomaterials, 2018. **179**: p. 83-95.
93. Li, H., et al., *Generation of cost-effective Mxene@ polydopamine-decorated chitosan nanofibrous wound dressing for promoting wound healing.* Biomaterials Advances, 2022. **140**: p. 213055.
94. Yang, Y., et al., *Photo-activated nanofibrous membrane with self-rechargeable antibacterial function for stubborn infected cutaneous regeneration.* Small, 2022. **18**(12): p. 2105988.
95. Davidson, E., et al., *Multi-functional chitosan nanovesicles loaded with bioactive manganese for potential wound healing applications.* Molecules, 2023. **28**(16): p. 6098.
96. Wu, Z., et al., *Manganese-doped calcium silicate nanowire composite hydrogels for melanoma treatment and wound healing.* Research, 2021.
97. Popescu, T., et al., *Influence of surfactant-tailored Mn-doped Zno nanoparticles on ROS production and DNA damage induced in murine fibroblast cells.* Scientific reports, 2020. **10**(1): p. 18062.
98. Morganti, D., et al., *Development, characterization and biological studies of Mn-doped Zno/Ti biomaterials for regenerative medicine.* Scientific Reports, 2025. **15**(1): p. 35952.
99. Alam, M.W., et al., *Phyto synthesis of manganese-doped zinc nanoparticles using carica papaya leaves: structural properties and its evaluation for catalytic, antibacterial and antioxidant activities.* Polymers, 2022. **14**(9): p. 1827.
100. Jiang, N., et al., *Using Hybrid MnO2-Au Nanoflowers to Accelerate ROS Scavenging and Wound Healing in Diabetes.* Pharmaceutics, 2024. **16**(10): p. 1244.
101. Jiang, X., et al., *Highly bioactive Mxene-M2-exosome nanocomposites promote*

angiogenic diabetic wound repair through reconstructing high glucose-derived immune inhibition. ACS nano, 2024. **18**(5): p. 4269-4286.

102. Gao, Y., et al., *Tissue-Adhesive and Antibacterial Hydrogel Promotes MDR Bacteria-Infected Diabetic Wound Healing via Disrupting Bacterial Biofilm, Scavenging ROS and Promoting Angiogenesis.* Advanced Healthcare Materials, 2025. **14**(10): p. 2404889.
103. Hu, Y., et al., *Mxene/zinc ion embedded agar/sodium alginate hydrogel for rapid and efficient sterilization with photothermal and chemical synergetic therapy.* Talanta, 2024. **266**: p. 125101.
104. Sang, Z., et al., *NIR sensitive Zno QDs decorated Mxene hydrogel promotes spinal cord repair via tunable controlled release of Zn^{2+} and regulating ROS microenvironment of mitochondrion.* Chemical Engineering Journal, 2024. **489**: p. 151343.
105. Li, T., et al., *Bioactive Mxene promoting angiogenesis and skeletal muscle regeneration through regulating M2 polarization and oxidation stress.* Advanced healthcare materials, 2023. **12**(4): p. 2201862.
106. Wu, M., et al., *Photoactivated Hydrogel Therapeutic System with Mxene-Based Nanoarchitectonics Potentiates Endogenous Bone Repair Through Reshaping the Osteo-Vascularization Network.* Small, 2024. **20**(51): p. 2403003.
107. Cheng, F., et al., *Photothermal Mxene@ Zn-MOF-decorated bacterial cellulose-based hydrogel wound dressing for infectious wound healing.* Cell Reports Physical Science, 2023. **4**(10).
108. Zhang, H., et al., *Bacterial cellulose cross-linked Mxene composite antimicrobial hemostatic sponges with photothermal properties for wound healing.* Materials Today Chemistry, 2025. **43**: p. 102520.
109. Ou, X., et al., *An Mxene nanocomposite hydrogel for enhanced diabetic infected wound healing via photothermal antibacterial properties and bioactive molecule integration.* Materials Today Bio, 2025. **31**: p. 101538.
110. Li, H., et al., *Mxene-based nanomaterials for antibacterial and wound healing.* Materials Research Letters, 2024. **12**(2): p. 67-87.
111. Cheng, X., et al., *Research on the antibacterial properties of Mxene-based 2D–2D composite materials membrane.* Nanomaterials, 2023. **13**(14): p. 2121.

112. Li, S., et al., *Mxene-enhanced chitin composite sponges with antibacterial and hemostatic activity for wound healing.* Advanced Healthcare Materials, 2022. **11**(12): p. 2102367.
113. Sun, L., et al., *Mxene-integrated microneedle patches with innate molecule encapsulation for wound healing.* Research, 2021.
114. Ye, S., et al., *Mxene: A wonderful nanomaterial in antibacterial.* Frontiers in Bioengineering and Biotechnology, 2024. **12**: p. 1338539.
115. Maleki, A., et al., *Biomedical applications of Mxene-integrated composites: regenerative medicine, infection therapy, cancer treatment, and biosensing.* Advanced Functional Materials, 2022. **32**(34): p. 2203430.
116. Blinov, A.V., et al., *Synthesis and characterization of zinc oxide nanoparticles stabilized with biopolymers for application in wound-healing mixed gels.* Gels, 2023. **9**(1): p. 57.
117. Dutta, G. and A. Sugumaran, *Bioengineered zinc oxide nanoparticles: Chemical, green, biological fabrication methods and its potential biomedical applications.* Journal of drug delivery science and technology, 2021. **66**: p. 102853.
118. Hassan, A., et al., *Investigation of angiogenesis and wound healing potential mechanisms of zinc oxide nanorods.* Frontiers in pharmacology, 2021. **12**: p. 661217.
119. Batool, M., et al., *Adsorption, antimicrobial and wound healing activities of biosynthesised zinc oxide nanoparticles.* Chemical Papers, 2021. **75**(3): p. 893-907.
120. Sukri, S.N.A.M., et al., *Cytotoxicity and antibacterial activities of plant-mediated synthesized zinc oxide (Zno) nanoparticles using Punica granatum (pomegranate) fruit peels extract.* Journal of Molecular Structure, 2019. **1189**: p. 57-65.
121. Mihai, M.M., et al., *Nanomaterials for wound healing and infection control.* Materials, 2019. **12**(13): p. 2176.
122. Venkateshalu, S. and A.N. Grace, *Ti3C2Tx Mxene and Vanadium nitride/Porous carbon as electrodes for asymmetric supercapacitors.* Electrochimica Acta, 2020. **341**: p. 136035.
123. Munir, S., et al., *Exploring the influence of critical parameters for the effective synthesis of high-quality 2D Mxene.* ACS omega, 2020. **5**(41): p. 26845-26854.
124. Kannan, K., et al., *Fabrication of Zno-Fe-Mxene based nanocomposites for efficient*

CO2 reduction. Catalysts, 2020. **10**(5): p. 549.

125. Al-Shmgani, H.S., et al., *Biosynthesis of silver nanoparticles from Catharanthus roseus leaf extract and assessing their antioxidant, antimicrobial, and wound-healing activities.* Artificial cells, nanomedicine, and biotechnology, 2017. **45**(6): p. 1234-1240.
126. Nasser, S., et al., *Concentration-Dependent Effects of Mxene Nanocomposite-Loaded Carboxymethyl Cellulose on Wound Healing.* Biotechnology Journal, 2024. **19**(10): p. e202400448.
127. Morris, C.J., *Carrageenan-induced paw edema in the rat and mouse.* Inflammation protocols, 2003: p. 115-121.
128. Haq, Y.-U., et al., *Synthesis and characterization of 2D Mxene: Device fabrication for humidity sensing.* Journal of Science: Advanced Materials and Devices, 2022. **7**(1): p. 100390.
129. Li, B., et al., *Structural health monitoring for polymer composites with surface printed Mxene/ink sensitive sensors.* Applied Physics A, 2020. **126**(10): p. 791.
130. Sharma, M., et al., *Structural, magnetic, and optical properties of Mn^{2+} doping in Zno thin films.* Surfaces, 2021. **4**(4): p. 268-278.
131. Priyadharsini, N., N. Bhuvaneswari, and J. Joshy, *Plant mediated synthesis of Zno and Mn doped Zno nanoparticles using carica papaya leaf extract for antibacterial applications.* Asian Journal of Applied Science and Technology (AJAST), 2021. **5**(4): p. 69-81.
132. Iqbal, A. and N.M. Hamdan, *Investigation and optimization of mxene functionalized mesoporous titania films as efficient photoelectrodes.* Materials, 2021. **14**(21): p. 6292.
133. Ramesh, A., et al., *Mn-doped Zno microspheres prepared by solution combustion synthesis for room temperature NH3 sensing.* Applied Surface Science Advances, 2022. **12**: p. 100349.
134. Satheeshkumar, E., et al., *One-step solution processing of Ag, Au and Pd@ Mxene hybrids for SERS.* Scientific reports, 2016. **6**(1): p. 32049.
135. Silambarasan, M., S. Saravanan, and T. Soga, *Mn-doped Zno nanoparticles prepared by solution combustion method.* e-Journal of Surface Science and Nanotechnology, 2014. **12**: p. 283-288.

136. Iqbal, M.A., et al., *Ti3C2-Mxene/bismuth ferrite nanohybrids for efficient degradation of organic dyes and colorless pollutants.* ACS omega, 2019. **4**(24): p. 20530-20539.
137. Hasan, M., et al., *Structural, optical, and photocatalytic efficacy of Ti3C2 and M2C (M= Ti, V, Cr, Nb) Mxene materials synthesized by etching technique.* AIP Advances, 2025. **15**(3).
138. Zahid, A., et al., *Synthesis of Mn-doped Zno nanoparticles and their application in the transesterification of castor oil.* Catalysts, 2023. **13**(1): p. 105.
139. Liu, X., et al., *A direct electrochemical H2S sensor based on Ti3C2Tx Mxene.* ChemElectroChem, 2021. **8**(19): p. 3658-3665.
140. Cao, Y., et al., *Enhanced thermal properties of poly (vinylidene fluoride) composites with ultrathin nanosheets of Mxene.* RSC advances, 2017. **7**(33): p. 20494-20501.
141. Tan, T.L., C.W. Lai, and S.B. Abd Hamid, *Tunable Band Gap Energy of Mn-Doped Zno Nanoparticles Using the Coprecipitation Technique.* Journal of Nanomaterials, 2014. **2014**(1): p. 371720.
142. Shatnawi, M., et al., *Influence of Mn doping on the magnetic and optical properties of Zno nanocrystalline particles.* Results in Physics, 2016. **6**: p. 1064-1071.
143. Ta, Q.T.H., N.M. Tran, and J.-S. Noh, *Rice crust-like Zno/Ti3C2Tx Mxene hybrid structures for improved photocatalytic activity.* Catalysts, 2020. **10**(10): p. 1140.
144. Khatun, Z., et al., *Green synthesis and Anti-bacterial activity of Silver Oxide nanoparticles prepared from Pinus longifolia leaves extract.* international Journal, 2015. **3**(11): p. 337-343.
145. Niaz, T., et al., *Potential of polymer stabilized nano-liposomes to enhance antimicrobial activity of nisin Z against foodborne pathogens.* Lwt, 2018. **96**: p. 98-110.
146. Amdekar, S., et al., *Anti-Inflammatory Activity of Lactobacillus on Carrageenan-Induced Paw Edema in Male Wistar Rats.* International journal of inflammation, 2012. **2012**(1): p. 752015.
147. Park, H., et al., *Sprayable Ti3C2 Mxene hydrogel for wound healing and drug release system.* Materials Today Bio, 2023. **23**: p. 100881.
148. Yin, R., et al., *Zno@ Mxene nanoplatform for near infrared induced elimination of drug resistant bacteria and Acceleration of infected wound healing.* Materials &

Design, 2025: p. 114816.

149. Khan, S.B., M.I. Khan, and J. Nisar, *Microwave-assisted green synthesis of pure and Mn-doped Zno nanocomposites: In vitro antibacterial assay and photodegradation of methylene blue.* Frontiers in materials, 2022. **8**: p. 710155.

Turnitin Originality Report

Processed on: 08-Jan-2026 16:15 PKT
ID: 2853932423
Word Count: 17687
Submitted: 1

Exploring the potential of Mn/ZnO@MXene in Biomedical Applications By Hina Murtaza Cit/sp24-r06-007/lhr

Similarity Index: 6%

Similarity by Source
Internet Sources: 3%
Publications: 4%
Student Papers: 0%

1% match (publications)
Mohammed Gulzar Ahmed, Sumel Ashique, Arshad Farid, Gokhan Zengin. "Nanomaterials for Wound Healing", CRC Press, 2025

< 1% match (Internet from 23-Dec-2025)
https://www.mdpi.com/2075-1729/12/9/1444/xml

< 1% match (Internet from 28-Feb-2020)
https://www.mdpi.com/1422-0067/18/12/2766/htm

< 1% match (Internet from 23-Dec-2025)
https://www.mdpi.com/2073-4344/13/1/51/xml

< 1% match (Internet from 28-Dec-2025)
https://www.mdpi.com/2072-6651/13/7/420/xml

< 1% match (Internet from 14-Mar-2025)
https://www.mdpi.com/1422-0067/23/17/10127

< 1% match (Internet from 07-Jan-2026)
https://www.mdpi.com/2079-4983/16/12/465/xml

< 1% match (Internet from 21-May-2025)
https://www.mdpi.com/2073-4360/14/15/3085

< 1% match (Internet from 03-Sep-2025)
https://www.mdpi.com/2227-9059/13/8/2003

< 1% match (Sandhiya Ravikumar, Kandavelu Velappan, Saravanabhavan Munusamy, Varnika M, Naveenaa S, Ramesh Shanmugam. "Emerging nanotechnologies in wound care: The role of metal and polymeric nanocomposites in enhancing healing and combating infections", International Journal of Pharmaceutics, 2025)
Sandhiya Ravikumar, Kandavelu Velappan, Saravanabhavan Munusamy, Varnika M, Naveenaa S, Ramesh Shanmugam. "Emerging nanotechnologies in wound care: The role of metal and polymeric nanocomposites in enhancing healing and combating infections", International Journal of Pharmaceutics, 2025

< 1% match (Internet from 30-Mar-2023)
https://www.researchgate.net/publication/331848428_Novel_coating_containing_molybdenum_oxide_nanoparticles_to_reduce_Staphylococcus_aureus_contamination_on_inanimate_surf

< 1% match (Internet from 26-Apr-2023)
https://www.researchgate.net/publication/306038691_Study_of_Phytochemical_Screening_Physicochemical_Analysis_and_Antimicrobial_Activity_of_Bacopa_monnieri_L_Extracts

< 1% match (J. Nandhini, E. Karthikeyan, S. Rajeshkumar. "Nanomaterials for wound healing: Current status and futuristic frontier", Biomedical Technology, 2024)
J. Nandhini, E. Karthikeyan, S. Rajeshkumar. "Nanomaterials for wound healing: Current status and futuristic frontier", Biomedical Technology, 2024

< 1% match (Internet from 02-Mar-2025)
https://www.benchchem.com/product/b073188

< 1% match (Internet from 23-Sep-2025)
https://www.benchchem.com/product/b2452652

< 1% match (Internet from 04-Aug-2023)
https://www.science.gov/topicpages/a/activated+inos+mediate.html

< 1% match (Internet from 14-Jun-2023)
https://www.science.gov/topicpages/i/inflammatory+cytokine+production

< 1% match (Internet from 05-Aug-2023)
https://bioresources.cnr.ncsu.edu/resources/structural-characterization-and-solid-state-properties-of-thermal-insulating-cellulose-materials-of-different-size-classifications/

< 1% match (Hossein Omidian, Renae L. Wilson, Erma J. Gill. "Advancements and Challenges in Self-Healing Hydrogels for Wound Care", Gels, 2024)
Hossein Omidian, Renae L. Wilson, Erma J. Gill. "Advancements and Challenges in Self-Healing Hydrogels for Wound Care", Gels, 2024

< 1% match (Nandhini J, Karthikeyan E, Rajeshkumar S. ""Green Synthesis of Zinc Oxide Nanoparticles: Eco-Friendly Advancements for Biomedical Marvels"", Resources Chemicals and Materials, 2024)
Nandhini J, Karthikeyan E, Rajeshkumar S. ""Green Synthesis of Zinc Oxide Nanoparticles: Eco-Friendly Advancements for Biomedical Marvels"", Resources Chemicals and Materials, 2024

< 1% match ("Innovative Pharmaceutical Excipients: Natural Sources", Springer Science and Business Media LLC, 2025)
"Innovative Pharmaceutical Excipients: Natural Sources", Springer Science and Business Media LLC, 2025

< 1% match (Hafezeh Nabipour, Moayad Hossaini Sadr, Ghasem Rezanejade Bardajee. " Release behavior, kinetic and antimicrobial study of nalidixic acid from [Zn (bdc) (dabco)] metal-organic frameworks ", Journal of Coordination Chemistry, 2017)
Hafezeh Nabipour, Moayad Hossaini Sadr, Ghasem Rezanejade Bardajee. " Release behavior, kinetic and antimicrobial study of nalidixic acid from [Zn (bdc) (dabco)] metal-organic frameworks ", Journal of Coordination Chemistry, 2017

< 1% match (Internet from 08-Dec-2025)
https://pmc.ncbi.nlm.nih.gov/articles/PMC10044335/

< 1% match (Internet from 03-Oct-2023)
https://www.omicsdi.org/dataset/biostudies/S-EPMC6813896

< 1% match (Internet from 25-Dec-2023)